

**Copyright**  
**By**  
**Michael Ericson Ahern**  
**2005**

**Design and Fabrication of a Compact Specimen for Evaluation of  
Corrosion Resistance of New Post-Tensioning Systems**

by

**Michael Ericson Ahern, B.S.**

**Thesis**

Presented to the Faculty of the Graduate School of

The University of Texas at Austin

in Partial Fulfillment

of the Requirements

for the Degree of

**Master of Science in Engineering**

**The University of Texas at Austin**

**May 2005**

**Design and Fabrication of a Compact Specimen for Evaluation of  
Corrosion Resistance of New Post-Tensioning Systems**

**APPROVED BY  
SUPERVISING COMMITTEE:**

---

**John E. Breen**

---

**Sharon L. Wood**

## **Dedication**

This work is dedicated to my entire family – the most important part of my life.

## **Acknowledgements**

Dr. Breen provided expert guidance for my degree and research, but I will remember him most for advising me on life and sharing his experiences. I learned more from Dr. Breen than any other person outside of my family.

My friends in the structures department made my two years at Texas a great experience. Spending time with them, in and out of the classroom, broadened my personal and geographic horizons. I wish them all well in the future – I am certain our paths will cross again.

My undergraduate research assistants – Kyle Steuck, Gregory Turco and Michael McCarty – were integral to my work at Ferguson Lab. I appreciate all their hard work and company, especially during last semester.

The technical and administrative staff at Ferguson Lab made my research possible. I appreciate all their expertise and assistance over the past two years.

May 6, 2005

# **Design and Fabrication of a Compact Specimen for Evaluation of Corrosion Resistance of New Post-Tensioning Systems**

Michael Ericson Ahern, M.S.E.

The University of Texas at Austin, 2005

SUPERVISOR: John E. Breen

This thesis focuses on the design and fabrication of a new compact research specimen for evaluation of corrosion resistance of potentially improved post-tensioning systems. The development of new post-tensioning materials and systems in recent years has made some of the durability research in this area obsolete. The current research is evaluating the corrosion resistance of both existing and potential post-tensioning materials as well as examining construction practices for the new systems. The new post-tensioning systems being investigated include combinations of strand, duct (with and without couplers),

bearing plates and electrical isolation. Possible combinations of the following materials were identified using a specimen matrix:

<b>Strands</b>	Conventional Copper Clad Stainless Clad Stainless Epoxy Coated Hot Dip Galvanized Electroplated Galvanized
<b>Ducts</b>	One-Way Ribbed Plastic (with Slip-On and Snap-On Couplers) Two-Way Ribbed Plastic (with Slip-On Couplers) Galvanized Corrugated Steel (No Couplers)
<b>Bearing Plates</b>	Non-Galvanized Galvanized
<b>Electrical Isolation</b>	Conventional Tendons Electrically Isolated Tendons

The experimental program includes both long-term exposure tests and accelerated corrosion tests. The long-term program is modeled after previous post-tensioning durability research at the University of Texas under Project 1405. To provide continuity between the two projects and comparable results, this research used construction practices, exposure methods and monitoring conditions similar to those used in the previous research, with the exception that the current specimen uses only one-eighth of the materials used in previous specimens. The compact specimens should yield data fully comparable to that from the larger specimens of the previous project. The accelerated testing of the materials and evaluation of construction practices will be completed in ongoing phases of the project.

## Table of Contents

<b>CHAPTER 1 INTRODUCTION.....</b>	<b>1</b>
1.1 Problem Statement .....	1
1.2 Background .....	1
1.2.1 Post-Tensioning.....	1
1.2.2 Post-Tensioning Corrosion.....	3
1.2.3 Electrochemistry.....	5
1.2.4 Influence of Cracking.....	8
1.2.5 Previous Testing.....	10
1.2.6 Field Experience with Post-Tensioning Corrosion .....	11
1.3 Project Objective .....	18
1.4 Thesis Objectives and Organization.....	18
<b>CHAPTER 2 IMPROVED POST-TENSIONING SYSTEMS .....</b>	<b>20</b>
2.1 Problems with Present Systems.....	20
2.2 Quest for New Materials .....	22
2.3 Materials.....	23
2.3.1 Specimen Matrix .....	23
2.3.2 Types of Strand .....	25
2.3.3 Types of Duct .....	32
2.3.3.1 Plastic .....	33
2.3.3.2 Galvanized Steel.....	37
2.3.4 Types of Bearing Plates.....	38
2.3.5 Types of Systems .....	39
<b>CHAPTER 3 DESIGN OF TEST SPECIMENS.....</b>	<b>42</b>
3.1 Objectives.....	42
3.1.1 Small Specimen.....	42
3.1.2 Controlled Cracking .....	44
3.1.3 Accelerated Results .....	46
3.1.4 Post-Tensioning Hardware Isolation.....	46
3.2 Design.....	47
3.2.1 Forces .....	47
3.2.2 Reinforcement .....	49



3.2.3 Concrete .....	50
<b>CHAPTER 4 CONSTRUCTION .....</b>	<b>52</b>
4.1 Objectives.....	52
4.2 Forms.....	52
4.3 Deformed Reinforcement Cage.....	54
4.4 Ducts.....	56
4.5 Strand .....	57
4.6 Concrete .....	57
4.7 Stressing .....	58
4.7.1 Target Values .....	58
4.7.2 Losses .....	59
4.8 Stressing .....	64
4.8.1 Prestress Procedure .....	64
4.8.2 Live Load Procedure .....	65
4.8.3 Data Acquisition.....	67
4.9 Grouting .....	69
4.10 Sealing Anchorage Techniques .....	71
<b>CHAPTER 5 EXPOSURE AND MONITORING TECHNIQUES .....</b>	<b>73</b>
5.1 Location.....	73
5.2 Cycled Exposure .....	76
5.2.1 Ponded Saltwater.....	76
5.2.2 Anchorage Exposure .....	77
5.3 Monitoring.....	78
5.3.1 Visual Examination .....	79
5.3.2 Half-Cell Potential Readings.....	79
5.3.3 AC Impedance.....	81
<b>CHAPTER 6 TEST SPECIMENS .....</b>	<b>83</b>
6.1 Introduction .....	83
6.2 Specimen Details.....	83
6.3 Specimen Data.....	89
6.3.1 Beam 1.1.....	89
6.3.1.1 Materials.....	89
6.3.1.2 Important Dates .....	89
6.3.1.3 Stressing History .....	90

6.3.1.4	Beam 1.1 Comments .....	91
6.3.2	Beam 2.2.....	92
6.3.2.1	Materials.....	92
6.3.2.2	Important Dates .....	92
6.3.2.3	Stressing History .....	93
6.3.2.4	Beam 2.2 Comments .....	94
<b>CHAPTER 7 CONCLUSION.....</b>		<b>95</b>
7.1	Brief Summary .....	95
7.2	Conclusions .....	96
7.3	Recommendations For Similar Research .....	97
7.4	Continuation of Project 4562 Research.....	98
7.4.1	Continued Exposure and Monitoring .....	98
7.4.2	Material Testing .....	99
7.4.3	Accelerated Corrosion Testing.....	99
7.4.4	Autopsy Research Specimens .....	99
<b>APPENDIX A ADDITIONAL MATERIAL INFORMATION.....</b>		<b>101</b>
A.1	Materials Summary .....	101
A.2	Workshop Summary.....	102
<b>APPENDIX B ADDITIONAL DESIGN INFORMATION.....</b>		<b>103</b>
B.1	Mild Reinforcement .....	103
B.1.1	Details.....	104
B.1.2	Bar Dimensions .....	105
B.2	Reference Comparison Specimen Design Calculations .....	109
<b>APPENDIX C BEAM DATA .....</b>		<b>110</b>
C.1	Beam Data .....	110
C.1.1	Beam 1.1.....	110
C.1.1.1	Beam 1.1 Materials.....	110
C.1.1.2	Beam 1.1 Important Dates .....	110
C.1.1.3	Beam 1.1 Stressing History .....	111
C.1.1.4	Beam 1.1 Comments.....	112
C.1.2	Beam 1.2.....	113
C.1.2.1	Beam 1.2 Materials.....	113
C.1.2.2	Beam 1.2 Important Dates .....	113

C.1.2.3	Beam 1.2 Stressing History .....	114
C.1.2.4	Beam 1.2 Comments.....	115
C.1.3	Beam 1.3.....	116
C.1.3.1	Beam 1.3 Materials.....	116
C.1.3.2	Beam 1.3 Important Dates .....	116
C.1.3.3	Beam 1.3 Stressing History .....	117
C.1.3.4	Beam 1.3 Comments.....	118
C.1.4	Beam 1.4.....	119
C.1.4.1	Beam 1.4 Materials.....	119
C.1.4.2	Beam 1.4 Important Dates .....	120
C.1.4.3	Beam 1.4 Stressing History .....	120
C.1.4.4	Beam 1.4 Comments.....	122
C.1.5	Beam 2.1.....	122
C.1.5.1	Beam 2.1 Materials.....	122
C.1.5.2	Beam 2.1 Important Dates .....	122
C.1.5.3	Beam 2.1 Stressing History .....	123
C.1.5.4	Beam 2.1 Comments.....	123
C.1.6	Beam 2.2.....	123
C.1.6.1	Beam 2.2 Materials.....	123
C.1.6.2	Beam 2.2 Important Dates .....	123
C.1.6.3	Beam 2.2 Stressing History .....	124
C.1.6.4	Beam 2.2 Comments.....	125
C.1.7	Beam 2.3.....	126
C.1.7.1	Beam 2.3 Materials.....	126
C.1.7.2	Beam 2.3 Important Dates .....	126
C.1.7.3	Beam 2.3 Stressing History .....	127
C.1.7.4	Beam 2.3 Comments.....	128
C.1.8	Beam 2.4.....	129
C.1.8.1	Beam 2.4 Materials.....	129
C.1.8.2	Beam 2.4 Important Dates .....	129
C.1.8.3	Beam 2.4 Stressing History .....	130
C.1.8.4	Beam 2.4 Comments.....	131
C.1.9	Beam 3.1.....	133
C.1.9.1	Beam 2.1 Materials.....	133
C.1.9.2	Beam 2.1 Important Dates .....	133
C.1.9.3	Beam 2.1 Stressing History .....	134
C.1.9.4	Beam 3.1 Comments.....	135

C.1.10	Beam 3.2.....	136
C.1.10.1	Beam 3.2 Materials.....	136
C.1.10.2	Beam 3.2 Important Dates.....	136
C.1.10.3	Beam 3.2 Stressing History.....	137
C.1.10.4	Beam 3.2 Comments.....	139
C.1.11	Beam 3.3.....	139
C.1.11.1	Beam 3.3 Materials.....	139
C.1.11.2	Beam 3.3 Important Dates.....	139
C.1.11.3	Beam 3.3 Stressing History.....	140
C.1.11.4	Beam 3.3 Comments.....	141
C.1.12	Beam 3.4.....	142
C.1.12.1	Beam 3.4 Materials.....	142
C.1.12.2	Beam 3.4 Important Dates.....	143
C.1.12.3	Beam 3.4 Stressing History.....	143
C.1.12.4	Beam 3.4 Comments.....	145
C.1.13	Beam 4.1.....	145
C.1.13.1	Beam 4.1 Materials.....	145
C.1.13.2	Beam 4.1 Important Dates.....	146
C.1.13.3	Beam 4.1 Stressing History.....	146
C.1.13.4	Beam 4.1 Comments.....	148
C.1.14	Beam 4.2.....	149
C.1.14.1	Beam 4.2 Materials.....	149
C.1.14.2	Beam 4.2 Important Dates.....	149
C.1.14.3	Beam 4.2 Stressing History.....	150
C.1.14.4	Beam 4.2 Comments.....	151
C.1.15	Beam 4.3.....	152
C.1.15.1	Beam 4.3 Materials.....	152
C.1.15.2	Beam 4.3 Important Dates.....	153
C.1.15.3	Beam 4.3 Stressing History.....	153
C.1.15.4	Beam 4.3 Comments.....	155
C.1.16	Beam 4.4.....	155
C.1.16.1	Beam 4.4 Materials.....	155
C.1.16.2	Beam 4.4 Important Dates.....	156
C.1.16.3	Beam 4.4 Stressing History.....	156
C.1.16.4	Beam 4.4 Comments.....	158
C.1.17	Beam 5.1.....	158
C.1.17.1	Beam 5.1 Materials.....	158

C.1.17.2	Beam 5.1 Important Dates .....	158
C.1.17.3	Beam 5.1 Stressing History .....	159
C.1.17.4	Beam 5.1 Comments.....	160
C.1.18	Beam 5.2.....	161
C.1.18.1	Beam 5.2 Materials.....	161
C.1.18.2	Beam 5.2 Important Dates .....	161
C.1.18.3	Beam 5.2 Stressing History .....	162
C.1.18.4	Beam 5.2 Comments.....	163
C.1.19	Beam 5.3.....	164
C.1.19.1	Beam 5.3 Materials.....	164
C.1.19.2	Beam 5.3 Important Dates .....	165
C.1.19.3	Beam 5.3 Stressing History .....	165
C.1.19.4	Beam 5.3 Comments.....	167
C.1.20	Beam 6.1 .....	168
C.1.20.1	Beam 6.1 Materials.....	168
C.1.20.2	Beam 6.1 Important Dates .....	168
C.1.20.3	Beam 6.1 Stressing History .....	168
C.1.20.4	Beam 6.1 Comments.....	168
C.1.21	Beam 6.2.....	169
C.1.21.1	Beam 6.2 Materials.....	169
C.1.21.2	Beam 6.2 Important Dates .....	169
C.1.21.3	Beam 6.2 Stressing History .....	169
C.1.21.4	Beam 6.2 Comments.....	169
C.1.22	Beam 6.3.....	170
C.1.22.1	Beam 6.3 Materials.....	170
C.1.22.2	Beam 6.3 Important Dates .....	170
C.1.22.3	Beam 6.3 Stressing History .....	170
C.1.22.4	Beam 6.3 Comments.....	170
C.1.23	Beam 7.1 .....	171
C.1.23.1	Beam 7.1 Materials.....	171
C.1.23.2	Beam 7.1 Important Dates .....	171
C.1.23.3	Beam 7.1 Stressing History .....	171
C.1.23.4	Beam 7.1 Comments.....	172
Beam 7.2.....		172
C.1.23.5	Beam 7.2 Materials.....	172
C.1.23.6	Beam 7.2 Important Dates .....	172
C.1.23.7	Beam 7.2 Stressing History .....	173

C.1.23.8	Beam 7.2 Comments.....	173
C.1.24	Beam 7.3.....	173
C.1.24.1	Beam 7.3 Materials.....	173
C.1.24.2	Beam 7.3 Important Dates.....	173
C.1.24.3	Beam 7.3 Stressing History.....	174
C.1.24.4	Beam 7.3 Comments.....	174
C.1.25	Beam 7.4.....	174
C.1.25.1	Beam 7.4 Materials.....	174
C.1.25.2	Beam 7.4 Important Dates.....	175
C.1.25.3	Beam 7.4 Stressing History.....	175
C.1.25.4	Beam 7.4 Comments.....	175
<b>REFERENCES.....</b>		<b>176</b>
<b>VITA.....</b>		<b>180</b>

## List of Tables

Table 2.1: Final Specimen Matrix.....	24
Table 2.2: Industry Standard vs. EIT Systems .....	39
Table 5.1: Interpretation of Half-Cell Potentials for Uncoated Reinforcing Steel.....	81
Table 6.1: Specimen Catalog (1 of 2) .....	84
Table 6.2: Specimen Catalog (2 of 2) .....	85
Table 6.3: Sorted Test Specimen Information .....	86
Table 6.4: Beam 1.1 Materials .....	89
Table 6.5: Beam 1.1 Important Dates .....	89
Table 6.6: Beam 2.2 Materials .....	92
Table 6.7: Beam 2.2 Important Dates .....	92
Table A.1: Material Acquisition Summary .....	101
Table A.2: Post-Tensioning Durability Workshop Invitation List (Ferguson Structural Engineering Lab – April 14-15, 2003) .....	102
Table C.1: Beam 1.1 Materials.....	110
Table C.2: Beam 1.1 Important Dates.....	110
Table C.3: Beam 1.2 Materials.....	113
Table C.4: Beam 1.2 Important Dates.....	113
Table C.5: Beam 1.3 Materials.....	116
Table C.6: Beam 1.3 Important Dates.....	116
Table C.7: Beam 1.4 Materials.....	119
Table C.8: Beam 1.4 Important Dates.....	120
Table C.9: Beam 2.1 Materials.....	122
Table C.10: Beam 2.1 Important Dates.....	122
Table C.11: Beam 2.2 Materials.....	123
Table C.12: Beam 2.2 Important Dates.....	123
Table C.13: Beam 2.3 Materials.....	126
Table C.14: Beam 2.3 Important Dates.....	126
Table C.15: Beam 2.4 Materials.....	129

Table C.16: Beam 2.4 Important Dates.....	129
Table C.17: Beam 3.1 Materials.....	133
Table C.18: Beam 3.1 Important Dates.....	133
Table C.19: Beam 3.2 Materials.....	136
Table C.20: Beam 3.2 Important Dates.....	136
Table C.21: Beam 3.3 Materials.....	139
Table C.22: Beam 3.3 Important Dates.....	139
Table C.23: Beam 3.4 Materials.....	142
Table C.24: Beam 3.4 Important Dates.....	143
Table C.25: Beam 4.1 Materials.....	145
Table C.26: Beam 4.1 Important Dates.....	146
Table C.27: Beam 4.2 Materials.....	149
Table C.28: Beam 4.2 Important Dates.....	149
Table C.29: Beam 4.3 Materials.....	152
Table C.30: Beam 4.3 Important Dates.....	153
Table C.31: Beam 4.4 Materials.....	155
Table C.32: Beam 4.4 Important Dates.....	156
Table C.33: Beam 5.1 Materials.....	158
Table C.34: Beam 5.1 Important Dates.....	158
Table C.35: Beam 5.2 Materials.....	161
Table C.36: Beam 5.2 Important Dates.....	161
Table C.37: Beam 5.3 Materials.....	164
Table C.38: Beam 5.3 Important Dates.....	165
Table C.39: Beam 6.1 Materials.....	168
Table C.40: Beam 6.1 Important Dates.....	168
Table C.41: Beam 6.2 Materials.....	169
Table C.42: Beam 6.2 Important Dates.....	169
Table C.43: Beam 6.3 Materials.....	170
Table C.44: Beam 6.3 Important Dates.....	170
Table C.45: Beam 7.1 Materials.....	171
Table C.46: Beam 7.1 Important Dates.....	171
Table C.47: Beam 7.2 Materials.....	172
Table C.48: Beam 7.2 Important Dates.....	172
Table C.49: Beam 7.3 Materials.....	173
Table C.50: Beam 7.3 Important Dates.....	173
Table C.51: Beam 7.4 Materials.....	174
Table C.52: Beam 7.4 Important Dates.....	175



## List of Figures

Figure 1.1: Surface Area of Bars and Strands .....	5
Figure 1.2: Passive-Active Behavior in Steel (Schokker 1999).....	7
Figure 1.3: Corrosion of Steel in Concrete (Schokker 1999).....	7
Figure 1.4: Point of View 1 – Increased Penetration of Moisture and Chlorides at Crack Location Accelerates the Onset and Severity of Corrosion (West 1999).....	9
Figure 1.5: Point of View 2: Cracking Accelerates Onset of Corrosion, But Over Time Corrosion is Similar in Cracked and Uncracked Concrete (West 1999).....	9
Figure 1.6: Plan View of Slipped Tendon at Deviation Saddle Niles Channel Bridge (FLDOT 2002) .....	14
Figure 1.7: Advanced Corrosion of Strands within Anchorage Niles Channel Bridge (FLDOT 2002) .....	14
Figure 1.8: The Mid-Bay Bridge, Florida (FLDOT 2002).....	15
Figure 1.9: Failure of Tendon 28-6 on the Mid-Bay Bridge (FLDOT 2002) .....	15
Figure 1.10: Failure of Tendon 57-1 on the Mid-Bay Bridge at Expansion Joint Diaphragm (FLDOT 2002).....	16
Figure 1.11: The Sunshine Skyway Bridge, Tampa, Florida (FLDOT 2002) .....	16
Figure 1.12: Tendon Corrosion inside the Sunshine Skyway Bridge Piers (FLDOT 2002) .....	17
Figure 2.1: Corroded Galvanized Steel Duct (Breen and Kreger 2003) .....	20
Figure 2.2: 0.5” Conventional Strand.....	25
Figure 2.3: 0.5” Hot Dip Galvanized Strand.....	26
Figure 2.4: 0.6” Stainless Steel Strand.....	28
Figure 2.5: 0.5” Copper Clad Strand.....	29
Figure 2.6: 0.6” Stainless Clad Strand .....	30
Figure 2.7: Unfilled (left) vs. Filled (right) Epoxy Coated Strand Cross Sections .....	31
Figure 2.8: 0.5” Flow Filled, Epoxy Coated Strand.....	32
Figure 2.9: GTI Plastic Ducts.....	34
Figure 2.10: GTI Slip-On Couplers with Heat Shrink Sleeves .....	35
Figure 2.11: GTI 76mm Plastic Duct Snap-On Coupler .....	35

Figure 2.12: VSL PT-Plus Plastic Duct .....	36
Figure 2.13: VSL PT-Plus Plastic Duct Coupler.....	37
Figure 2.14: Galvanized Steel Duct .....	37
Figure 2.15: Non-Galvanized (Left) and Galvanized (Right) VSL EC5-7 Bearing Plates.....	38
Figure 2.16: Conventional System Detail (FIB Commission 5) .....	40
Figure 2.17: Electrically Isolated Tendon System Detail (FIB Commission 5) ..	40
Figure 2.18: VSL Electrically Isolated Tendon Materials .....	41
Figure 3.1: Project 1405 Research Specimen.....	43
Figure 3.2: Project 4562 Research Specimen.....	45
Figure 3.3: External and Internal Forces .....	46
Figure 4.1: Research Specimen Profile .....	53
Figure 4.2: End Walls, Dead (left) and Live (right).....	53
Figure 4.3: Assembled Forms .....	54
Figure 4.4: Completed Passive Reinforcement Cage.....	55
Figure 4.5: Grout Vent Connection Detail .....	57
Figure 4.6: Seating Loss Experiment Setup.....	61
Figure 4.7: Stressing Sequence (Live End Shown).....	62
Figure 4.8: Prestressing Setup.....	64
Figure 4.9: Dywidag Assembly, Live End (Left) and Dead End (Right) .....	66
Figure 4.10: Data Acquisition Hardware .....	68
Figure 4.11: Data Acquisition Equipment.....	68
Figure 4.12: Grouting Procedure.....	69
Figure 4.13: Grouting Specimens (Kyle Steuck pictured) .....	70
Figure 4.14: Temporary Grouting Caps .....	71
Figure 4.15: Pour Back Process .....	72
Figure 5.1: General Beam Location by Aerial Photo (Terraserver).....	73
Figure 5.2: Non-Anchorage Exposure Specimens .....	74
Figure 5.3: Anchorage Exposure Specimens .....	75
Figure 5.4: Saltwater Exposure Detail .....	78
Figure 5.5: Half-Cell Potential Reading Schematic .....	80
Figure 5.6: Half-Cell Potential Reading Sampling Grid .....	80
Figure 5.7: EIT Monitoring Connections Detail .....	82

Figure 6.1: Specimen Labeling System.....	87
Figure 6.2: Characteristic Load-Deformation Plot.....	88
Figure 6.3: Beam 1.1 Live Load Application Plot .....	90
Figure 6.4: Beam 1.1 Crack Map .....	91
Figure 6.5: Beam 2.2 Live Load Application Plot .....	93
Figure 6.6: Beam 2.2 Crack Map .....	94
Figure 7.1: New Specimens (Foreground) and Previous Specimens (Background) in Service at the North End of Ferguson.....	96
Figure 7.2: Corbel Design Planes.....	98
Figure 7.3: PSU Strand Accelerated Corrosion Test Specimen (Salcedo 2003) 100	
Figure B.1: Mild Reinforcement Cage Details.....	104
Figure B.2: Ends and Midsection Details.....	104
Figure B.3: Rebar Dimensions (1 of 3) .....	105
Figure B.4: Rebar Dimensions (2 of 3).....	106
Figure B.5: Rebar Dimensions (3 of 3) .....	107
Figure B.6: Bend 5 Detail .....	108
Figure C.1: Beam 1.1 Live Load Application Plot .....	111
Figure C.2: Beam 1.1 Crack Map .....	112
Figure C.3: Beam 1.2 Live Load Application Plot .....	114
Figure C.4: Beam 1.2 Crack Map .....	115
Figure C.5: Beam 1.3 Live Load Application Plot .....	117
Figure C.6: Beam 1.3 Crack Map .....	118
Figure C.7: Beam 1.4 Live Load Application Plot .....	120
Figure C.8: Beam 1.4 Crack Map .....	121
Figure C.9: Beam 2.2 Live Load Application Plot .....	124
Figure C.10: Beam 2.2 Crack Map .....	125
Figure C.11: Beam 2.3 Live Load Application Plot .....	127
Figure C.12: Beam 2.3 Crack Map .....	128
Figure C.13: Beam 2.4 Live Load Application Plot .....	130
Figure C.14: Beam 2.4 Crack Map .....	131
Figure C.15: Beam 3.1 Live Load Application Plot .....	134
Figure C.16: Beam 3.1 Crack Map .....	135
Figure C.17: Beam 3.2 Live Load Application Plot .....	137

Figure C.18: Beam 3.2 Crack Map .....	138
Figure C.19: Beam 3.3 Live Load Application Plot .....	140
Figure C.20: Beam 3.3 Crack Map .....	141
Figure C.21: Beam 3.4 Live Load Application Plot .....	143
Figure C.22: Beam 3.4 Crack Map .....	144
Figure C.23: Beam 4.1 Live Load Application Plot .....	146
Figure C.24: Beam 4.1 Crack Map .....	147
Figure C.25: Beam 4.2 Live Load Application Plot .....	150
Figure C.26: Beam 4.2 Crack Map .....	151
Figure C.27: Beam 4.3 Live Load Application Plot .....	153
Figure C.28: Beam 4.3 Crack Map .....	154
Figure C.29: Beam 4.4 Live Load Application Plot .....	156
Figure C.30: Beam 4.4 Crack Map .....	157
Figure C.31: Beam 5.1 Live Load Application Plot .....	159
Figure C.32: Beam 5.1 Crack Map .....	160
Figure C.33: Beam 5.2 Live Load Application Plot .....	162
Figure C.34: Beam 5.2 Crack Map .....	163
Figure C.35: Beam 5.3 Live Load Application Plot .....	165
Figure C.36: Beam 5.3 Crack Map .....	167

# **CHAPTER 1**

## **Introduction**

### **1.1 PROBLEM STATEMENT**

Post-tensioning has many potential benefits including crack control, smaller and irregular cross sections, and the possibility of rapid construction with minimal traffic interference when combined with precast members. Although post-tensioning is not a new form of construction, it is being improved with the introduction of new construction practices and materials. Before these developments are implemented, it is important to consider the durability of the post-tensioning system and overall structure. In particular, chloride-induced corrosion from a marine environment or deicing salts is a very real concern for all types of bridges. Research in this area for post-tensioned bridges is limited in part due to the long-term nature of durability studies (Schokker 1999).

The development of new post-tensioning materials and systems in recent years has made some of the durability research in this area obsolete. The current research focuses on evaluating the corrosion resistance performance of state-of-the-art, as well as potential, post-tensioning materials and construction practices. The experimental program includes both long-term exposure tests and electrically accelerated corrosion tests.

### **1.2 BACKGROUND**

#### **1.2.1 Post-Tensioning**

Concrete is strong in compression, but weak in tension. Therefore it will crack in tension well before crushing in compression. To supplement the

relatively low tensile strength of concrete, steel is embedded in concrete to transfer tensile loads and control concrete cracking. The concrete and steel composite is reinforced concrete.

Prestressed concrete is a form of reinforced concrete in which high-strength steel reinforcement in the form of bars, wires or strands has been tensioned against the concrete. This tensioning, or stressing, operation results in a self-equilibrating system of internal stresses (tensile stresses in steel and compressive stresses in the concrete) which improves the response of the concrete to external loads (Collins and Mitchell). In order for prestressed concrete to crack, the tensile stresses must overcome not only the tensile capacity of the concrete, but the precompression of the concrete due to the prestressed steel as well. The ability of prestressed concrete to minimize or eliminate cracking and control deflections allow for smaller concrete members than if using non-prestressed concrete.

There are two forms of prestressed concrete – pretensioned and post-tensioned. In pretensioned concrete, the prestressing steel is stressed before placing the concrete. Once the concrete reaches sufficient strength, the strands are released and the steel tensile force is transferred to the concrete. The tensile force is sustained by the bond between the prestressing steel and the surrounding concrete. The steel tensile stresses are internally equilibrated by compressive stresses in the concrete and the concrete member is prestressed.

In post-tensioned concrete, the prestressing steel is placed within ducts and is stressed after the concrete has been placed and gains sufficient strength. The steel tensile force is sustained by anchorages at the end of the prestressing steel. There are two types of post-tensioning – external and internal – depending on whether the prestressing steel is inside or outside the concrete cross-section. The void for placing internal prestressing steel in hardened concrete is created

with duct placed in the section before casting concrete. Internal tendons (complete post-tensioning assemblies) are classified as either bonded or unbonded. For bonded tendons, the ducts are filled with high-strength cementitious grout in order to bond the prestressing steel to the surrounding concrete along the entire length of the tendon. Unbonded tendons are only attached to the surrounding concrete at the anchorages. External tendons, regardless of the presence of grout, are always considered to be unbonded.

### **1.2.2 Post-Tensioning Corrosion**

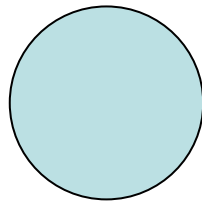
Post-tensioned concrete has several corrosion protection advantages over non-prestressed concrete, but there are also inherent drawbacks. Some of the potential corrosion protection disadvantages for post-tensioned concrete can be eliminated with proper design and construction. Several important points of post-tensioning corrosion are included in this section, but a detailed review is given in Chapter 2 in West (1999).

As discussed in Section 1.2.1, one of the benefits of prestressed concrete is the mitigation or elimination of cracks. By controlling cracking, the direct access of chlorides and oxygen to the post-tensioning hardware may be limited. Therefore, the concrete will be a more effective layer of corrosion protection. In traditional reinforced concrete, the concrete is the only layer of corrosion protection. In special cases, an additional layer is provided by bar coatings such as epoxy or zinc. Post-tensioned concrete corrosive performance benefits from multiple layers of corrosion protection for the prestressing strand – concrete, duct, grout and any strand coatings. Proper grouting of the post-tensioning ducts is necessary for corrosion protection and bond transfer, but complete grouting can be difficult due to the lack of visibility and access to all parts of the duct (Schokker 1999).

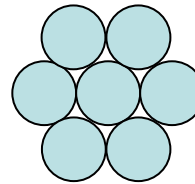
The consequences of prestressing steel corrosion are potentially more severe than corrosion of mild steel reinforcement (West 1999). This is primarily due to the higher strength of the prestressing steels, and the high level of stress in the steel. Prestressing steels normally experience stress levels in service on the order of 70% to 80% of their tensile strength. This percentage is much lower in mild steel reinforcement. Due to the lower stress levels, the loss of cross-sectional area due to corrosion is less likely to lead to tensile failure of mild steel reinforcing bars. The higher strength of prestressing steel also means that there is less steel area in the member cross-section. As a result, the loss of one prestressing strand or bar will have a more significant effect on the capacity of the member than the loss of an equivalent sized mild steel bar.

Prestressing steels are generally believed to be more susceptible to corrosion than mild steel reinforcement for several reasons. In the case of 7-wire prestressing strands, the surface area to volume ratio is larger than for the equivalent diameter bar, as illustrated in Figure 1.1. This means that more surface area is available for corrosion, and the cross-sectional area of the strand may be reduced at a faster rate. The configuration of the 7-wire prestressing strand also makes the strand more susceptible to crevice corrosion. This is a type of severe corrosion occurring in small spaces or crevices, such as the interstices between wires. The geometric constraints of the crevice enhance the formation of chloride ion concentration cells. Once corrosion has initiated, it progresses similar to pitting corrosion. Due to the geometry of the crevice,  $\text{Fe}^{2+}$  ions can not disperse easily, and chloride ions are drawn into the crevice by the positive charge accumulation. The process becomes autocatalytic as the presence of chloride ions leads to formation of hydrochloric acid (HCl) and higher corrosion rates ensue (West 1999).





**0.5" Diam. Bar (#4 Bar)**



**0.5" Diam. 7-Wire Strand**

*Surface Area Per Foot Length:*

**18.9 in<sup>2</sup>**

**44.0 in<sup>2</sup>**

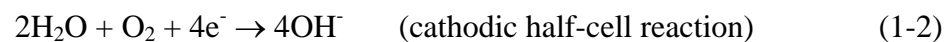
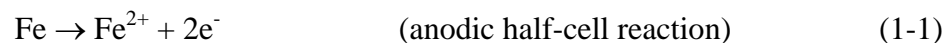
*∴ Surface Area of 0.5" Diam. 7-Wire Strand is 2.33 Times  
the Surface Area of 0.5" Diam. Bar of the Same Length*

***Figure 1.1: Surface Area of Bars and Strands***

High strength prestressing steel is also more prone to other forms of corrosion related deterioration that do not occur in mild steel reinforcement. This includes stress corrosion cracking, hydrogen embrittlement, fretting fatigue and corrosion fatigue. These types of deterioration mechanisms are very difficult to detect, and can lead to brittle failure with little or no sign of warning.

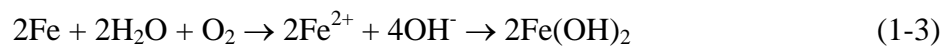
### **1.2.3 Electrochemistry**

Before considering the corrosion of prestressing steel in concrete, a general corrosion theory for metals must be understood (Schokker 1999). Corrosion of iron is an electrochemical process governed by Equations 1-1 and 1-2, commonly known as half-cell reactions:

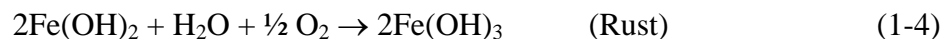


The anode (where electrochemical oxidation takes place) and the cathode (where reduction takes place) form on the metal surface. Iron is oxidized into ferrous ions at the anode as shown in Equation 1-1. The ferrous ions are

converted to Fe(OH)<sub>3</sub> (commonly known as rust) through a number of reactions. A summary of rust formation is shown in Equations 1-3 and 1-4 (Jones).



which can further react to give:



The anodic and cathodic areas are regions of different electrochemical potential that develop due to contact of two different metals (which therefore have different potentials) or a single metal with surface differences (metallurgical or local variations in electrolyte) (Rosenberg). The anode and cathode locations can change often and have an irregular pattern leading to a somewhat uniform corrosion or the locations can be more fixed and localized.

#### Passivity

Steel is an active-passive metal, and therefore its corrosion rate depends on potential as shown in Figure 1.2. Under typical conditions, steel in concrete is in a passive state and a passive protective film is found on the steel surface. Chlorides (and lowered pH) in the surrounding concrete have been shown to cause a breakdown of the passive film at potentials that should be well within the passive region (Fontana).

#### Corrosion of Steel in Concrete

In the case of corrosion of steel in concrete, the anodes and cathodes are formed on the steel surface with the cement paste pore solution acting as an electrolyte. Figure 1.3 shows the basic corrosion process for steel in concrete. The rust product occupies a much larger volume than the products that go into its formation which can cause splitting tensile stresses in the concrete.

A detailed review of the corrosion process and different forms of corrosion are included in Chapter 2 in West.

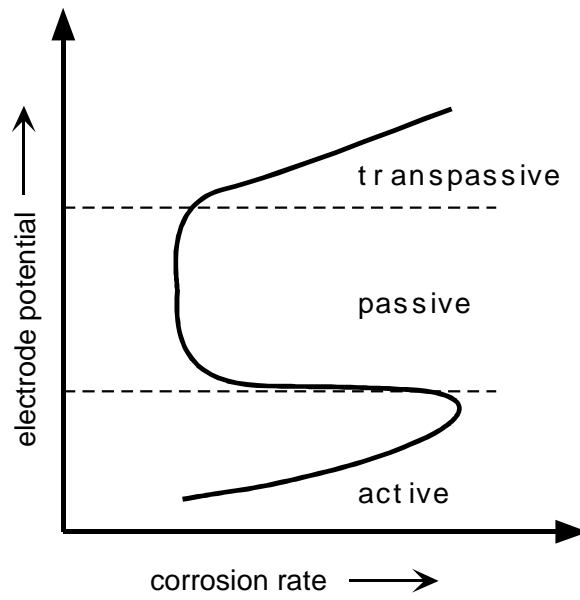


**Figure 1.2: Passive-Active Behavior in Steel (Schokker 1999)**

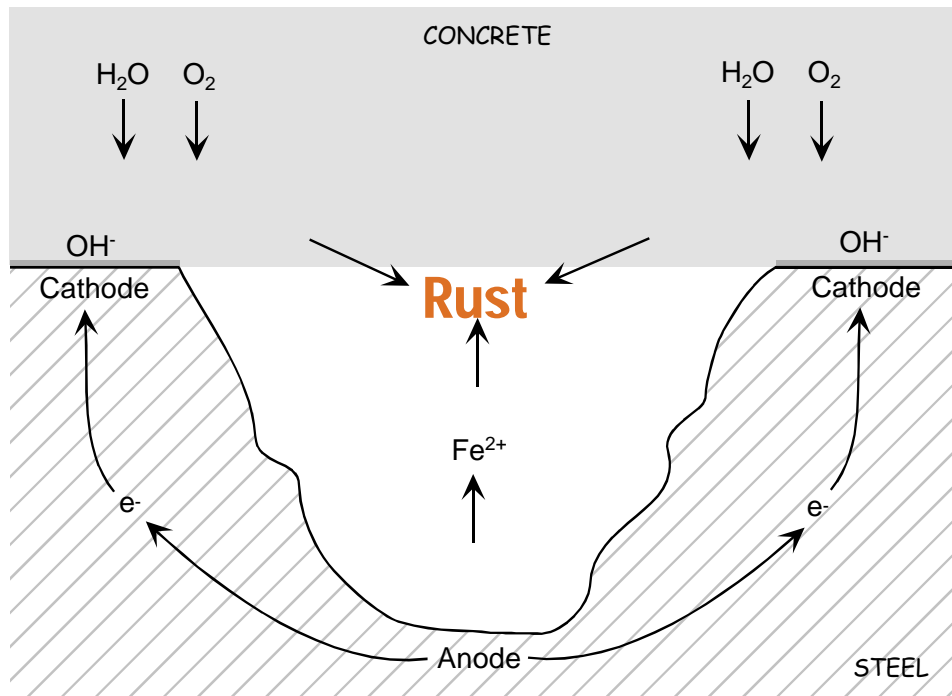


**Figure 1.3: Corrosion of Steel in Concrete (Schokker 1999)**

#### 1.2.4 Influence of Cracking

The influence of cracking and crack widths on the corrosion of steel reinforcement in concrete members is a subject that has received much debate (West 1999). In the past, considerable research and discussion has been devoted to this topic without arriving at a general consensus. In general, two points of view exist (ACI Committee 222 1996):

- 1.) Cracks reduce the service life of the structure by permitting a more rapid means of access for moisture, chloride ions and oxygen to reach the reinforcement, thus accelerating the onset of corrosion (i.e., cracking has a significant effect on corrosion).
- 2.) Cracks may accelerate the onset of corrosion, but such corrosion will be localized to the region of the crack. It is suggested that over time, chloride ions will eventually penetrate even uncracked concrete, initiating more widespread corrosion. Thus, after a long service life, the difference between the amount of corrosion in cracked and uncracked concrete will be minor (i.e., cracking does not have a significant effect on corrosion).

The two points of view are illustrated in Figures 1.4 and 1.5. Both points of view indicate that the presence of cracks will accelerate the onset of corrosion. The first point of view suggests that the accelerated onset of corrosion will lead to more corrosion damage in a shorter period, and thus reduce the service life of the structure. The second point of view suggests that the corrosion rate in uncracked concrete will reach the corrosion rate at the crack locations after some duration. This point of view implies that the length of time between corrosion initiation at a crack,  $t_i$ , and corrosion initiation in uncracked concrete,  $t_{icr}$ , is not significant. This means that the two curves in Figure 1.5 are close together when the entire service life is considered, and thus the early onset of corrosion at cracks has little

effect on the service life in comparison to the case where the concrete was entirely uncracked.

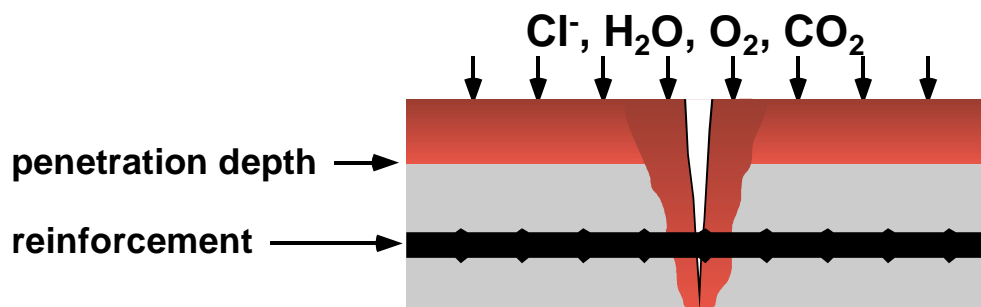


*Figure 1.4: Point of View 1 – Increased Penetration of Moisture and Chlorides at Crack Location Accelerates the Onset and Severity of Corrosion (West 1999)*

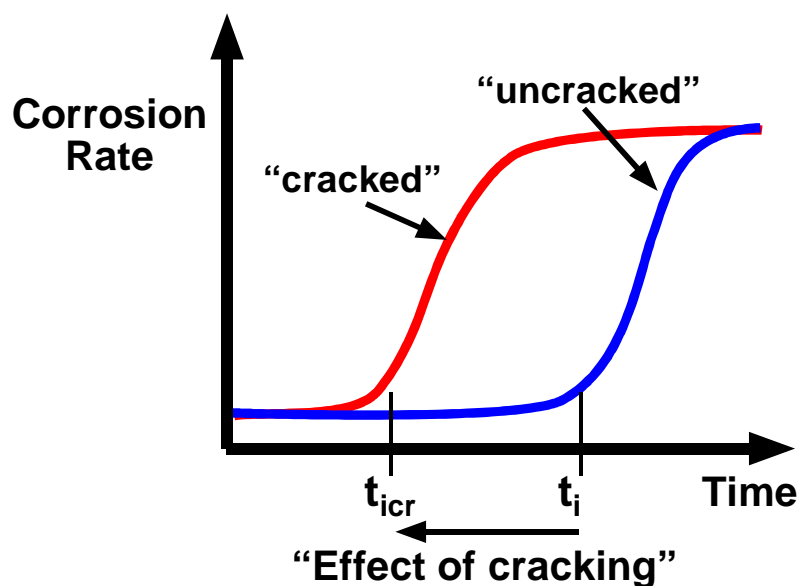


*Figure 1.5: Point of View 2: Cracking Accelerates Onset of Corrosion, But Over Time Corrosion is Similar in Cracked and Uncracked Concrete (West 1999)*

The opinions presented in the preceding paragraph are primarily based on past research and experience related to corrosion in reinforced concrete before the development of modern high performance, low permeability concrete. Much of

this research (West 1999) and experience has focused on relating crack width to corrosion, and trying to determine whether there is a critical crack width (i.e., a crack width below which corrosion will not occur or is negligible) for corrosion.

Either or both of these opinions are normally reflected in design code provisions for crack control. While there are other important reasons for crack control in concrete structures, the concern for corrosion is often prevalent. Code provisions and design recommendations normally recognize different exposure conditions and assign crack control requirements that become more strict as the exposure becomes more severe.

Refer to Chapter 1 in West (1999) for a more detailed review of the effects of concrete cracking on steel reinforcement corrosion.

### **1.2.5 Previous Testing**

Previous post-tensioning durability research at Ferguson Structural Engineering Lab (FSEL) focused on the corrosion resistance performance of several critical facets of post-tensioned concrete:

- combinations of prestressing and mild reinforcement
- types of duct and applicable duct splices
- types of grout used to bond and protect prestressing strand
- construction joints between precast segments
- construction joints between precast columns and foundations

Both the previous and current research projects were supervised by Dr. John Breen. The research was conducted by Salas, Schokker and West with the assistance of several graduate students and undergraduate research assistants. The dissertations of Salas (2003), Schokker (1999) and West (1999) are referenced throughout this thesis, especially in the project background information in Chapter 1.

During the design of the current experiment, efforts were made to provide continuity between the previous and current post-tensioning durability research projects in order to compare future results. The various considerations to connect the data of the two research projects are included throughout the thesis: design (Chapter 3), construction (Chapter 4) and exposure and monitoring (Chapter 5).

### **1.2.6 Field Experience with Post-Tensioning Corrosion**

Out of the total number of bridges in the USA, approximately 20% are prestressed concrete bridges (Salas 2003); only 3% of these were classified, in 1998, as structural deficient (bridges that can no longer sustain the loads for which they were designed) (Yunovich 2003).

A comprehensive survey performed in 1999 by the American Segmental Bridge Institute (ASBI) found that concrete segmental bridges were performing well with time. Based on inspection reports using Federal Highway Administration (FHWA) guidelines, all segmental bridges were rated as “fair” or better. Of the 131 bridges, 99 percent had superstructure ratings of “satisfactory” or better, 79 percent had superstructure ratings of “good” or better, and 31 percent had superstructure ratings of “very good” or better (Miller 2000).

The first segmental bridge constructed in the US, in 1971, the John F. Kennedy Memorial Causeway near Corpus Christi, Texas, was inspected extensively in a Federal Highway Administration study in 1988, and no indications of distress or corrosion of the prestressing tendons were found (West 1999). This bridge was constructed using match-cast epoxy joints, as required by designers, considering the hot, humid, seawater environment of the Gulf of Mexico.

Recently, some tendon failures and corrosion related problems have come to light, especially in the state of Florida (Freyermuth 2001 and FLDOT 2002). In

1999, one of the external tendons in the Niles Channel Bridge built in 1983, failed due to corrosion at an expansion joint. A 9-inch movement of the tendon through one of the deviation saddles was noticed first. When the tendon was removed for replacement, a void in the grout and heavy pitting in the prestressing strands inside the anchor head were found (see Figures 1.6 and 1.7). In 2000, eleven tendons out of a total of 846 were replaced in the Mid-Bay Bridge built in 1993. Ten of the eleven tendons that were replaced were located at expansion joints (see Figures 1.8, 1.9 and 1.10). Also, in 2000, several corroded tendons were discovered in segmental piers of the Sunshine Skyway Bridge, built in 1986, where the corrosion resulted from seawater in ducts, permeable concrete anchorage protection at the top of piers and splitting of polyethylene ducts (Freyermuth 2001) (see Figures 1.11 and 1.12).

In addition to the figures below, inspections in Florida bridges have revealed a large number of bleed water voids at anchorages, partially grouted tendons and ungrouted tendons, the same type of problems that were found in the Sidney Lanier Cable Stayed Bridge in Georgia and in the Boston Central Artery bridges (Freyermuth 2001).

Freyermuth (2001) has indicated that the major portion of the bridge tendon corrosion problems that have been observed in the U.S. have been identified with the following:

- An aggressive environment (northeast U.S. and Florida)
- Areas with a low volume of post-tensioned construction
- Contractors with no experience or expertise in post-tensioned construction
- Grossly inadequate construction supervision
- Design details without adequate provision for corrosion protection of tendons
- Failures to respond to or correct construction problems



In particular, after analyzing the problems encountered in bridges located in the state of Florida, it appears that the tendon corrosion problems were due to:

- Voids associated with accumulation of bleed water at tendon anchorages
- Recharge of ungrouted tendon anchorages with salt water or surface drainage during construction.
- Leakage through end anchorage protection details
- Quality of the grout installation and grout materials
- Splitting of polyethylene ducts
- Deficiencies in implementation and inspection of grouting procedures.

The findings in Florida have led to some immediate recommendations, with respect to the use of bonded post-tensioning systems (Theryo 2002):

- No precast concrete hollow column section should be specified below the waterline.
- No PT tendons should be located in columns below the highest water splash zone elevation.
- Grouting operation for vertical tendons should be carefully planned, tested and monitored. Stage and vacuum grouting should be specified in the upper section of tendons in combination with a pressurized sealed PT system and zero bleed grout.
- Provide multiple levels of protection at anchorages, including permanent grout cap, epoxy material pour-back and polymer coating over the pour-back.



*Figure 1.6: Plan View of Slipped Tendon at Deviation Saddle Niles Channel Bridge (FLDOT 2002)*

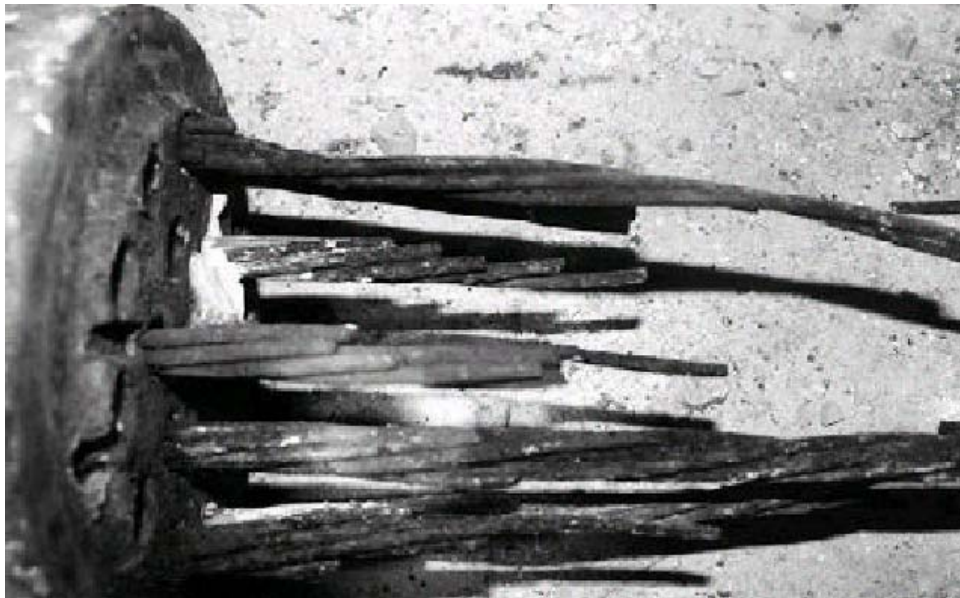


*Figure 1.7: Advanced Corrosion of Strands within Anchorage Niles Channel Bridge (FLDOT 2002)*



*Figure 1.8: The Mid-Bay Bridge, Florida (FLDOT 2002)*



*Figure 1.9: Failure of Tendon 28-6 on the Mid-Bay Bridge (FLDOT 2002)*



*Figure 1.10: Failure of Tendon 57-1 on the Mid-Bay Bridge at Expansion Joint Diaphragm (FLDOT 2002)*



*Figure 1.11: The Sunshine Skyway Bridge, Tampa, Florida (FLDOT 2002)*





***Figure 1.12: Tendon Corrosion inside the Sunshine Skyway Bridge Piers  
(FLDOT 2002)***

- PT redundancy system or practical replacement capabilities should be incorporated.
- The impact of construction methods on the corrosion vulnerability of PT system should be thoroughly analyzed and designed for, especially for critical elements in aggressive corrosive environments.
- Corrosion detection methods should be included during the construction and service life of the structure.

In spite of the above, and as mentioned by Freyermuth, the durability performance of prestressed and segmental post-tensioned bridges has been superior to all other types of construction. Recent improvements in grouting materials technology (anti-bleed, thixotropic grouts), and training programs for grouting supervisors and inspectors are expected to yield significant results, reducing the incidence of corrosion problems in grouted tendons.

### **1.3 PROJECT OBJECTIVE**

The objective of Project 4562, Phase II is to evaluate the corrosive resistance performance of recent and upcoming commercially available post-tensioning products. The materials were identified by meeting with post-tensioning industry representatives regarding the upcoming durability research. The initial project meeting occurred at Ferguson Lab in April 2003 – a list of attendees is included in Appendix A. In addition to meeting with industry, post-tensioning materials were also selected and researched during the literature review process.

### **1.4 THESIS OBJECTIVES AND ORGANIZATION**

The overall objective of the thesis is to document the initial portion of Project 4562, Phase II. Towards the broad thesis purpose, there are several specific thesis objectives:

- To introduce the basis of the research project, explain project background information and provide thesis overview (Chapter 1)
- To list and describe all post-tensioning materials to be evaluated for corrosion performance (Chapter 2)
- To explain the design goals and methods of the research specimens (Chapter 3)

- To document and depict construction practices utilized during the production of research specimens (Chapter 4)
- To describe exposure and monitoring techniques (Chapter 5)
- To catalog information pertaining to individual specimens such as content, procedural dates, etc. (Chapter 6)
- To provide conclusions for the initial portion of Project 4562, Phase II and recommendations for continued research (Chapter 7)

## CHAPTER 2

### Improved Post-Tensioning Systems

#### 2.1 PROBLEMS WITH PRESENT SYSTEMS

The conventional internal bonded tendon consists of bare high-carbon steel strand in a galvanized steel duct bonded and protected with a Portland cement grout. The galvanized steel duct and grout in combination with the surrounding concrete are supposed to provide redundant layers of corrosion protection for the steel strand. According to previous post-tensioning durability research at the University of Texas by West, Schokker and Salas, galvanized steel ducts are an ineffective means of providing corrosion protection. An example of corroded galvanized steel duct autopsied from Project 1405 research specimen is shown in Figure 2.1. West (1999) concluded:

Galvanized steel ducts were corroded in all cases. Duct corrosion led to concrete cracking along the line of the tendon in many specimens. Ducts were corroded through in nearly two-thirds of the specimens, eliminating the duct as corrosion protection for the prestressing tendon. Test results indicate the potential for durability problems when using galvanized ducts in aggressive exposures.



*Figure 2.1: Corroded Galvanized Steel Duct (Breen and Kreger 2003)*



In addition to the ineffectiveness of the duct itself, the industry standard galvanized steel duct splice required for most practical post-tensioning applications is also insufficient. The industry standard splice for galvanized steel duct is an oversized piece of steel duct placed over the two ends of the individual ducts to be spliced and sealed along the edges with duct tape. A possible improved splice utilizes heat-shrink sleeves instead of duct tape to seal the edges of the oversized duct. Both methods of coupling were investigated in the Project 1405 post-tensioning durability research. Salas concluded that neither the industry standard splice nor the heat shrink splice appears to be a satisfactory duct splice for the corrosion protection of a galvanized steel duct.

In bonded internal post-tensioning tendons, the grout is provided to bond the tendon to the structure as well as to protect the strand. It may be a flawed form of corrosion protection since the Portland cement grout is pumped into the duct after the prestress force is applied. The grout is not prestressed while the surrounding concrete is under precompression. Therefore, the grout is more susceptible to cracking since there is no precompression to overcome before cracking as in the surrounding prestressed concrete.

As described in Chapter 1, high strength steel prestressing strand is more susceptible to corrosion and the penalties of strand corrosion can be more severe than corrosion of mild steel reinforcement. Therefore, providing effective corrosion protection for the prestressing strand is critical to ensure the integrity of the structure. Due to the ineffectiveness of conventional systems, there is a need to evaluate new systems and other possibilities for protecting prestressing tendons from corrosion. The objective of Project 4562 is to assess the corrosion resistance of recent and upcoming commercially available post-tensioning systems. The materials of interest included different types of prestressing strands, plastic ducts, bearing plates and tendon systems.

## **2.2 QUEST FOR NEW MATERIALS**

In April 2003, a meeting with various members of the post-tensioning community was held at FSEL. New post-tensioning materials and possible future industry trends were identified. The list of attendees is included in Appendix A. In addition to the meeting with industry, new materials were also discovered through literature review.

Once materials of interest were identified, an initial specimen matrix was developed to determine specimen makeup and material quantities. The specimen matrix is discussed in Section 2.3.1. Post-tensioning suppliers were contacted to obtain the research materials. Most of the materials were donated by the various companies. Some of the materials were difficult to obtain due to limited availability in the United States. Procurement notes are included in the individual descriptions of the various materials and material summary in Appendix A.

Two materials of interest were not included in the research due to circumstances beyond the control of the project – MMFX strand and After-Bond systems. Steel that is made using MMFX’s proprietary technology is allegedly not only stronger and tougher (not brittle), but also significantly more corrosion resistant than conventional steel. The improved corrosion resistance is due to removal of carbides from the steel matrix. At the time of specimen construction, MMFX strand was not available commercially. While prestressing strand was planned for the future, but the production timeframe was uncertain. After-Bond systems combine prestressing strand with plastic duct and a slow-hardening epoxy into a single product. The initial benefits are the ease of placement and reduced friction while stressing due to the uncured epoxy. The epoxy and plastic duct provide delayed bonded behavior and corrosion protection over the service life of the tendon. Due to the high quantity of epoxy, After-Bond is a relatively expensive form of prestressing. Another consideration is the restricted working

time with After-Bond systems – the stressing process must be completed before the epoxy cures. While initial contacts seemed favorable, the foreign suppliers declined to provide sample tendons in a timely manner for inclusion in the research program.

## **2.3 MATERIALS**

### **2.3.1 Specimen Matrix**

Materials of research interest include strand, ducts, duct couplers, bearing plates and electrically isolated tendon systems. Considering all available materials, project timetables and project finances, a specimen matrix was used to generate and evaluate potential combinations of post-tensioning hardware of research interest. The primary focus of the matrix was to establish strand-duct combinations. The final specimen matrix is shown in Table 2.1.

A control specimen was built using industry standard post-tensioning materials: conventional strand, galvanized steel duct and non-galvanized bearing plates. This specimen will serve as a benchmark for the corrosive resistance performance of the other specimens.

In addition to prestressed specimens, two non-prestressed specimens are included in the experiment to serve as reference comparisons for the post-tensioned specimens. Both comparison specimens have steel reinforcing bars in the same position as the post-tensioning hardware it is replacing (see Appendix B for design calculations). Of the two non-prestressed specimens, the surface of one set of longitudinal bars is epoxy coated while the other is not.

**Table 2.1: Final Specimen Matrix**

*Project 4562: Final Material Matrix*

Duct	Prestressed – Strand Type							Non-Prestressed
	<i>Conventional</i>	<i>Hot Dip Galvanized</i>	<i>Electroplated Galvanized</i>	<i>Copper Clad</i>	<i>Stainless Clad</i>	<i>Stainless</i>	<i>Flowfilled</i>	<i>Conventional Rebar</i>
<i>Galvanized</i>	GB <sup>1.4</sup> NGB <sup>1.1</sup>	NGB <sup>2.2</sup>	NGB <sup>6.1</sup>	NGB <sup>1.2</sup>	NGB <sup>1.3</sup>	NGB <sup>4.1</sup>	<u>NGB<sup>2.1</sup></u>	
<i>One-Way Ribbed Plastic*</i>	NGB <sup>2.3</sup>	NGB <sup>3.4</sup>	NGB <sup>6.2</sup>	NGB <sup>2.4</sup>		NGB <sup>4.2</sup>		
<i>Two-Way Ribbed Plastic*</i>	<u>GB<sup>5.1</sup></u> <u>NGB<sup>3.1</sup></u>	<u>NGB<sup>3.2</sup></u>	<u>NGB<sup>6.3</sup></u>	<u>NGB<sup>3.3</sup></u>	<u>NGB<sup>5.2</sup></u>	<u>NGB<sup>5.3</sup></u>		
<i>Fully Encapsulated</i>	<u>NGB(2)<sup>7.1,7.2</sup></u>	<u>NGB<sup>7.3</sup></u>					<u>NGB<sup>7.4</sup></u>	
<i>No Duct</i>								1 black <sup>4.4</sup> 1 epoxy <sup>4.3</sup>

GB = galvanized bearing plate, NGB = non-galvanized bearing plate

<sup>X.Y</sup> = “Y” Beam in the “X” Series or Cast Group

(Bearing Plate)<sup>X.Y</sup> = Dead End Anchorage Exposure

*NOTE: For each specimen with plastic ducts, one duct will be coupled and the other will be continuous.*

### 2.3.2 Types of Strand

Seven types of strands are being evaluated in the various specimens.

#### Conventional

Conventional refers to the industry standard 0.5", 7-wire, bare-steel, low-relaxation strand. The 0.5" conventional strand is shown in Figure 2.2.

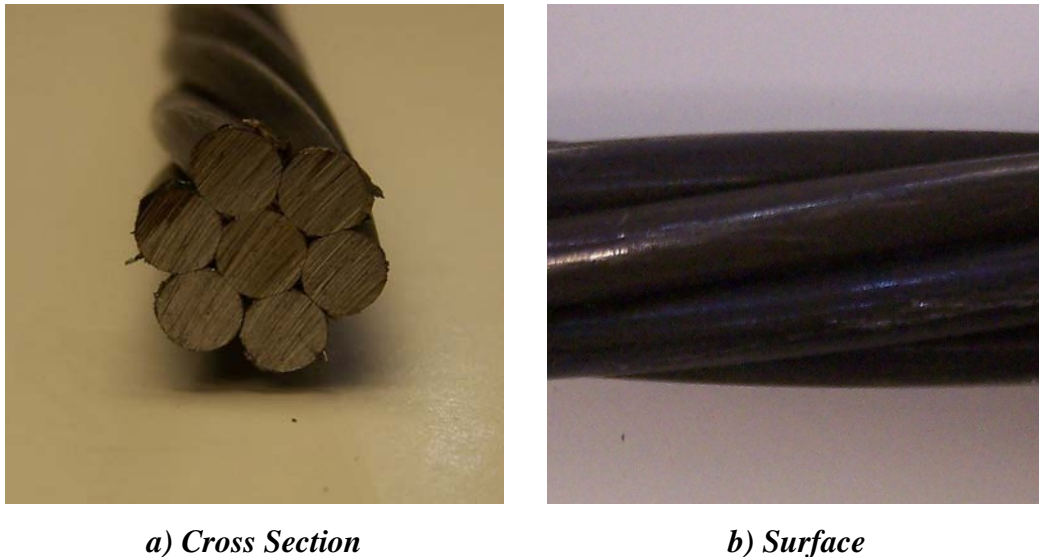


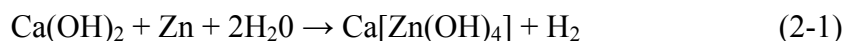
***Figure 2.2: 0.5" Conventional Strand***

#### Hot Dip Galvanized

Conventional 0.5" steel strand is coated in molten zinc during a standard hot dip galvanization process. The hot dip galvanized strand from VSL is shown in Figure 2.3. The zinc provides active, galvanic corrosion protection since it has a more active corrosion potential than steel. The zinc coating is sacrificed to corrosion as long as it is available on the steel surface (fib Bulletin 11 2001). The corrosion protection is still effective at breaks or scratches in the coating surface. Zinc is galvanically corroded at breaks in the coating to protect the exposed steel cathodically (Jones 1996).

Although the zinc coating is beneficial to the strand's corrosive performance, the strand strength is affected by the galvanization process. Heating during galvanizing reduces the tensile strength to approximately 240 ksi (FHWA 2004). In addition to decreasing strength, the hot dip coating process also does not allow for uniform zinc coating. The zinc coating could block the grooves on the inside surface of the wedge and cause the stand to slip during anchoring.

Hydrogen embrittlement of the prestressing strand may also be a concern for hot dip zinc coating. The zinc reacts with the alkaline Portland environment of fresh cement grout or concrete and evolves hydrogen (see Equation 2-1).



*a) Cross Section*

*b) Surface*

***Figure 2.3: 0.5" Hot Dip Galvanized Strand***

#### Electroplated Galvanized

The electroplated galvanized strand provides the same type of protection as the hot dip galvanized, but the zinc is applied by a chemical reaction instead of dipping the strand in molten zinc. The high carbon steel strand is coated with zinc by cathodic polarization of zinc ions in an electroplating solution. The reaction for the electroplated galvanization process is shown in Equation 2.2.



By removing molten zinc from the galvanization process, some of the drawbacks of hot dip galvanization, such as reduced strength and inconsistent surface coating, are avoided while the corrosion resistance benefits are retained. Electrogalvanized-zinc coatings may be applied in preference to hot dipping for improved surface finish and finer control of dimensions (Jones 1996).

Similarly to hot dip galvanized strand, the formation of hydrogen by the zinc coating reacting with the alkaline environment of fresh grout or concrete is a concern for electroplated galvanized strand. The hydrogen product may cause hydrogen embrittlement of the prestressing strand.

While the initial search for the electroplated galvanized strand seemed promising, suppliers were not able to provide the strand by the completion of this thesis. Alternative materials such as non-prestressing grade zinc plated barrier cables were considered, but also unavailable at the time of thesis completion. Beams for the electroplated galvanized stand were cast, but were not completed (prestressed, grouted, cracked, etc.) due to the lack of the strand.

### Stainless Steel

Stainless steels are alloys with at least 12% chromium in iron. Chromium is noted for formation of very stable, thin, resistant surface films in less oxidizing conditions, when alloyed with other metals, especially iron and nickel. Thus, chromium additions provide the basis for stainless steels and other corrosion-resistant alloys (Jones 1996). In the presence of chlorides, stainless steel may be susceptible to crevice corrosion and stress corrosion cracking due to breakdown of the protective passive film.

The stainless steel strand shown in Figure 2.4 was provided by Techalloy Company, Inc. The stainless strand was originally produced for a bridge project in California. The strand became available to the research project when the

bridge project switched to conventional strand. The stainless strand provided was 0.6" strand, but the post-tensioning hardware was designed for 0.5" strand. Because the stainless strand was rare and donated, special anchor heads were machined by VSL to accommodate the three 0.6" strands in the 0.5" bearing plate.



*a) Cross Section*

*b) Surface*

***Figure 2.4: 0.6" Stainless Steel Strand***

### Copper Clad

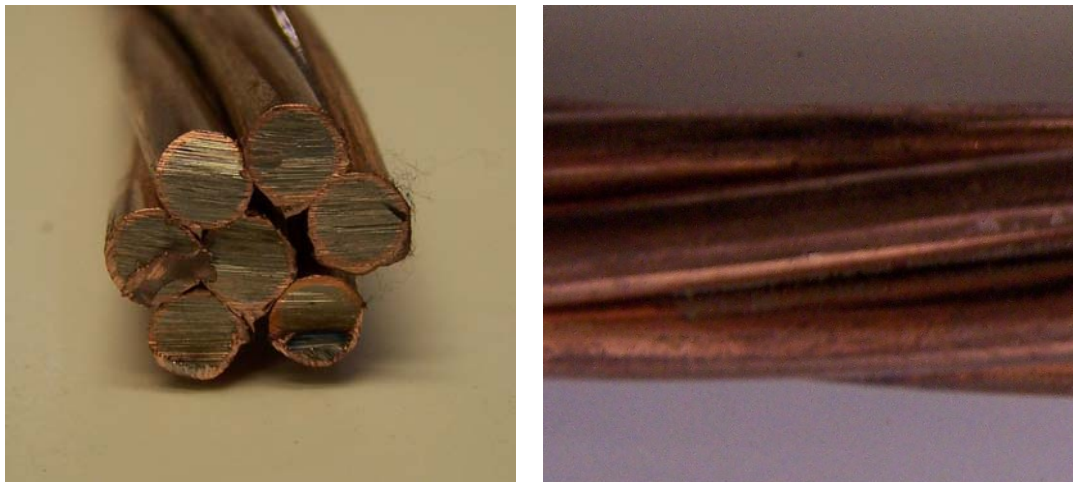
The individual wires of copper clad strand are composites consisting of a steel core with a thin layer of copper metallurgically bonded to the surface. The copper clad strand from Copperweld is shown in Figure 2.5. The cladding process is accomplished through continuous, hot, solid-cladding process using pressure rolling for primary bond.

The thermodynamic tendency for copper corrosion is low, as measured by a low free energy of chemical reaction with aqueous solutions and relatively noble potentials in the emf series and galvanic series. Thus, copper and its alloys are quite corrosion resistant in many atmospheric and nonoxidizing aqueous environments (Jones 1996).



Copper clad strand couples the strength of steel with the corrosion resistance of copper. The advantage of clad materials is that the end product combines the superior properties of each metal – strength, corrosive resistance, cost, etc. – to produce a material superior to that of the individual materials. Noble metal cladding such as copper, nickel and stainless steels have historically been investigated but have not been used extensively due to initial cost considerations (FHWA 2004). Improved manufacturing methods have made clad materials more affordable.

The cross section of the copper clad strand is exposed at the very ends of the strand due to the cutting of excess strand after stressing. Therefore, the steel cores of the individual wires at the end of the strand are uncovered and may be vulnerable to corrosion beyond the anchorages.



*a) Cross Section*

*b) Surface*

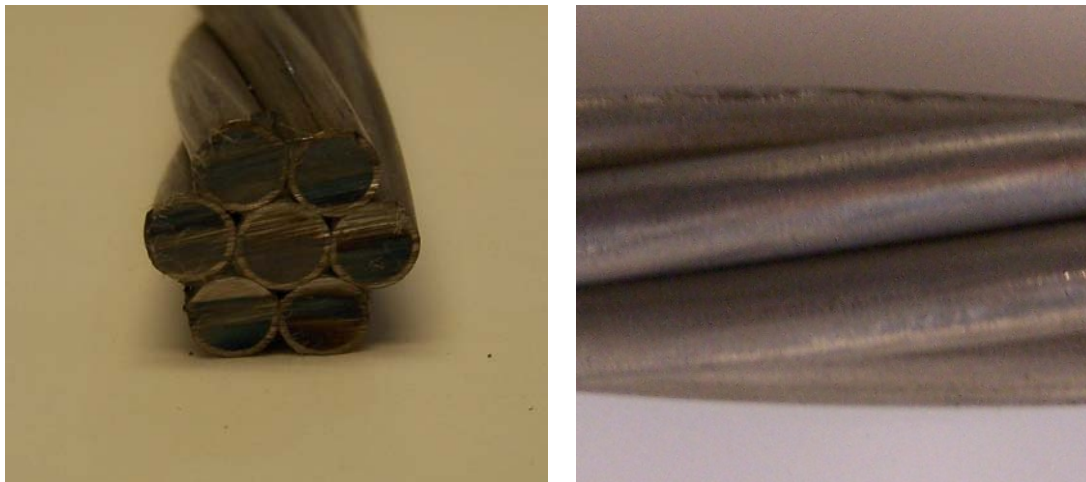
***Figure 2.5: 0.5” Copper Clad Strand***

### Stainless-Clad

Similarly to the copper clad process, a thin layer of stainless steel is bonded to a high carbon steel core to create a composite wire. Stainless clad strand benefits from the corrosion resistance of stainless steel without having the

entire cross-section stainless. It couples the strength and relative cost of conventional prestressing steel with the corrosion resistance of stainless steel. The stainless-clad strand provided by Dywidag Systems International (DSI) is shown in Figure 2.6. Due to limited quantities, the stainless clad strand was sent to FSEL in two separate shipments – Summer 2004 and Spring 2005. Similarly to the stainless strand, the stainless clad was also 0.6” and had to be accommodated with special anchor heads.

The cross section of the stainless clad strand is exposed at the very ends of the strand due to the cutting of excess strand after stressing. Therefore, the high carbon steel cores of the individual wires at the end of the strand are uncovered and may be vulnerable to corrosion beyond the anchorages.



*a) Cross Section*

*b) Surface*

***Figure 2.6: 0.6” Stainless Clad Strand***

#### Flow Filled, Epoxy Coated Strand

The epoxy coating provides a protective barrier around the strand. The 0.5” flow filled epoxy coated strand from Sumiden Wire is shown in Figure 2.8. When first introduced, the outside of the strand was coated while the interstices between strands were unfilled. Humidity could enter the interstices around the

core wires, the wires then corroded and the bond with the coating reduced (FIB Bulletin 11 2001). As the strand-coating bond is reduced, the bond between strand and structure for bonded post-tensioning response may be affected. Today, the seven-wire strand is opened during coating and closed again. Therefore, all wires are completely coated and there no voids in the cross-section. The unfilled and filled epoxy strand cross sections are shown in Figure 2.7.

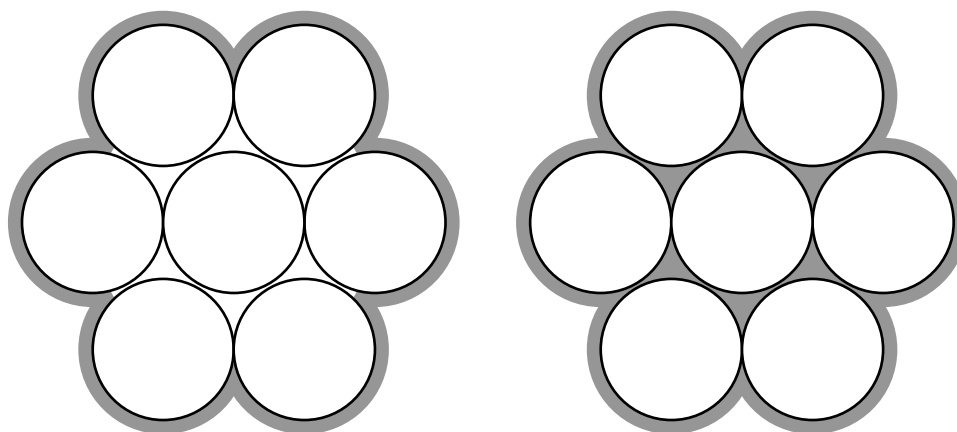
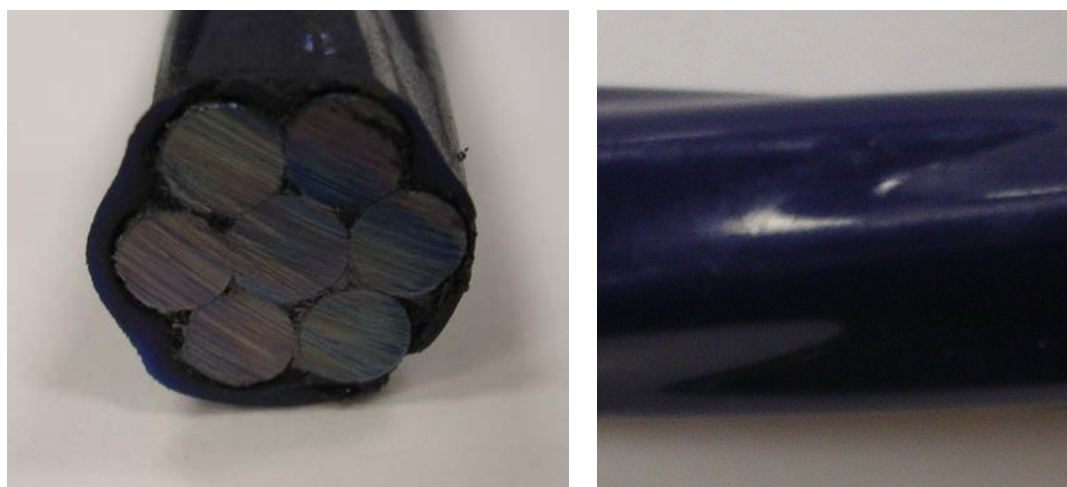


***Figure 2.7: Unfilled (left) vs. Filled (right) Epoxy Coated Strand Cross Sections***

Coating is effective as long it remains intact. Macroscopic and microscopic defects, such as pinholes, voids and mechanical scrapes and scratches, are inevitable in coatings, allowing access of the environment to the substrate metal (Jones 1996). The imperfections in the coating can initiate cathodic disbondment or oxide lifting. Cathodic disbondment is delamination of the coating by oxygen and water migrating to the cathodic reaction under the coating while the anodic reaction takes place at the coating defect. Oxide lifting occurs when the anodic corrosion products from cyclical wet and dry cycles accumulate under the surface of the coating and raise the coating from the substrate metal surface. Cathodic disbondment is a more common form of coating failure than oxide lifting.

Special wedges with deeper and wider teeth are required to anchor epoxy coated strand. Sumiden Wire supplied the required wedges and corresponding anchor heads. The wedges must penetrate the protective coating in order to make contact with the steel so the strand does not slip during anchoring. Therefore, epoxy coated strand is inherently vulnerable at anchorage zones since the coating must be broken in order for the wedges to hold the strand in place.

The cross section of the epoxy coated strand is exposed at the very ends of the strand due to the cutting of excess strand after stressing. Therefore, the steel cores of the individual wires at the end of the strand are uncovered and may be vulnerable to corrosion beyond the anchorages.



*a) Cross Section*

*b) Surface*

***Figure 2.8: 0.5" Flow Filled, Epoxy Coated Strand***

### **2.3.3 Types of Duct**

Originally, duct was considered primarily as a means of forming a void through the concrete for the tendon and little attention was paid to the possible role of the duct as a barrier to corrosive agents (FHWA 2004). After discovering cracks and voids in the grout, more emphasis has been placed on the reliability of

duct as a means of protecting the strand. Grout is injected into the duct subsequent to post-tensioning. Therefore, the grout is not prestressed and may crack earlier than the surrounding prestressed concrete. Voids in grout can be caused by poor grouting procedures and/or accumulated bleed water. Proper grouting of the post-tensioning ducts is necessary for corrosion protection and bond transfer, but complete grouting can be difficult due to the lack of visibility and access to all parts of the duct (Schokker 1999).

#### **2.3.3.1 Plastic**

High density plastic ducts of polyethylene or polypropylene are used to create an effective moisture barrier. According to Salas, “the superiority of plastic ducts is evident” based on his macro cell research at FSEL under Project 1405.

Plastic duct and couplers from two suppliers were investigated in the current research: General Technologies Inc. (GTI) and VSL.

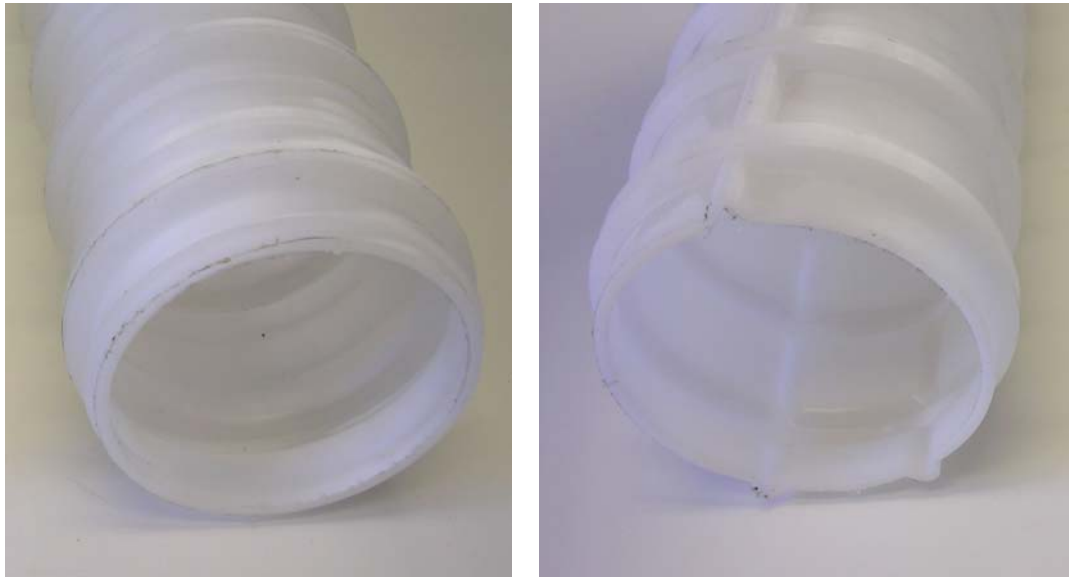
##### GTI

GTI produces plastic ducts with two ribbing schemes: 1) circumferential ribs and 2) circumferential and longitudinal ribs. The longitudinal ribbing is intended to minimize voids from air that is trapped at the high point of corrugations and improve grout flow. The size of each type of duct used in the specimens corresponded to the smallest available coupler for the particular style of duct: 3.00” (76 mm) one-way ribbed duct and 3.35” (85 mm) two-way ribbed duct. The two GTI plastic ducts are shown in Figure 2.9.

Rigid plastic couplers are used to splice together sections of duct when more than one length is needed. GTI produces slip-on and snap-on plastic couplers. The GTI slip-on couplers are designed to fit over the to-be-coupled ends of the plastic duct. Once the coupler is in place, heat-shrink sleeves are

installed over the edges of the coupler to seal the duct connection. Grouting vents were installed into the slip-on couplers by the supplier. The GTI slip-on couplers and heat-shrink sleeves are shown in Figure 2.10.

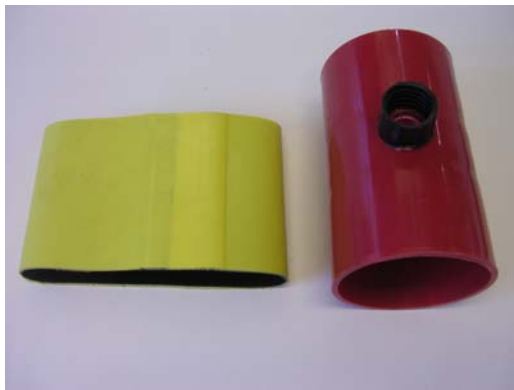
The snap-on couplers provided by GTI are designed for the one-way ribbed duct and can not accommodate the two-way ribbed duct due to the additional ribbing. Plastic hinges connect the three segment of the snap-on coupler: two half-shells and a rigid fold-over section that holds the coupler together. Rubber rings inside the half-shells seal the splice; therefore, it is not necessary to seal the edges of the coupler using heat-shrink sleeves or any other means. Grouting vents were built into the snap-on couplers. The GTI snap-on coupler is shown in Figure 2.11.



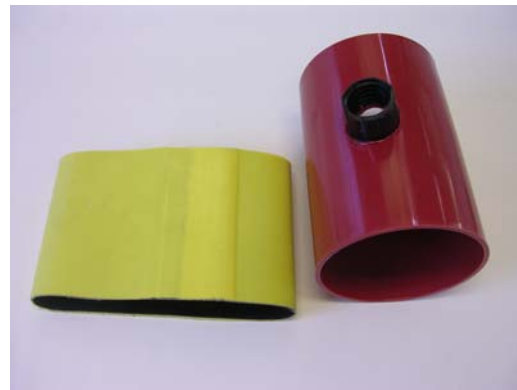
*a) 76 mm One-Way Ribbed*

*b) 85 mm Two-Way Ribbed*

**Figure 2.9: GTI Plastic Ducts**



*a) 76 mm*



*b) 85 mm*

**Figure 2.10: GTI Slip-On Couplers with Heat Shrink Sleeves**



*a) Assembled*



*b) Unassembled*

**Figure 2.11: GTI 76mm Plastic Duct Snap-On Coupler**

## VSL

VSL produces the PT Plus plastic duct (59 mm) utilized for current research specimens and is shown in Figure 2.12. The duct is ribbed circumferentially and can be coupled with a robust four-part system: two half shells and two locking tabs along the sides. The VSL coupler is shown in Figure

2.13. VSL couplers with manufacturer installed grout vents were not available at the time of specimen production. Therefore grout vents were installed in the couplers by researchers at FSEL. A plastic male adaptor was threaded into a hole in the coupler and sealed by heat welding. VSL couplers with manufacturer installed grout vents were made available to the researchers after the completion of specimen production.

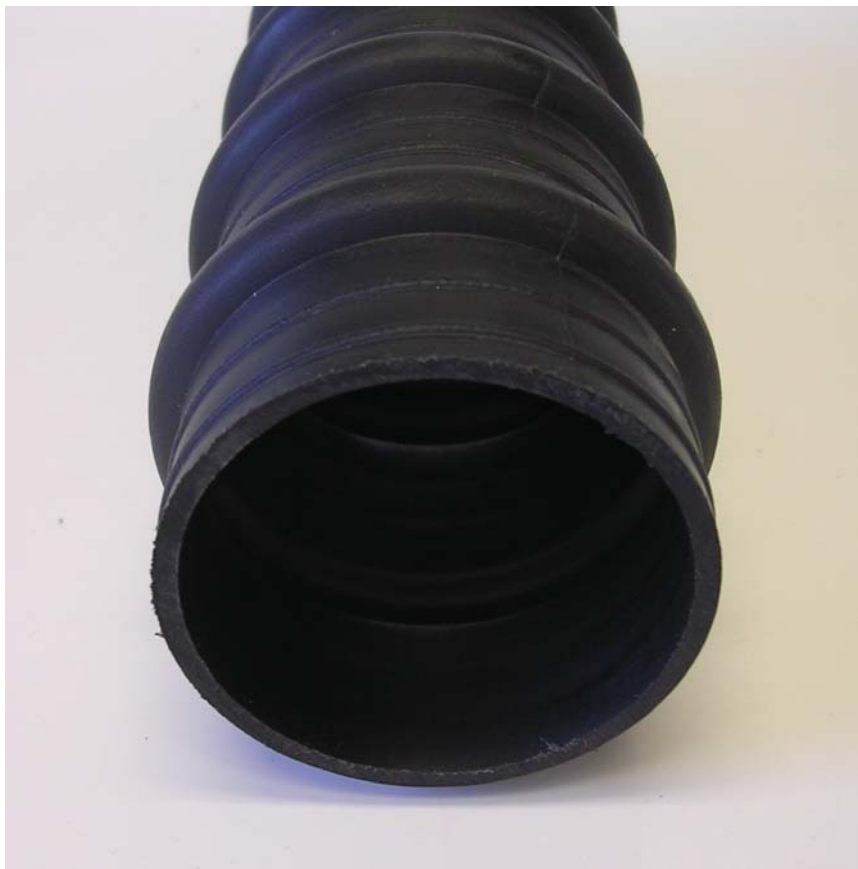


*Figure 2.12: VSL PT-Plus Plastic Duct*





*a) Assembled*



*b) Unassembled*

**Figure 2.13: VSL PT-Plus Plastic Duct Coupler**

### **2.3.3.2 Galvanized Steel**

Galvanized steel duct (2 in. diameter) provided by VSL is shown in Figure 2.14. Splices for galvanized steel duct were investigated during previous post-tensioning durability research at FSEL.



**Figure 2.14: Galvanized Steel Duct**

### 2.3.4 Types of Bearing Plates

The specimen was originally designed for the VSL E5-3 bearing plate which accommodates three 0.5” strands. At the onset of specimen construction, VSL determined they would not be able not to supply the E5-3 bearing plates because they are not commonly available in the United States. The smallest available bearing plate for 0.5” strand was the EC5-7 by VSL which accommodated seven 0.5” strands. The four extra holes in the anchor heads were plugged with epoxy to seal the tendon. The epoxy used to plug the anchor heads was also used to coat the anchorage pocket before backfilling it with mortar (see Sections 4.9 and 4.10).

Both non-galvanized and hot-dip galvanized versions of the VSL EC5-7 bearing plates were used in the specimens. The benefits of hot dip galvanization are described for hot dip galvanized strand in Section 2.3.2. Both types of bearing plates are shown in Figure 2.15.



*Figure 2.15: Non-Galvanized (Left) and Galvanized (Right) VSL EC5-7 Bearing Plates*

### 2.3.5 Types of Systems

The research project investigated both industry standard and electrically isolated tendon systems.

Conventional systems do not have active means of corrosion resistance. Through metal-to-metal contact on components, the tendon is electrically connected to the other post-tensioning hardware including steel ducts and bearing plates. Temporary protection caps are used for grouting, but are removed before the anchorage pockets are backfilled with grout. The connection between the bearing plate trumpet and duct is sealed with duct tape. See Figure 2.16 for an example detail of a conventional system from FIB Commission 5 (2004).

Electrically isolated tendon (EIT) systems employ several levels of active corrosion protection. The tendon is electrically isolated from the rest of the post-tensioning hardware by means of an isolating insert between the anchor head and bearing plate. Plastic duct is standard and is connected to the plastic bearing plate trumpet by a rigid plastic coupler. A permanent plastic isolation protection cap seals the anchorage during grouting of the tendons and backfilling of the anchorage pocket with grout. See Figure 2.17 for an example detail of an EIT system from FIB Commission 5 (2004). The materials for the EIT specimens provided by VSL Switzerland are shown in Figure 2.18.

An itemized comparison between conventional and electrically isolated tendon systems is shown in Table 2.1.

**Table 2.2: Industry Standard vs. EIT Systems**

<b>System</b>	<b>Industry Standard</b>	<b>EIT</b>
<b>Duct</b>	Steel or Plastic	Plastic
<b>Trumpet-Duct Connection</b>	Duct Tape	Plastic Coupler
<b>Permanent Protective Cap</b>	No	Yes
<b>Electrically Isolated Tendon</b>	No	Yes

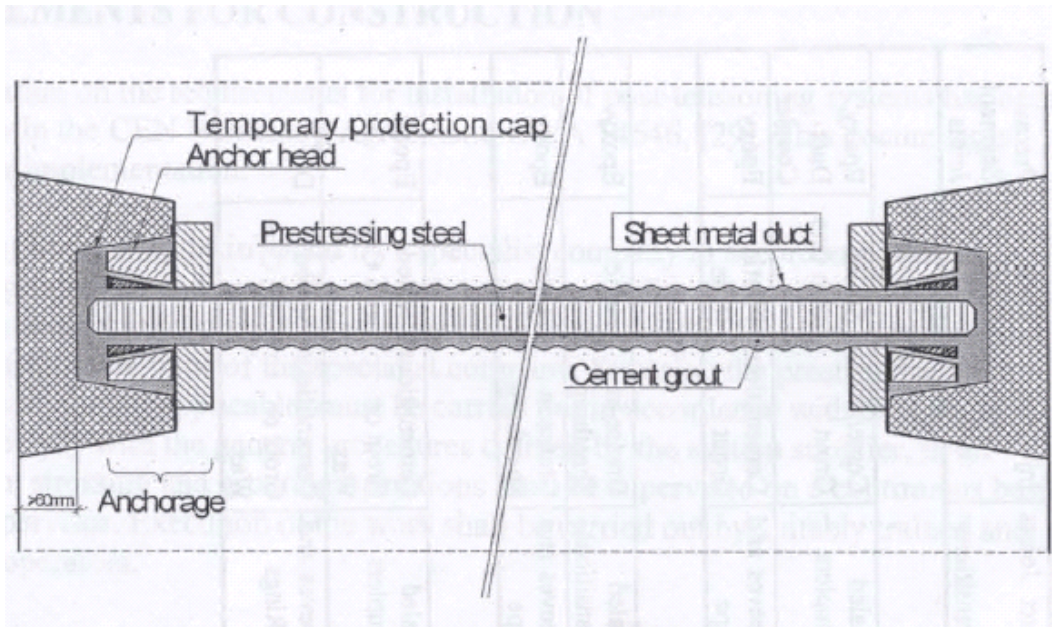


**Figure 2.16: Conventional System Detail (FIB Commission 5)**

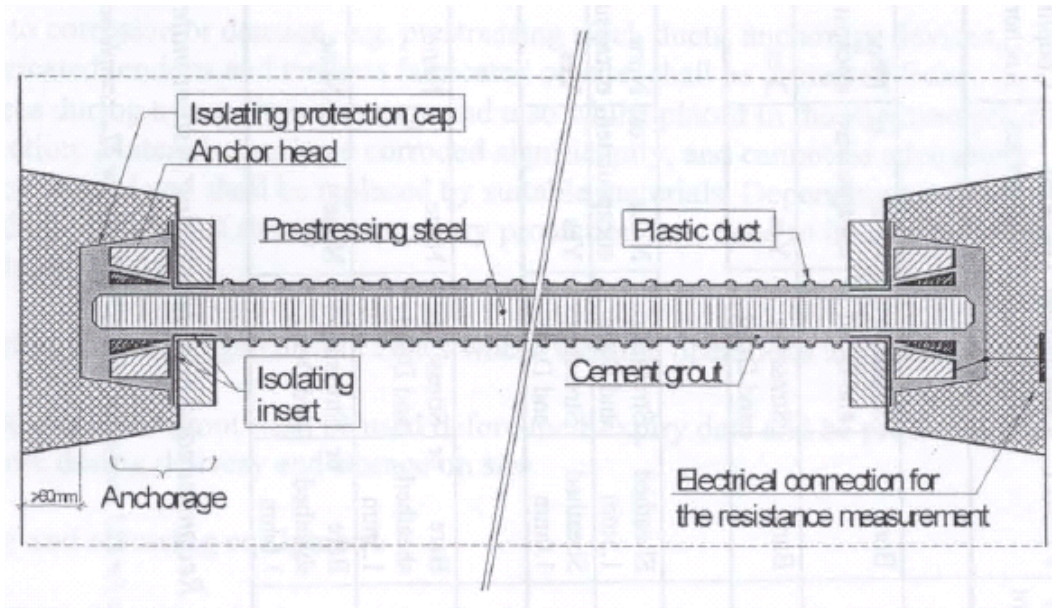


**Figure 2.17: Electrically Isolated Tendon System Detail (FIB Commission 5)**



*a) CS2000 6-7 Bearing Plate*



*b) Insulation Plate*



*c) Protection Cap*

*Figure 2.18: VSL Electrically Isolated Tendon Materials*

## **CHAPTER 3**

### **Design of Test Specimens**

#### **3.1 OBJECTIVES**

The design of the test specimens was focused on creating a small specimen, in which cracking behavior could be controlled and post-tensioning hardware isolated, that would yield comparative durability results in a reasonable amount of time.

##### **3.1.1 Small Specimen**

In order to investigate many different material combinations by maximizing the number of specimens, size was an important factor in the design. By designing small and efficient specimens, the potential value of each specimen is increased. In addition to financial considerations, limited storage space for the long term exposure, ease of handling and future autopsies were also motivators for the small specimen.

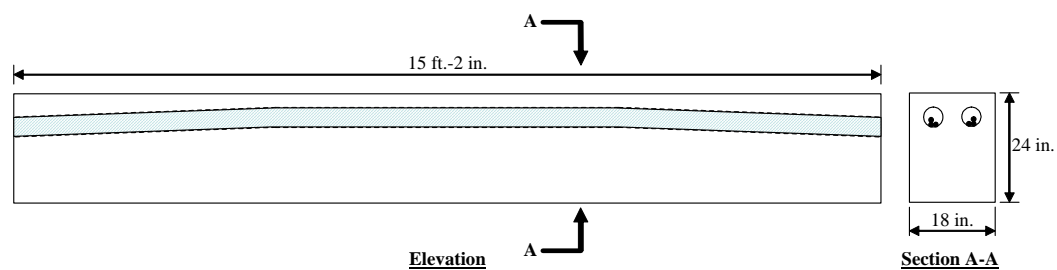
Large beam specimens from Project 1405 were still under load at the north end of FSEL during the design of the new specimens. The 1405 specimen consists of double-stacked beams with identical dimensions, but different content. The lower beam is heavily reinforced and serves as a reaction beam to load against. The upper beam was post-tensioned to various levels and the focus of the research. In each prestressed upper beam, there were two draped ducts with three strands per tendon. On the top surface of the upper beam, thin plastic walls sealed with silicon form a pool in order to pond saltwater. The region of research interest was directly beneath the pool. The saltwater exposure region is approximately the width of the beam and 4 ft. long, centered along the 15 ft.-2 in.



length. Therefore, only a small portion of the beam was being exposed and monitored. In addition to the exposure on the top surface, saltwater was also sprayed over the dead end anchorage zones on Beams 2.7, 2.9 and 2.12. The double-stacked research specimen from Project 1405 is shown in Figure 3.1a and detailed in Figure 3.1b.



*a) In-Service Project 1405 Research Specimen*



*b) Project 1405 Research Specimen Detail*

**Figure 3.1: Project 1405 Research Specimen**

The new research specimens were designed to provide the same type and quantity of results using much less materials in a more efficient approach than the previous specimens. As in Project 1405, the new specimens each have two ducts with three strands per tendon. While the new specimen is over 9 ft. shorter than the old specimens, the saltwater exposure region is only 1 ft. shorter than old specimens. Therefore, the quantity of durability exposed post-tensioning duct and strand in each specimen is quite comparable for the current and past research specimens. Saltwater will also be sprayed on the anchorage zones of the new beams similarly to the 1405 beams. All loads in the new specimens are self-contained. Therefore, there is no need for a reaction beam. The new research specimens are shown in Figure 3.2a and detailed in Figure 3.2b. The same steel sections in contact with the 1405 and 4562 test specimens in Figures 3.1a and 3.2b provide a means of comparing the size of the specimens.

### **3.1.2 Controlled Cracking**

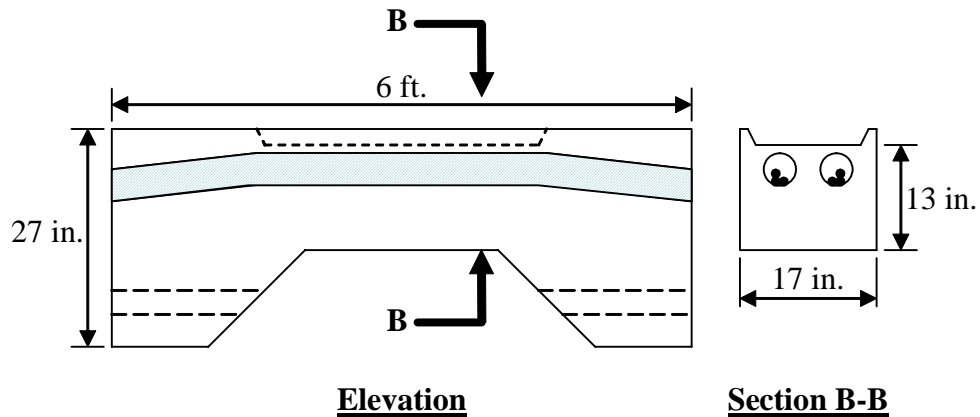
To provide a realistic, aggressive concrete environment for the research materials, the concrete surrounding the post-tensioning ducts was cracked. Cracks provide a direct means of access for moisture and chlorides to the post-tensioning hardware. In addition to the presence of cracks, the location and widths of cracks were also important and thus controlled.

The cracking objective of the specimen design was to provide fine cracks in the specimen throughout the depression for the salt bath on the top surface of the beam. By reducing the cross section and moment of inertia of the specimen at the middle of the beam, cracks can be restricted to the middle portion of the beam (see Section 3.2.4 for design calculations). In addition to the reduced cross section, the midsection is lightly reinforced longitudinally with mild steel to control cracking in the region. The beam is subjected to uniform moment and





*a) Completed Project 4562 Research Specimen*



*b) Project 4562 Research Specimen Detail*

*Figure 3.2: Project 4562 Research Specimen*

axial load by the eccentrically applied prestress force and an external Dywidag bar force through the center of the corbels. The conduit through the center of the corbels was created with PVC pipe. The Dywidag force represents live load in the experiment. See Figures 3.3 for a detail of the applied and internal forces.

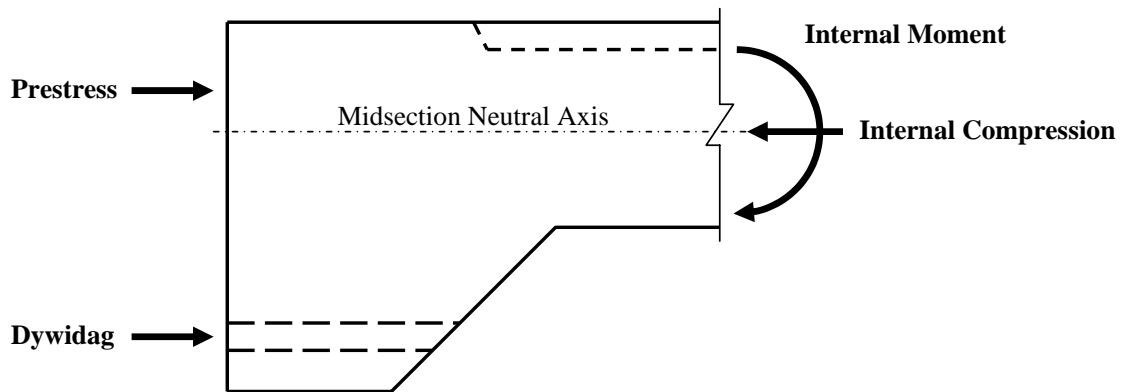


*Figure 3.3: External and Internal Forces*

### 3.1.3 Accelerated Results

In order to achieve results in a reasonable amount of time, the corrosion process was accelerated by using a reduced concrete cover above the ducts and by pre-cracking the specimen. The thickness of the concrete between the bottom of the depression for the salt bath and top of the cage is 1 in. The duct is draped against the top of the cage and #3 bars are used as transverse reinforcement. Therefore, the concrete cover over the ducts at the apex of the drape in the middle portion of the beam is 1-3/8 in.

In addition to the reduced cover, the beam is also cracked through the middle portion as discussed in Section 3.1.2. In prior post-tensioning durability research conducted at the University of Texas, Salas (2003) compared crack widths with localized corrosion. Based on Salas's work, the goal of the live load application are crack widths on the order of 0.010 in.

### 3.1.4 Post-Tensioning Hardware Isolation

In Project 1405 specimens, corrosion of the transverse reinforcement caused uncontrolled cracking and may have influenced the half-cell potential readings. Half-cell potentials are a non-destructive means of monitoring

corrosion of the post-tensioning hardware and are discussed in Section 5.3.2. The transverse reinforcement provided in 1405 specimens was not coated. In order to avoid similar corrosion problems, epoxy coated reinforcing bars were used for all non-prestressed reinforcement in the current study.

In addition to problems with corrosion of the transverse reinforcement, the metal chairs used to control concrete cover in the 1405 specimens also corroded. Since the 1405 specimens were cast upside-down – the top surface of the beam was the bottom surface of the forms – metal chairs are located along the top, exposed surface of the beam. To avoid potential corrosion of the chairs, plastic chairs were used to control concrete cover in the current study. After construction began, possible problems with cracking around the plastic chairs arose due to difference in thermal expansion coefficients for concrete and plastic. Due to the non-critical locations of the chairs, possible uncontrolled cracks around the plastic chairs should not be an issue.

In order to move the specimens, two  $\frac{3}{4}$  in. straight coil loop lifting anchors were placed in the top surface on either side of the depression for the salt bath. The lifting anchors were galvanized so they would not corrode and possibly affect the half-cell potential readings. Before initiation of long-term exposure cycles and outdoor storage, the lifting anchors were sealed with plastic inserts and a bead of silicon to preserve the anchors for future specimen movements. The inclusion of galvanized lifting anchors was not prompted by problems in 1405 specimens.

## **3.2 DESIGN**

### **3.2.1 Forces**

In order to represent the post-tensioning materials in an appropriate environment, the tendon was stressed. The presence of prestress – not the level of prestress – was the important factor. In order to meet the goals listed in Section

3.1 and still have a reasonable level of prestress, a level of 25% GUTS (Guaranteed Ultimate Strength = 270 ksi) was initially determined by conducting a parameter study. The specimen design was optimized by varying the level of prestress and mid-section dimensions and solving for the Dywidag force. The level of prestress was later dropped to 15% GUTS in order to develop larger cracks as discussed in Section 4.7.1. Cracks in the trial specimens stressed to 25% were too narrow for research objectives. The design equation to estimate the initial cracking forces assumes linear elastic behavior and superposition of stresses due to moments and axial loads (see Equation 3-1).

$$\frac{Mc}{I} \pm \frac{P}{A} = \frac{[F_D e_D - F_P e_P]c}{I} - \frac{F_D + F_P}{A} = f_t \quad (3-1)$$

Where  $F_D$  = Dywidag Force

$e_D$  = Dywidag Eccentricity

$F_P$  = Prestress Force =  $A_p f_p$

$f_p$  = Level of Prestress

$A_p$  = Area of Prestress Strand =  $6[0.153 \text{ in.}^2]$

$e_p$  = Prestress Eccentricity

$I$  = Moment of Inertia at Midsection =  $\frac{bh^3}{12}$

$b$  = Beam Width

$h$  = Beam Height at Midsection

$c$  = Distance from Neutral Axis to Extreme Fiber =  $\frac{h}{2}$

$A$  = Gross Area of Midsection =  $bh$

$f_t$  = Assumed Tensile Strength of Concrete =  $12\sqrt{f'_c}$

$f'_c$  = Design Compressive Strength of Concrete

The calculated Dywidag force was compared with the capacity of the Dywidag system which was controlled by the squash load of the nested springs used to maintain Dywidag force over time. Three concentric springs of equal lengths and various diameters form the nested spring. The squash load of a nested spring was experimentally determined in a compression machine to be approximately 35 kips. Two parallel nested springs are used in the Dywidag assembly; therefore the capacity of the assembly is approximately 70 kips. See Section 4.8.2 for description, pictures and stressing procedures of the Dwyidag system. The dimensions of the final optimized design are such that half of the Dywidag assembly capacity is used to crack the specimen as discussed in Section 3.1.2 while the remaining capacity is used to increase the crack widths as discussed in Section 3.1.3.

Most calculations were based on 0.5 in. diameter strand when selecting a prestress force (15% GUTS and 6.2 kip per strand) that would be sufficient to maintain a reasonable prestress after anticipated losses. However, the only available stainless and stainless clad strands were 0.6 in. diameter (see Section 2.3.2). If 15% GUTS was used for the prestress force in these specimens, the resulting prestress level in the concrete section would be too high to overcome with the Dywidag bar to produce cracking. After substantial calculations, it was decided to reduce the tendon stress level to 12.8% GUTS or 7.5 kip per strand. Even though this change increases the concrete stress level, it was felt that any lower tendon stress might result in too drastic a loss in prestress.

### **3.2.2 Reinforcement**

As described in Section 3.1.4, all steel reinforcing bars were epoxy coated. Minimal reinforcement was provided through the midsection of the beam. As described in Section 3.1.2, the longitudinal reinforcement was limited for

cracking purposes. Four #5 bars at the corners of the rectangular cage provide a reinforcement ratio at the midsection of only 0.56%. The longitudinal bars had 180 degree hooks at both ends in order to develop the bars mechanically. #3 bar stirrups were provided at the maximum spacing of half of the depth of the tension steel as per ACI318-02 Section 11.5.4. The spirals provided were specified by VSL for the E5-3 bearing plate, but were used on the EC5-7 bearing plate due to the post-design hardware change. The E5-3 spiral is slightly smaller than the EC5-7 spiral, but still adequate.

The corbel reinforcement was designed to meet ACI318-02 Section 11.9 requirements. The main reinforcement is a #7 bar bent in separate three planes. The hooks at the ends of the main bar mechanically anchor the main bar to the rest of the beam and are positioned so the width of the specimen was not increased to accommodate the hooks. In addition to meeting ACI318-02 Section 11.9 requirements, the corbel stirrups also provide continuity between the corbel and beam reinforcement.

During the live load application for the trial specimens, cracks formed at the reentrant corner near the shear face of the corbel due to a lack of reinforcement in the area. Inclined #3 bars were placed across the crack plane in all subsequent cages to control cracking of that region.

Figure 4.4 is a picture of a completed steel reinforcement cage. Reinforcement drawings and order specifications are included in Appendix B.

### **3.2.3 Concrete**

In order to match materials used in Project 1405 and provide a realistic environment for the post-tensioning hardware, Texas Department of Transportation (TxDOT) Class C Concrete for substructures was used in the

specimens. The criteria and uses for Type C Concrete are listed in Section 421.9 of the TxDOT Standard Specifications.

The concrete was delivered by Capitol Aggregates of Austin, Texas. Mix #164 was recommended based on project needs. Maximum 3/8 in. aggregate was used to facilitate proper consolidation of the concrete around the closely spaced steel reinforcement cage. In addition to the small aggregate, a 6 in. slump was also specified to prevent voids and minimize vibration. Concrete information such as casting dates and strengths are included in the Specimen Catalog, Tables 6.1 and 6.2.

## **CHAPTER 4**

### **Construction**

#### **4.1 OBJECTIVES**

The objective of the construction process was to develop practical and efficient methods of producing viable research specimens. In an effort to link the results from these specimens to previous post-tensioning durability research completed at FSEL under Project 1405, the same construction practices were used for current specimens when applicable.

#### **4.2 FORMS**

Two sets of wood forms were built using  $\frac{3}{4}$ -in. plywood and 2-in. x 4-in. studs. Two specimens can be cast in each set of forms. Therefore, four specimens can be cast simultaneously. This was done to minimize concrete variation as well as to conserve lab floor space and was achieved by using a common form wall between two specimens. Each set of forms has two side walls, two end walls, one middle wall, two salt bath block-out forms and two trapezoidal forms to create the reduced cross section in the middle of the specimen. A profile of the specimen with reduced cross section is shown in Figure 4.1.

The side walls, trapezoidal forms and salt bath forms on each side of the common form wall are identical, but the end walls differed depending on whether the end of the specimen would be the live-end or the dead-end. As discussed in Chapter 3, an open live-end is utilized to provide additional room for stressing equipment. Both the live-end and dead-end pockets are created using wood forms attached to the respective end wall. Holes were drilled through the pocket forms and end walls to attach the bearing plates to the forms using  $\frac{1}{2}$  in. threaded rods,



washers and bolts. The bearing plate-wood form interface was sealed using silicone to prevent moisture from fresh concrete penetrating behind the bearing plate. The dead-end form is covered in plastic and tapered for removal purposes. The end walls, with non-galvanized bearing plates attached, are shown in Figure 4.2.



*Figure 4.1: Research Specimen Profile*



*Figure 4.2: End Walls, Dead (left) and Live (right)*

The forms used to create the cast-in depressions for salt baths in the top surface of the beam were built to be adjustable. A combination of threaded rods,

washers and bolts allow for the form position to be adjusted so that the bottom of the salt-bath is consistently 1 in. above the top of the reinforcement cage against which the duct is draped.

The common middle wall and trapezoidal forms used to create the reduced middle cross section are fixed to the floor. The side walls and end walls are attached to the fixed portion of the forms after the cage and ducts were in place and before casting. The assembled forms are shown in Figure 4.3 just prior to casting specimens.



*Figure 4.3: Assembled Forms*

#### **4.3 DEFORMED REINFORCEMENT CAGE**

The epoxy-coated reinforcing steel was ordered from the ABC Coating, Inc. in Waxahatchie, Texas. At the time of construction, ABC was the only company in Texas and immediate surrounding area that could provide epoxy-

coated rebar. All information provided to ABC regarding reinforcing steel lengths and bends is included in Appendix B. Due to the unusual nature of the primary corbel reinforcement, pictures of a paperclip bent in the desired shape were emailed to the supplier.

The reinforcing steel was delivered to FSEL bent and epoxy-coated as specified. As specified by the supplier, cages were tied together using coated wire provided by the supplier. Conventional wire ties could not be used because the bare wire might damage the epoxy coating. A completed steel reinforcement cage is shown in Figures 4.4.



***Figure 4.4: Completed Passive Reinforcement Cage***

To regulate concrete cover, plastic chairs were tied along the bottom of the completed cage with coated tie wire before the cage was placed in the forms. Plastic chairs were used in order to prevent corrosion of the metal chairs from



damaging and staining the surfaces of the beam. The decision to use plastic chairs was a direct result of observed chair corrosion in Project 1405 beams.

#### **4.4 DUCTS**

All ducts were cut to length using either a grinder (steel ducts) or power miter saw (plastic ducts). To allow for a grouting vent at the apex of the drape, a hole was drilled through one wall of ducts that were not coupled. For coupled ducts, grouting vents were built into the coupler. The GTI snap-on couplers came with vents already in the coupler, but both the GTI slip-on and VSL PT-Plus couplers had to be modified to provide a grouting vent. The modifications to the GTI product were completed by the company while the VSL coupler modifications were made at FSEL – both processes incorporate drilling into the coupler and heat welding a plastic connector at the hole to attach a hose. The hole in the uncoupled ducts was centered  $\frac{3}{4}$  in. to the side to the middle of the duct to allow space for the stirrup at the middle of the beam. The duct was placed through the spirals into the cage before attaching the vent.

To provide a sturdy grouting vent for uncoupled ducts, the threaded portion of a plastic male adaptor was cut off and the remainder was placed inside the duct so the small portion could extend out of the hole while the large section remained inside as a bearing surface against the interior wall of the duct. A detail of the connection is shown in Figure 4.5.

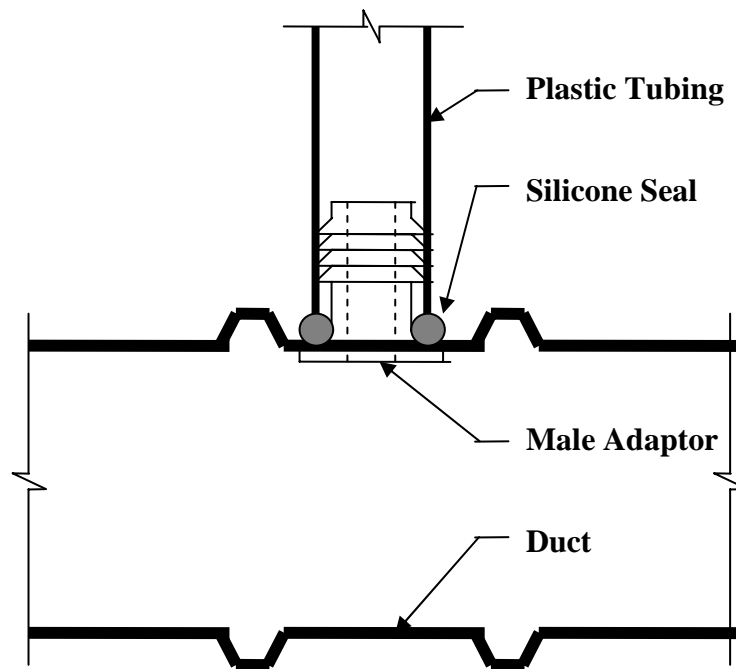


*Figure 4.5: Grout Vent Connection Detail*

#### **4.5 STRAND**

The strand was delivered to FSEL from various suppliers arriving in continuous rolls ranging from 2.5 to 6 ft. in diameter and held together with wire, tape or zip ties. The strand was cut into 8-ft. lengths with a grinder in order to be placed in the specimens for stressing. To accomplish the cutting safely, the strand rolls were placed in a steel cage before being released. The bottom and sides were lined with plywood and metal edges of the cage that would come in contact with the strand were covered with foam pipe insulation to protect the integrity of the surfaces of the coated strands.

#### **4.6 CONCRETE**

Concrete from Capitol Aggregates was delivered by ready mix truck and placed using the one cubic-yard bucket and overhead crane. Special attention was

given to not damaging the grout vent in the middle of the duct with the bucket or falling concrete. Once the concrete was in the forms, vibrators were used to consolidate the mix. The forms required to create depressions in the top surface for the salt baths were positioned before finishing. Concrete cylinders were placed on top of the salt bath forms to counteract the buoyancy forces from the displaced concrete. The top surface of the specimen was finished with trowels and then two 6 in. x  $\frac{3}{4}$  in. galvanized straight coil loop lifting anchors were set into the concrete along the centerline on both sides of the salt bath block out. Concrete was kept out of the threaded portion of the lifting anchor by placing a short length of greased foam backer rod into the threads.

Nine, 6 in. x 12 in. companion cylinders were cast from each batch of concrete. Three cylinders each were tested at 7, 14 and 28 days to monitor strength. The concrete strengths for all beams are reported in Chapter 6.

## **4.7 STRESSING**

### **4.7.1 Target Values**

The presence of prestress was crucial, but the specific level of prestress was not as important. Due to the small-scale specimen utilized, applying the maximum amount of prestress was not practical. Instead, a small percentage of the guaranteed ultimate strength (GUTS) was used.

The initial level of prestress was set at 25% GUTS for the trial specimens, but reduced to 15% GUTS for the remaining specimens for crack width control. The crack widths achieved in the initial trial specimens with a prestress level of 25% GUTS were on the order of 0.005 in. As mentioned in Chapter 3, the desired crack widths for accelerated results were on the order of 0.010 in. Therefore, the cracks in the trial specimens were too narrow.

By reducing the level of prestress, the beams would crack at a lower applied Dywidag force and the crack could be opened further using the remaining Dywidag assembly capacity. However, if the initial level of prestress was too low, a significant portion of the applied post-tensioning force could have been lost due to creep – creep losses are described in Section 4.7.2. After considering long-term creep effects and factors affecting crack widths, 15% GUTS provided the best balance.

As discussed in Section 3.2.1, the level of prestress was reduced for specimens with 0.6-in. strands to 12.8% or 7.5 kip per strand. If 15% GUTS was used for the prestress force in the 0.6-in. specimens, the resulting prestress level in the concrete section would be too high to overcome with the Dywidag bar to produce cracking. It was felt that any lower tendon stress might result in too drastic a loss of prestress.

#### **4.7.2 Losses**

Losses in stress due to seating, shortening, relaxation, creep and shrinkage were considered during design of the specimens.

##### Seating Losses

After tensioning the strand with the ram, the strand was released from the ram and the force was transferred to the anchor head. During the transfer, the tapered outer wedge walls came into contact with the matching tapered walls of the holes in the anchor head and the teeth of the inside face of the wedge “bite” into the strand to hold it in place. The loss occurred as the wedge places, or seats, itself into the anchor head and the strand is allowed to shorten. Seating losses were especially important in very short specimens such as those intended for the present study. The actual shortening as the wedges seat was divided by the tendon length to reduce the initial strain in the tendon. This is called the seating

loss. Seating losses can be minimized by power seating or pushing the wedges forward into the anchor head. Most commercially available post-tensioning equipment has incorporated power seating capabilities.

Because the strands are less than 6 ft. long, a quite small amount of uncompensated seating loss could render the prestress force negligible. Therefore, it was important to determine seating losses for the strand length and stressing equipment used. Once determined, overstressing the tendon can compensate for seating losses. To determine seating losses for both sets of stressing equipment used for the three strand and seven strand anchor heads, an existing steel frame of approximately the same length as the test specimen was modified with 2-in. thick steel bearing plates welded at the ends. The stressing frame is shown in Figure 4.6.

The trial specimens used different anchor heads and stressing techniques than the other specimens due to material availability problems described in Section 2.3.4. The procedure for determining seating losses using stressing methods employed in all test beams (other than the initial trial specimens) is as follows:

1. Place strands through frame, center-hole ram and anchor heads and install wedges at each end. The overall setup is seen in Figure 4.6.
2. Stress each strand individually to desired force and power seat using equipment built into the nose of the ram. The description of the ram is included in Section 4.8.1.
3. Once the entire tendon has been stressed and seated, incrementally apply pressure to the center-hole ram and measure elongation using a dial gauge magnetically attached to the center-hole ram. The dial gauge setup can be seen in Figure 4.6. When the force in the center-hole ram overcomes the force in the tendon, the tendon will begin to



elongate; therefore, the seating loss is the difference between the expected force to which the tendon was initially stressed and the actual force in the tendon determined by pressurizing the center-hole ram and measuring tendon elongation.

Three seating loss experiments were conducted at various levels of tension. The seating losses were determined to be approximately 7.25 kip per strand. This indicated that great care and overstressing were required in seating the actual specimens. In order to achieve an end result of 15% GUTS or 6.2 kip per strand, each strand needed be stressed to approximately 13.5 kip.



***Figure 4.6: Seating Loss Experiment Setup***

### Friction Losses

Friction losses in post-tensioning is a function of the type of materials used, length of duct and curvature. Since the ducts in the specimen are only 4.5 ft. long and the angle change is only 10 degrees through the negative drape, friction losses were assumed to be negligible and therefore ignored.

### Elastic Shortening Losses

When stressing is completed sequentially instead of all at once, induced tensile forces in elements stressed early in the stressing process can be reduced as compressive strain from subsequent stressed elements allow already stressed elements to relax. Due to equipment limitations caused by material availability, individual strands, not full tendons, were stressed sequentially. Although the shortening losses were assumed to be negligible due to the low levels of prestress (15% GUTS), steps were taken to minimize potential effects. Stressing of individual strands was alternated between the two tendons. The stressing sequence is detailed in Figure 4.7.

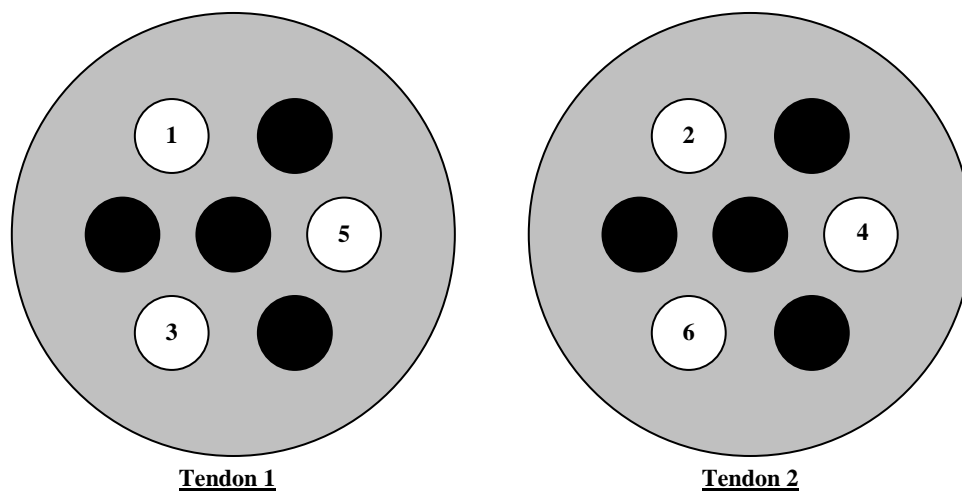


***Figure 4.7: Stressing Sequence (Live End Shown)***

### Relaxation Losses

Relaxation is the loss of stress in a stressed material held at constant length (Nilson 2004). In prestressing strand, essentially no relaxation occurs if the initial stress in the tendon is less than 55% of the yield stress. Therefore, relaxation losses were ignored due to the low level of prestress used in the research specimens.

### Creep Losses

Creep is the slow deformation of concrete over considerable lengths of time at constant stress or load (Nilson 2004). As creep takes place and the beam shortens, the tendons shorten and loose prestress. Long-term creep calculations were made. These indicated that the creep losses would be quite low due to the low level of prestress and relatively mature concrete at stressing. The calculations indicated that there should be a reasonable level of prestress through the life of the specimen.

### Shrinkage Losses

Shrinkage is the volume reduction of concrete due to evaporation of water from the concrete mixture. Shrinkage, which continues at a decreasing rate for several months, depending on the configuration of the member, is a detrimental property of concrete in several respects (Nilson 2004). Concrete shrinkage may lead to cracking and partial loss of initial prestress. Due to the maturity of the concrete at the time of prestressing, shrinkage losses were neglected during specimen design.

### Conclusion

Consideration of all losses indicated that the tendon should remain at reasonable level of prestress throughout the duration of the research.

## 4.8 STRESSING

There were two independent stressing operations: prestress and live load. Prestressing was the first procedure completed after casting of concrete. Live load application occurred after grouting and sealing of anchorages discussed in Sections 4.9 and 4.10 respectively.

### 4.8.1 Prestress Procedure

Stressing was completed with a monostrand ram with power seating capabilities. To make handling the ram and stressing less cumbersome, the ram was suspended from a winch on a swinging beam installed above the work area at the north end of FSEL. The stressing setup is shown in Figure 4.8.



*Figure 4.8: Prestressing Setup*

The stressing process is listed below. In addition to the actual stressing procedures, preparation steps are listed as well.

#### Preparation

1. Clean ducts of dust and debris using pressurized air.
2. Attach data acquisition equipment (see data acquisition description in Section 4.8.3).
3. Place strand through duct and place anchor heads against bearing plates with wedges in place.
4. Suspend ram from winch above worksite and attach hydraulics.

#### Stressing

5. Overstress each strand to 13.5 kip as described in Section 4.7.2 and then power seat and release.
6. Repeat Step 5 for all 6 strands following the sequence shown in Figure 4.7.
7. Trim the tails of the strand at the live end to approximately 1.25 in. using a grinder. Tails at the dead end were set at approximately 1.25 in. before stressing when setting the strands and wedges in place.

### **4.8.2 Live Load Procedure**

Live load was applied to the specimen via a Dywidag bar placed through a PVC pipe in the corbels. The length of the bar was approximately 9 ft. to allow for the length of the beam, springs, hardware and stressing equipment. The Dywidag assemblies for both ends, with stressing equipment in place, are shown in Figure 4.9. The preparation and stressing procedures for the Dywidag live load assembly are listed below.

### Preparation

1. Place Dywidag bar through both corbels of the specimen and place all permanent hardware along the Dywidag bar at the ends of the specimen.
2. Attach data acquisition equipment (see data acquisition description in Section 4.8.3).
3. Place feet of the stressing chair against the web of the channel at the live end and place the center hole ram against the surface of the chair.

### Stressing

4. Incrementally stress Dywidag bar and check for cracks between loading; if cracks are present, trace crack with a marker and record crack width and corresponding load.
5. Once acceptable cracking according to Section 3.1.2 has taken place, tighten the Dywidag nut at the live end to maintain level of force and then release ram pressure.

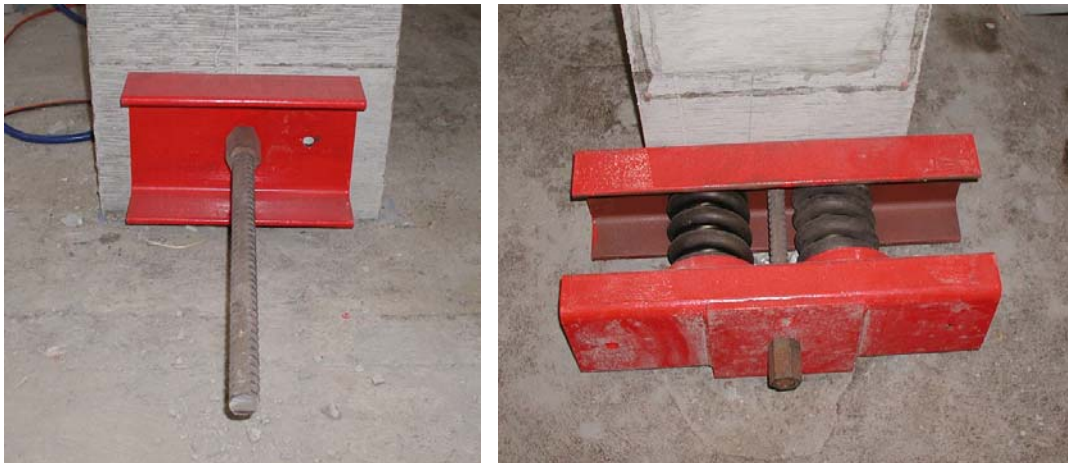


***Figure 4.9: Dywidag Assembly, Live End (Left) and Dead End (Right)***

Cracks extending from the reentrant corner at the live end formed in the corbel during the live load application process. The unintentional cracks were

sealed with the same pre-mixed concrete patch used to cover the anchorage pockets (see Section 4.10). The cracks along the sides of the reduced midsection of the specimen were sealed with an epoxy. Otherwise, ponded saltwater in the depression along the top surface of the beam would leak through the cracks out the sides of the specimen (see Section 5.2 for saltwater exposure details). The cracks along the top surface of the midsection of the beam were left open for accelerated results (see Sections 3.1.2 and 3.1.3).

#### **4.8.3 Data Acquisition**

During the stressing processes, a data acquisition system was used to record strain along the top of the beam and applied force. The change in length along the top surface was measured using two LVDTs – one on each side of the beam – and a rigid assembly attached to the beam using the lifting anchor inserts; therefore, LVDTs measured total change in length in the region between the lifting anchors which includes the reduced section of interest. The hardware for measuring elongation and compression along the top of the beam is shown in Figure 4.10 while the data collection equipment is shown in Figure 4.11.

Force was measured using a pressure transducer attached to the pump. The applied force is the pump pressure multiplied by the effective area of the ram. Redundant mechanical systems were in place to check the electronic output before and during stressing. A dial gauge assembly was attached parallel to the LVDTs and a pressure gauge was placed inline with the pressure transducer.





*a) overview*

*b) close-up*

**Figure 4.10: Data Acquisition Hardware**

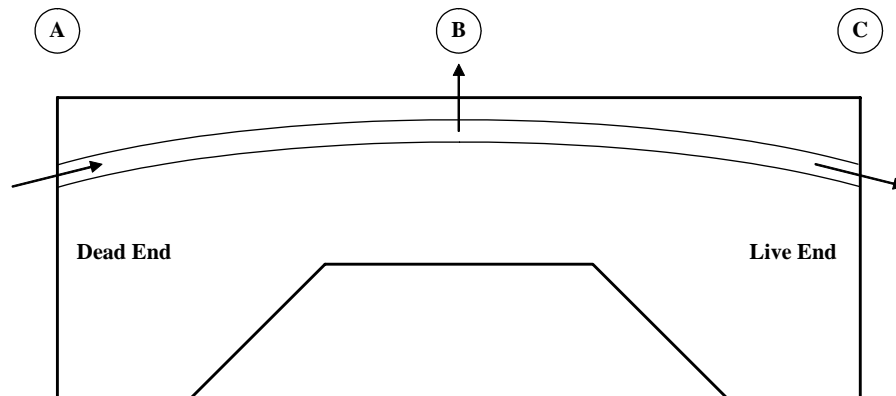


**Figure 4.11: Data Acquisition Equipment**



## 4.9 GROUTING

Grouting was completed within 48 hours of stressing as required in Section 426.9 of Texas Standard Specifications. Sika Grout 300 PT was used to grout the ducts. Sika is a non-bleed, high flow and sand free grout. The grout was proportioned according to bag instructions and mixed in a bucket using an electric hand drill and paddle. A hand pump was used to place the grout into the ducts. There were three openings along the length of the duct: two grouting ports in the bearing plates and a grouting vent at the apex of the drape. Plastic hose provided by VSL was threaded into the grout ports. The hose for the vent at the apex was already in place. Plastic caps were placed at the end of all hoses to stop grout and seal the duct. The grouting procedure adopted from VSL (2002) is listed in Figure 4.12 and is shown in progress in Figure 4.13.



1. Pump grout into ducts at A.
2. Cap grout vent at B once consistent flow is observed from the vent.
3. Cap grout vent at C once consistent flow is observed from the vent.
4. Maintain grout pressure with vents closed for approximately 1 minute and then open vent at B to allow any trapped air to escape. Recap vent at B once even flow resumes.
5. Cap grout vent at A.

**Figure 4.12: Grouting Procedure**

Temporary grouting caps provided by VSL were used to prevent loss of grout through gaps of the wedges. Grout flow from the unused anchor head holes was prevented by epoxy plugs described in Section 2.3.4. The caps were placed against the back of the anchor head and over the tails of the strand. In order for air to escape, the temporary grouting caps were also vented with small holes that were plugged with golf tees once consistent flow was observed from the vent. The temporary grouting caps and plastic hoses threaded into the grouting ports at the dead end are shown in Figure 4.14.



*Figure 4.13: Grouting Specimens (Kyle Steuck pictured)*



*Figure 4.14: Temporary Grouting Caps*

#### **4.10 SEALING ANCHORAGE TECHNIQUES**

In order to protect the post-tensioning hardware, the 2004 TxDOT Standard Specifications require anchorage pockets to be backfilled with concrete or mortar. All surfaces to be covered must be cleaned of rust, grout and other materials and then coated with TxDOT Type V or VII epoxy conforming to TxDOT DMS-6100 prior to placing the pour back concrete or mortar. The mortar or concrete is to be placed while the epoxy is still tacky. The two-part Type V epoxy provided by Unitex was used to coat all surfaces to be covered. The epoxy was proportioned according to instructions on the container and mixed in plastic 6 in. x 12 in. cylinder forms with an electric hand drill and paddle. Masterflow 928 provided by Degussa Building Systems was used to backfill the anchorage

pockets. The non-shrink mortar was proportioned according to bag instructions and mixed in plastic buckets with an electric hand drill and paddle.

The TxDOT Type V epoxy is a two-part epoxy and was mixed according to instructions on the packaging. A wire brush was used to clean the surfaces. After the surface preparation, the epoxy was applied using a paintbrush.

Forms were built to fit the dead end and live end anchorage pockets. The dead end form was attached to the specimen using plastic anchors in concrete and sealed with silicone. The live end was attached with bar clamps and sealed with silicon. Plastic buckets, funnels and plastic hoses were used to fill the anchorage pockets with Masterflow 928. The pour back process is shown in Figure 4.15.

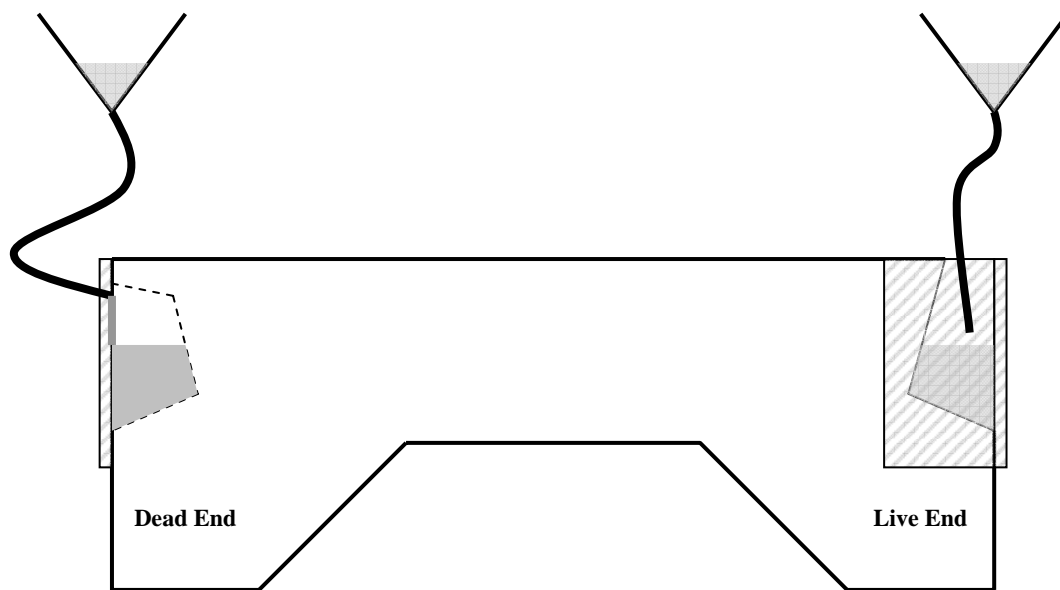


*Figure 4.15: Pour Back Process*

The anchorage pour back forms were removed after a minimum of two days of moist curing. Pre-mixed concrete patch was spread over both anchorage pockets to fill imperfections in the grout and produce a more uniform surface.

## CHAPTER 5

### Exposure and Monitoring Techniques

#### 5.1 LOCATION

The research beams were placed in two groups at the north end of FSEL for long-term monitoring and testing. The location of each beam depended on whether or not it was to be subjected to saltwater drips over the dead end anchorage zones. Refer to Section 5.2 for more details of the dead end anchorage exposure. To avoid moving Project 1405 beams and blocking access to the north door of FSEL, the Project 4562 beams were placed in the vacant spaces around the existing Project 1405 beams. A general location map is shown in Figure 5.1. Detailed placement maps of both sections are shown in Figures 5.2 and 5.3.

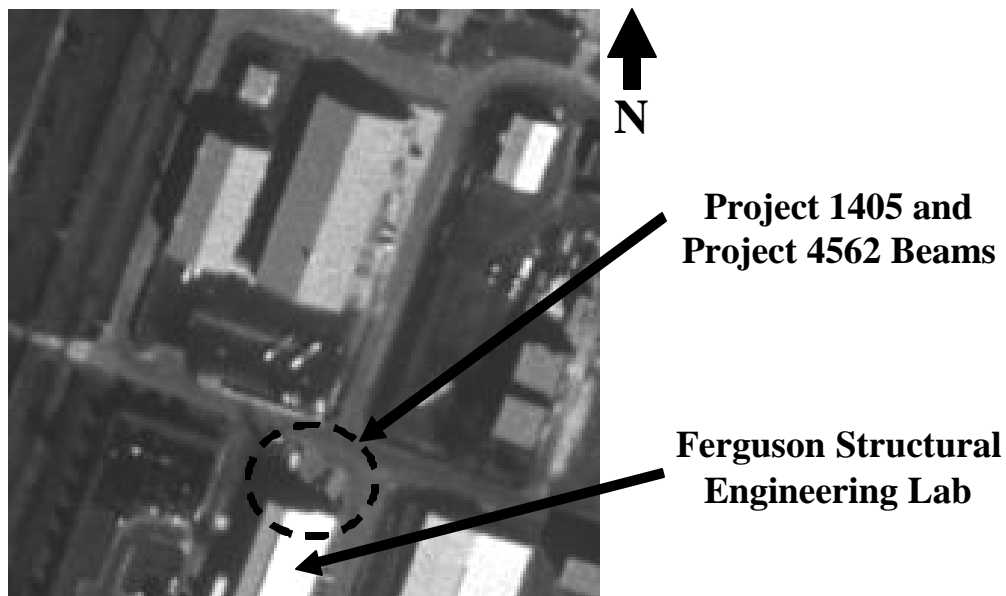


*Figure 5.1: General Beam Location by Aerial Photo (Terraserver)*

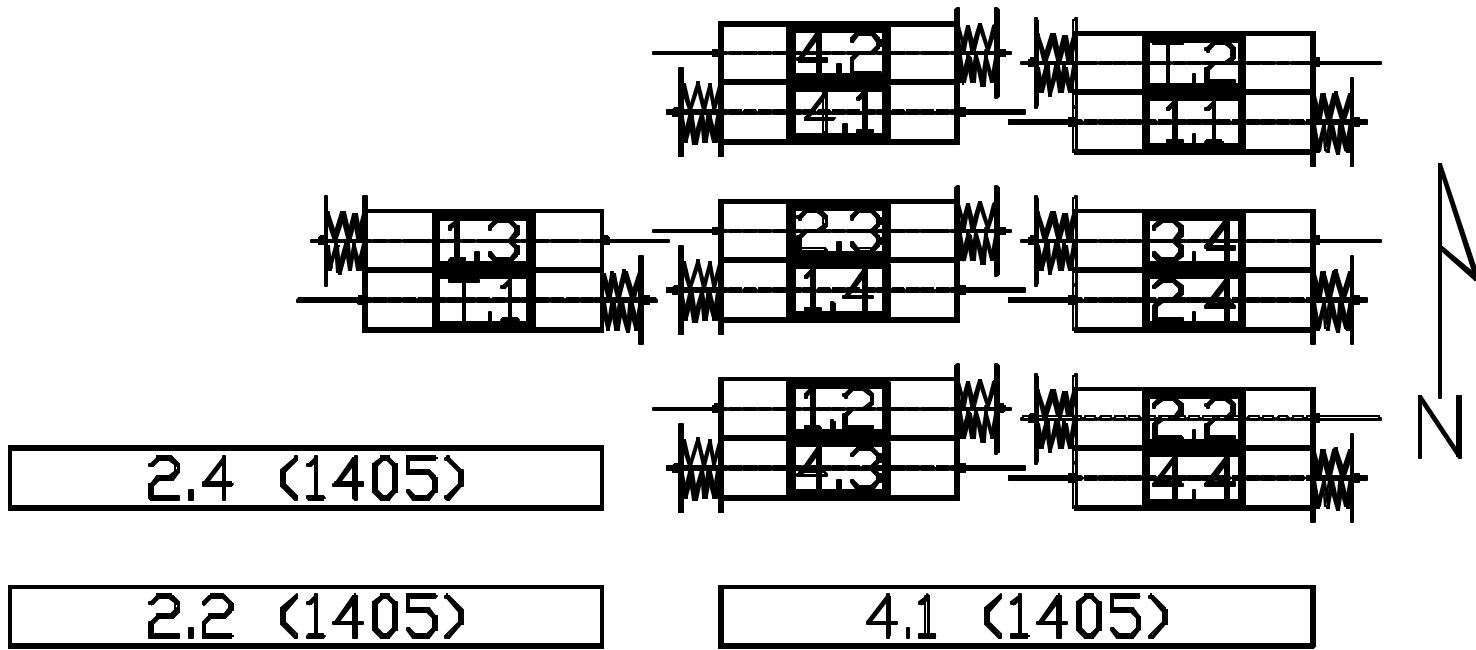
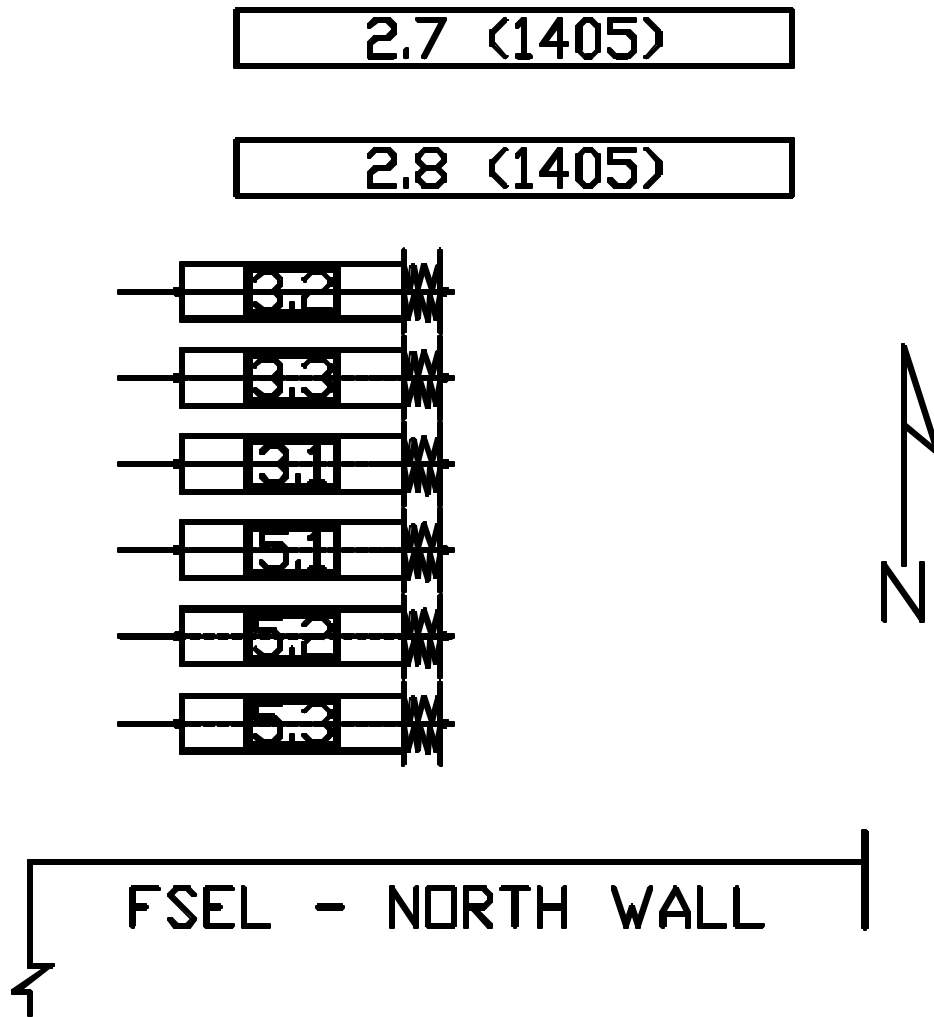


Figure 5.2: Non-Anchorage Exposure Specimens



*Figure 5.3: Anchorage Exposure Specimens*

## **5.2 CYCLED EXPOSURE**

The research beams are subjected to cycled saltwater exposure to simulate aggressive chloride environments such as coastal regions and locations that utilize deicing salts. All specimens are subjected to ponded saltwater at the center of the top surface of the beam directly over the post-tensioning ducts. In addition to the ponded saltwater, several specimens are also subjected to dead end anchorage exposure. Specimens subjected to dead end anchorage exposure are double-underlined in the specimen matrix shown in Table 2.1.

### **5.2.1 Ponded Saltwater**

A cast-in-place depression was provided in the top surface of the beam in order to pond saltwater directly above the post-tensioning tendons. Project 1405 created a pond for saltwater with plastic walls and silicone seals on the top surface of the beam, but the ponds were prone to leaking and would not always retain the saltwater for the salt solution exposure duration. Therefore, the saltwater ponds were built into the Project 4562 specimens in order to avoid possible future maintenance issues. Figure 5.4 is a detail of the saltwater exposure.

In an effort to provide continuity between Project 1405 and Project 4562 research results, the salt solution exposure cycles match those used in the previous post-tensioning durability research: alternating two-week cycles of wet and dry. During the wet cycle, 3.5% saltwater is ponded in the cast-in-place depression and covered. The 3.5% salt (NaCl) solution was taken from ASTM G109 when West started, although the most recent version of the testing standard specifies 3% instead of 3.5%. It was decided to maintain continuity of the experiments by using 3.5%. At the beginning of the dry cycles, all remaining saltwater and residue will be removed from the depression with freshwater and a sponge. The depression should remain uncovered until dry and then recovered. Covers for the



depressions are provided to block rain and wind and limit evaporation of the salt solution during the wet cycle.

### **5.2.2 Anchorage Exposure**

In order to evaluate the corrosive resistance of the post-tensioning tendon at the anchorage zones, saltwater is sprayed over the dead end anchorage pocket. As described in Section 4.10, the surface of the post-tensioning anchorage hardware is coated with epoxy, backfilled with a non-shrink grout and then covered with a premixed concrete patch. Similarly to the ponded exposure on the top surface, 3.5% saltwater is also used over the anchorage zones. An exposure loop was established in order to reduce production of saltwater and operation tasks. The salt solution is pumped to the specimens, sprayed over the dead end anchorage pockets, collected towards the bottom of the beam and recycled back to the pump. Garden sprinkler components are used to create a planar, 45 degree fanned spray of saltwater across the backfilled surface of the anchorage pocket. A saltwater exposure detail is shown in Figure 5.4.

To match exposure cycles from Project 1405, the dead end anchorage exposure will be conducted one day for at least 6 hours every 4 weeks. The dead end anchorage exposure coincides with the beginning of the wet cycle to combine similar tasks.

As stated in Section 5.1, all specimens were not subjected to dead end anchorage exposure. The beams with the two-way ribbed plastic duct/non-galvanized bearing plates combination were selected to provide a direct comparison for six of the seven types of strands used in the research specimens. There was not an epoxy coated strand/two way ribbed plastic duct combination included in the matrix. Therefore, the epoxy coated strand/galvanized steel duct

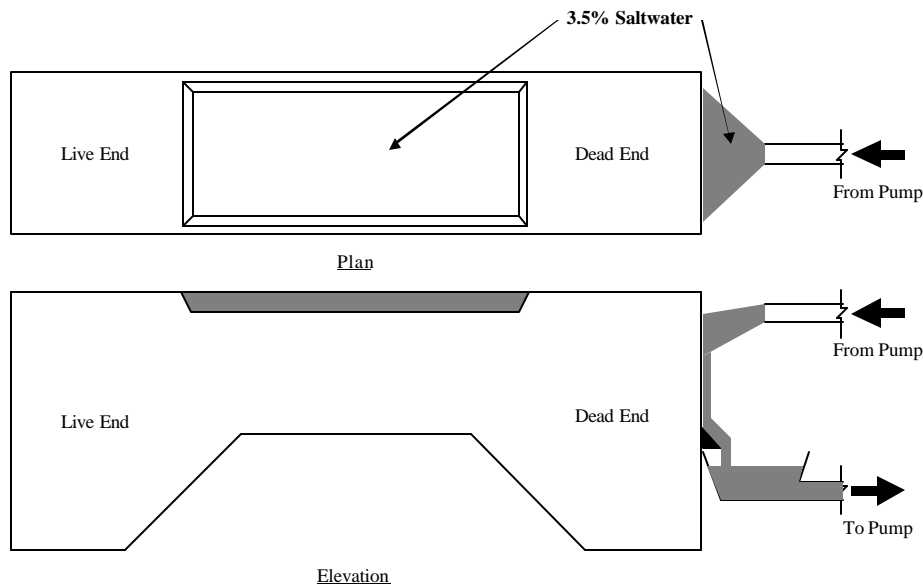


**Figure 5.4: Saltwater Exposure Detail**

specimen (Beam 2.1) was added to the dead end anchorage exposure group in order to test epoxy coated strand anchorages. The electrically isolated tendon (EIT) specimens were selected to evaluate the potential corrosion protection of the permanent cap over the anchor head. In order to test the possible corrosion performance benefits of galvanized bearing plates, the combination of conventional strand/galvanized bearing plates/two way ribbed plastic duct (Beam 5.1) was included as a direct comparison with a similar beam with non-galvanized bearing plates (Beam 3.1). The final specimen matrix is shown in Table 2.1 – the anchorage exposure specimens are double underlined.

### 5.3 MONITORING

To provide continuity between future results from Project 4562 specimens and existing Project 1405 data, the same forms of non-destructive corrosion monitoring techniques, such as visual examination and half-cell potentials, are used on both sets of specimens. In addition to Project 1405 methods, AC

impedance measurements were added for the electrically isolated tendon specimens.

### **5.3.1 Visual Examination**

During regular maintenance, monitoring and exposure, the specimens are inspected for visual signs of corrosion such as rust stains, changes in cracking, and concrete spalling.

### **5.3.2 Half-Cell Potential Readings**

The magnitude of the half-cell potential readings can indicate the probability of active corrosion, but can not determine the rate or magnitude of the degradation. Taken at regular intervals, the half-cell potential readings can determine the time of corrosion initiation.

As explained in Section 1.2.3, electrochemical cells consist of a two half-cells – one anodic and the other cathodic. By making one of the half-cells a known or reference half-cell, the second cell can be isolated for measurement or study (Jones 1996). The saturated calomel electrode (SCE) is the most common form of reference electrode and is used to monitor the Project 4562 and 1405 research specimens. The standard hydrogen electrode (SHE) is the benchmark for reference electrodes with a reference potential of 0.000V. The reference potential of a SCE with respect to a SHE is +0.241V. The isolated half-cell reaction of interest is the corrosion of the prestressing materials. Ground clamps were connected to both prestressing tendons with wires extending out of the concrete at the live end of the specimen. Readings are taken by a voltmeter connected between the reference electrode and the prestressing hardware. Saltwater that permeated into the concrete during the wet cycle serves as an indirect connection between the two half-cells. Therefore, half-cell potential readings are taken immediately following the two-week wet cycle described in Section 5.2.1. A

schematic of the half-cell potential reading is shown in Figure 5.5. Readings are taken along a grid established within the depression on the top surface of the beam. The grid spacing is 6" along the length of the beam and 3" laterally. The half-cell potential sampling grid is show in Figure 5.6.

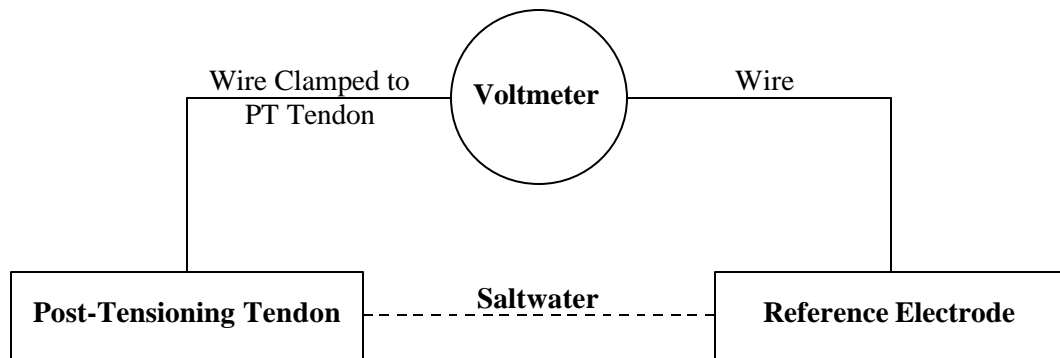


**Figure 5.5: Half-Cell Potential Reading Schematic**

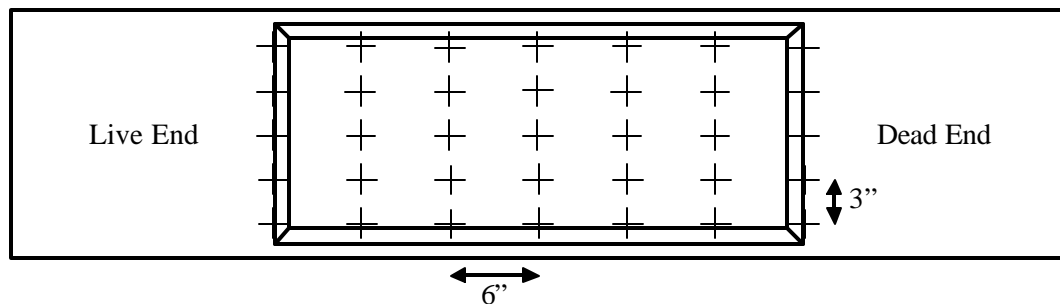


**Figure 5.6: Half-Cell Potential Reading Sampling Grid**

The relationship between the half-cell potential readings and the probability of corrosion is shown in Table 5.1. The magnitudes in Table 5.1 are ASTM C876 standards for corrosion of uncoated reinforcing steel in concrete and are not directly intended for post-tensioned concrete. In general, half-cell

potentials are not an effective method for monitoring corrosion activity in bonded post-tensioned structures. However, due to the lack of non-destructive methods of monitoring corrosion activity in post-tensioned concrete, it was decided to use regular half-cell potentials to monitor specimen condition (West 1999).

**Table 5.1: Interpretation of Half-Cell Potentials for Uncoated Reinforcing Steel**

<b>Measured Potentials (vs. SCE)</b>	<b>Probability of Corrosion</b>
More positive than -130 mV	less than 10% probability of corrosion
between -130mV and -280mV	corrosion activity uncertain
More negative than -280mV	Greater than 90% probability of corrosion

### **5.3.3 AC Impedance**

AC impedance measurements are used to monitor the condition of electrically isolated tendons during service life. The measurements require a sound electrical connection to each individual tendon and another connection to the rebars (VSL 2003). The tendon connection is a wire attached to the anchor head that goes through the protection cap and out the concrete surface at the live end of the specimen. The rebar connection could not be made directly to the main reinforcement cage due to the epoxy coating. Therefore, two additional bare steel rebars with connection wires were placed on each side and parallel to the post-tensioning duct with similar concrete cover to conduct the AC impedance measurements. The additional bare steel reinforcement and monitoring connections are shown in Figure 5.7. Monitoring of the electrically isolated tendons is performed with AC impedance measurements at frequency of 1 kHz. From laboratory studies the limiting values for a sound encapsulation was found to be 500 kW\*m (VSL 2003).

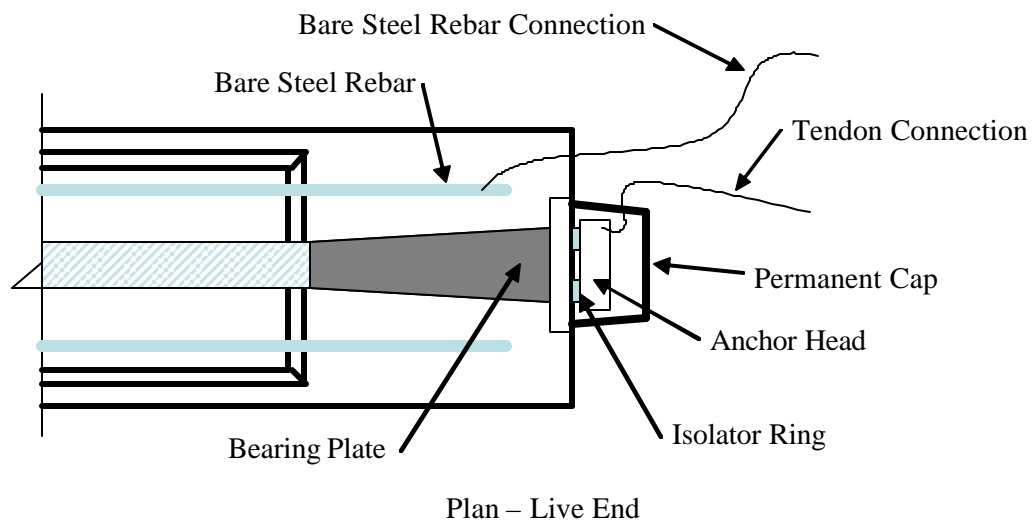


**Figure 5.7: EIT Monitoring Connections Detail**

# **CHAPTER 6**

## **Test Specimens**

### **6.1 INTRODUCTION**

The objective of Chapter 6 is to catalog all information pertaining to the 4562 test specimens. The records are needed in order to evaluate the corrosion resistance performance of the tested materials when the test specimens are autopsied at a future date.

During production of the test specimens, the important test specimen information – such as materials used, concrete strengths and important dates – was organized into a Specimen Catalog. The catalog was continuously updated throughout the production portion of the research project. The final Specimen Catalog is shown in Tables 6.1 and 6.2.

### **6.2 SPECIMEN DETAILS**

All pertinent information regarding the contents and history of each beam is given in Section 6.3. The information is sorted into four categories – materials, important dates, stressing history and comments. Table 6.3 shows the scope of material under each category.

**Table 6.1: Specimen Catalog (1 of 2)**

Cast Group	PROJECT 4562 - SPECIMEN CATALOG (1 of 2)						
	Specimen Name	Specimen ID	Anchor	Anchor Head	Strand	Duct	Coupler
T	T.1	TEST-GA-CON-CS-CG-T	Non-Galvanized	0.5" 3-Hole	Conventional	Corrugated Steel	None
	T.2	TEST-NGA-CON-CS-CG-T	Galvanized	0.5" 3-Hole	Conventional	Corrugated Steel	None
1	1.1	NGA-CON-CS-CG-1	Non-Galvanized	0.5" 7-Hole	Conventional	Corrugated Steel	None
	1.2	NGA-CU-CS-CG-1	Non-Galvanized	0.5" 7-Hole	Copper Clad	Corrugated Steel	None
	1.3	NGA-SC-CS-CG-1	Non-Galvanized	0.6" 3-Hole	Stainless Clad	Corrugated Steel	None
	1.4	GA-CON-CS-CG-1	Galvanized	0.5" 7-Hole	Conventional	Corrugated Steel	None
2	2.1	NGA-FF-CS-CG-2	Non-Galvanized	<i>Not Available</i>	Flow-Filled	Corrugated Steel	None
	2.2	NGA-HDG-CS-CG-2	Non-Galvanized	0.5" 7-Hole	Hot Dip Galvanized	Corrugated Steel	None
	2.3	NGA-CON-1P-CG-2	Non-Galvanized	0.5" 7-Hole	Conventional	GTI One-Way Plastic	Snap-On (Duct 1)
	2.4	NGA-CU-1P-CG-2	Non-Galvanized	0.5" 7-Hole	Copper Clad	GTI One-Way Plastic	Snap-On (Duct 1)
3	3.1	NGA-CON-2P-CG-3	Non-Galvanized	0.5" 7-Hole	Conventional	GTI Two-Way Plastic	Slip-On (Duct 1)
	3.2	NGA-HDG-2P-CG-2	Non-Galvanized	0.5" 7-Hole	Hot Dip Galvanized	GTI Two-Way Plastic	Slip-On (Duct 1)
	3.3	NGA-CU-2P-CG-3	Non-Galvanized	0.5" 7-Hole	Copper Clad	GTI Two-Way Plastic	Slip-On (Duct 1)
	3.4	NGA-HDG-1P-CG-3	Non-Galvanized	0.5" 7-Hole	Hot Dip Galvanized	VSL One-Way Plastic	Snap-On (Duct 1)
4	4.1	NGA-SS-CS-CG-4	Non-Galvanized	0.6" 3-Hole	Stainless	Corrugated Steel	None
	4.2	NGA-SS-1P-CG-4	Non-Galvanized	0.6" 3-Hole	Stainless	VSL One-Way Plastic	Snap-On (Duct 1)
	4.3	Comparison-Epoxy-4	Non-Galvanized	None	None	None	None
	4.4	Comparison-Uncoated-4	Non-Galvanized	None	None	None	None
5	5.1	GA-CON-2P-CG-5	Galvanized	0.5" 7-Hole	Conventional	GTI Two-Way Plastic	Slip-On (Duct 1)
	5.2	NGA-SC-2P-CG-5	Non-Galvanized	0.6" 3-Hole	Stainless Clad	GTI Two-Way Plastic	Slip-On (Duct 1)
	5.3	NGA-SS-2P-CG-5	Non-Galvanized	0.6" 3-Hole	Stainless	GTI Two-Way Plastic	Slip-On (Duct 1)
6	6.1	NGA-EG-CS-CG-6	Non-Galvanized	<i>Not Available</i>	Electroplated Galvanized	Corrugated Steel	None
	6.2	NGA-EG-1P-CG-6	Non-Galvanized	<i>Not Available</i>	Electroplated Galvanized	VSL One-Way Plastic	Snap-On (Duct 1)
	6.3	NGA-EG-2P-CG-6	Non-Galvanized	<i>Not Available</i>	Electroplated Galvanized	GTI Two-Way Plastic	Slip-On (Duct 1)
7	7.1	EIT-CON-CG-7	EIT (CS2000)	<i>Not Available</i>	Conventional	VSL One-Way Plastic	Snap-On (Duct 1)
	7.2	EIT-CON-CG-7	EIT (CS2000)	<i>Not Available</i>	Conventional	VSL One-Way Plastic	Snap-On (Duct 1)
	7.3	EIT-HDG-CG-7	EIT (CS2000)	<i>Not Available</i>	Hot Dip Galvanized	VSL One-Way Plastic	Snap-On (Duct 1)
	7.4	EIT-FF-CG-7	EIT (CS2000)	<i>Not Available</i>	Flow-Filled	VSL One-Way Plastic	Snap-On (Duct 1)



Table 6.2: Specimen Catalog (2 of 2)

Cast Group	PROJECT 4562 - SPECIMEN CATALOG (2 of 2)									
	Specimen Name	Concrete Data				Important Dates				
		Date Cast	7-Day (psi)	14-Day (psi)	28-Day (psi)	Prestressing	Grouting	Protection	Live Load	Exposure Initiation
T	T.1	9-Apr-04	4460	5290	5920	Not Available	Not Available	Not Available	Not Available	Not Available
	T.2	9-Apr-04	4460	5290	5920	Not Available	Not Available	Not Available	Not Available	Not Available
1	1.1	16-Aug-04	3720	4370	4860	25-Jan-05	27-Jan-05	3-Feb-05	22-Feb-05	Not Available
	1.2	16-Aug-04	3720	4370	4860	17-Feb-05	17-Feb-05	24-Feb-05	3-Mar-05	Not Available
	1.3	16-Aug-04	3720	4370	4860	18-Apr-05	18-Apr-05	21-Apr-05	26-Apr-05	Not Available
	1.4	16-Aug-04	3720	4370	4860	25-Jan-05	27-Jan-05	3-Feb-05	22-Feb-05	Not Available
2	2.1	18-Oct-04	3030	3590	4080	Not Available	Not Available	Not Available	Not Available	Not Available
	2.2	18-Oct-04	3030	3590	4080	16-Feb-05	17-Feb-05	24-Feb-05	3-Mar-05	Not Available
	2.3	18-Oct-04	3030	3590	4080	27-Jan-05	1-Feb-05	3-Feb-05	22-Feb-05	Not Available
	2.4	18-Oct-04	3030	3590	4080	16-Feb-05	17-Feb-05	24-Feb-05	3-Mar-05	Not Available
3	3.1	8-Dec-04	4260	5430	7260	27-Jan-05	1-Feb-05	3-Feb-05	22-Feb-05	Not Available
	3.2	8-Dec-04	4260	5430	7260	9-Mar-05	9-Mar-05	15-Mar-05	22-Mar-05	Not Available
	3.3	8-Dec-04	4260	5430	7260	16-Feb-05	17-Feb-05	24-Feb-05	3-Mar-05	Not Available
	3.4	8-Dec-04	4260	5430	7260	9-Mar-05	9-Mar-05	15-Mar-05	22-Mar-05	Not Available
4	4.1	10-Feb-05	5990	6810	7120	9-Mar-05	9-Mar-05	15-Mar-05	22-Mar-05	Not Available
	4.2	10-Feb-05	5990	6810	7120	9-Mar-05	9-Mar-05	15-Mar-05	22-Mar-05	Not Available
	4.3	10-Feb-05	5990	6810	7120	None	None	None	1-Mar-05	Not Available
	4.4	10-Feb-05	5990	6810	7120	None	None	None	1-Mar-05	Not Available
5	5.1	3-Mar-05	4710	5610	6180	16-Mar-05	17-Mar-05	21-Apr-05	26-Apr-05	Not Available
	5.2	3-Mar-05	4710	5610	6180	18-Apr-05	18-Apr-05	21-Apr-05	26-Apr-05	Not Available
	5.3	3-Mar-05	4710	5610	6180	16-Mar-05	17-Mar-05	21-Apr-05	26-Apr-05	Not Available
6	6.1	17-Mar-05	4210	4920	5730	Not Available	Not Available	Not Available	Not Available	Not Available
	6.2	17-Mar-05	4210	4920	5730	Not Available	Not Available	Not Available	Not Available	Not Available
	6.3	17-Mar-05	4210	4920	5730	Not Available	Not Available	Not Available	Not Available	Not Available
7	7.1	5-May-05	Not Available	Not Available	Not Available	Not Available	Not Available	Not Available	Not Available	Not Available
	7.2	5-May-05	Not Available	Not Available	Not Available	Not Available	Not Available	Not Available	Not Available	Not Available
	7.3	5-May-05	Not Available	Not Available	Not Available	Not Available	Not Available	Not Available	Not Available	Not Available
	7.4	5-May-05	Not Available	Not Available	Not Available	Not Available	Not Available	Not Available	Not Available	Not Available

**Table 6.3: Sorted Test Specimen Information**

<b>Materials</b>	<ul style="list-style-type: none"> <li>• Material Variables (strand, duct, coupler and bearing plate)</li> <li>• 28-Day Concrete Strength</li> </ul>
<b>Important Dates</b>	<ul style="list-style-type: none"> <li>• Casting Date</li> <li>• Prestress Application</li> <li>• Grouting Date</li> <li>• Anchorage Protection</li> <li>• Live Load Application</li> <li>• Exposure Initiation</li> </ul>
<b>Comments</b>	<ul style="list-style-type: none"> <li>• Special Circumstances</li> <li>• Abnormalities</li> </ul>
<b>Stressing History</b>	<ul style="list-style-type: none"> <li>• Crack Widths</li> <li>• Live Load Application Data</li> <li>• Crack Map</li> </ul>

The 28-day concrete strengths were determined by testing a minimum of three 6 in. x 12 in. companion cylinders. In addition to determining the 28-day strengths, cylinders were tested at 7 and 14 days to ensure proper strength gain. All information regarding the test specimens was initially tabulated in the Specimen Catalog shown in Tables 6.1 and 6.2.

In order to identify locations on the specimens, the orientations shown in Figure 6.1 were established. All recorded specimen information is consistent with the labeling system in Figure 6.1.

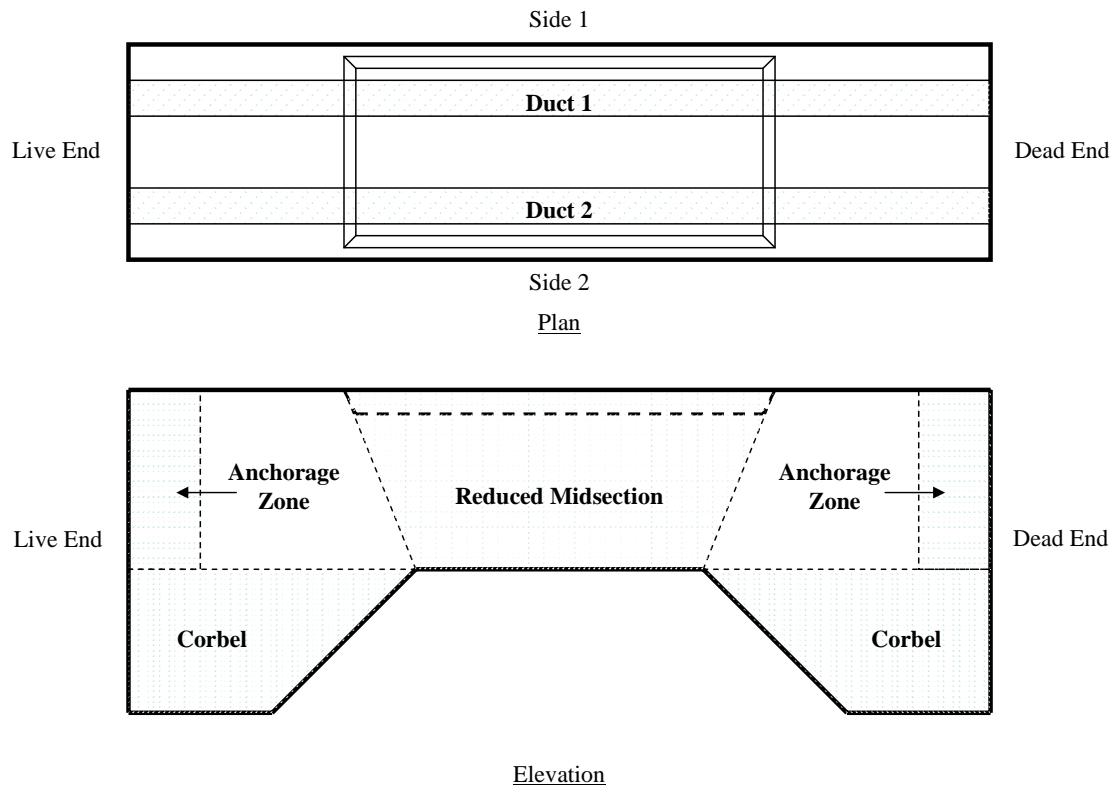


**Figure 6.1: Specimen Labeling System**

Included in the stressing history sections of each beam is a plot of the live load application data. In each plot, there are two load-deformation curves – the live load is plotted against the specimen elongation of each side of the specimen along the top surface. A characteristic load-deformation curve is shown in Figure 6.2. There are several important features of the characteristic load-deformation plot:

- initial precompression of concrete due to prestress force
- change in specimen stiffness (slope of curve) due to cracking
- final top surface elongation after losses due to locking off the live load assembly and releasing pressure in the center-hole ram

The differences between the curves plotted for each side of the specimen are due to unequal precompression values. The disparity in initial precompression within a specimen may have developed due to material variability and accidental lateral eccentricities in the post-tensioning hardware.

Cracks in the concrete were traced with a marker as they formed. The crack widths were determined using an optical crack microscope. Magnified cracks were compared to a scale with 0.001 in. increments seen through the lens to determine width.

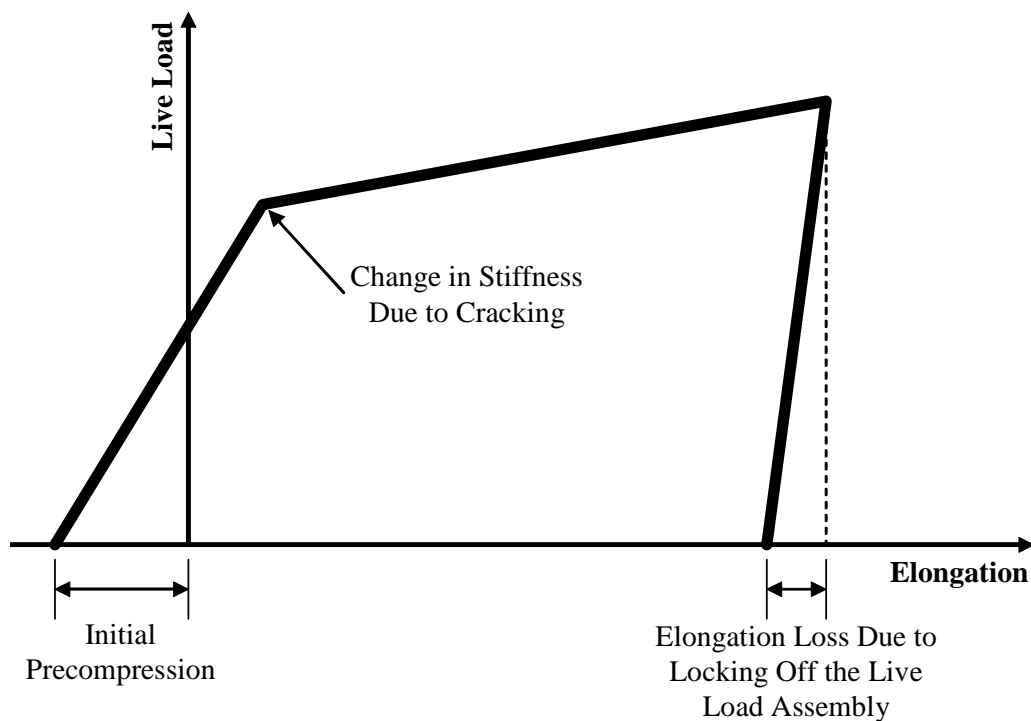


*Figure 6.2: Characteristic Load-Deformation Plot*

### 6.3 SPECIMEN DATA

Two examples of the specimen data cataloging format are shown in Sections 6.3.1 and 6.3.2 for Beams 1.1 and 2.2 respectively. Similar information for all research specimens is included in Appendix C.

#### 6.3.1 Beam 1.1

##### 6.3.1.1 Materials

*Table 6.4: Beam 1.1 Materials*

<b>Strand</b>	Conventional
<b>Duct</b>	Corrugated Steel
<b>Coupler</b>	None
<b>Bearing Plate</b>	Non-Galvanized
<b>28-Day Concrete Strength, <math>f'_c</math></b>	4860 psi

##### 6.3.1.2 Important Dates

*Table 6.5: Beam 1.1 Important Dates*

<b>Casting</b>	August 16, 2004
<b>Prestress Application</b>	January 25, 2005
<b>Grouting</b>	January 27, 2005
<b>Anchorage Protection</b>	February 3, 2005
<b>Live Load Application</b>	February 22, 2005
<b>Exposure Initiation</b>	<i>Not Available</i>

### 6.3.1.3 Stressing History

#### Live Load Application Plot

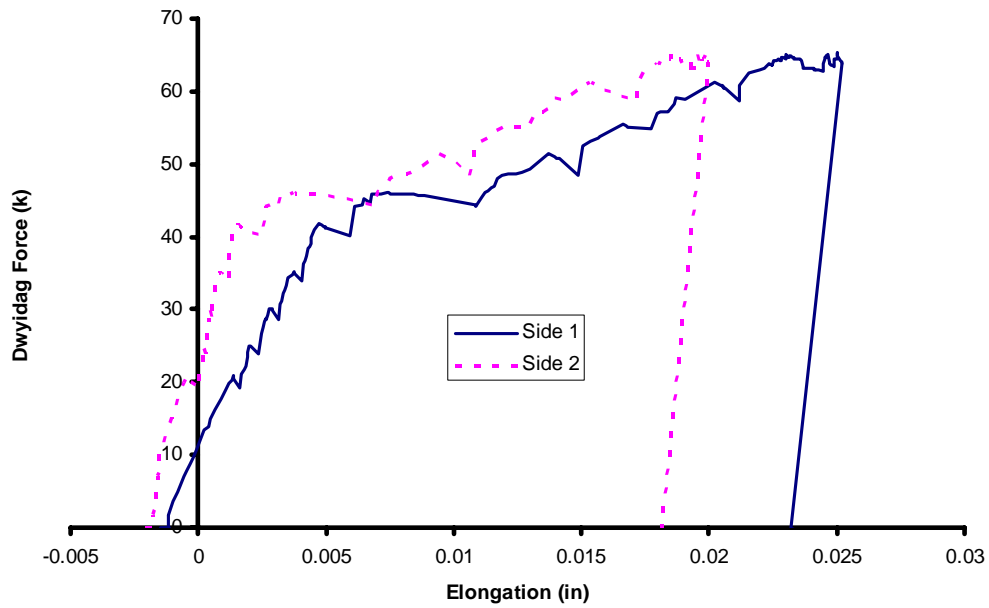


**Figure 6.3: Beam 1.1 Live Load Application Plot**

#### Crack Widths

The maximum measured crack width on the top of the specimen within the depression for the salt bath is 0.008 in. See the crack map within this section for additional information regarding location and widths of cracks.

### Crack Map

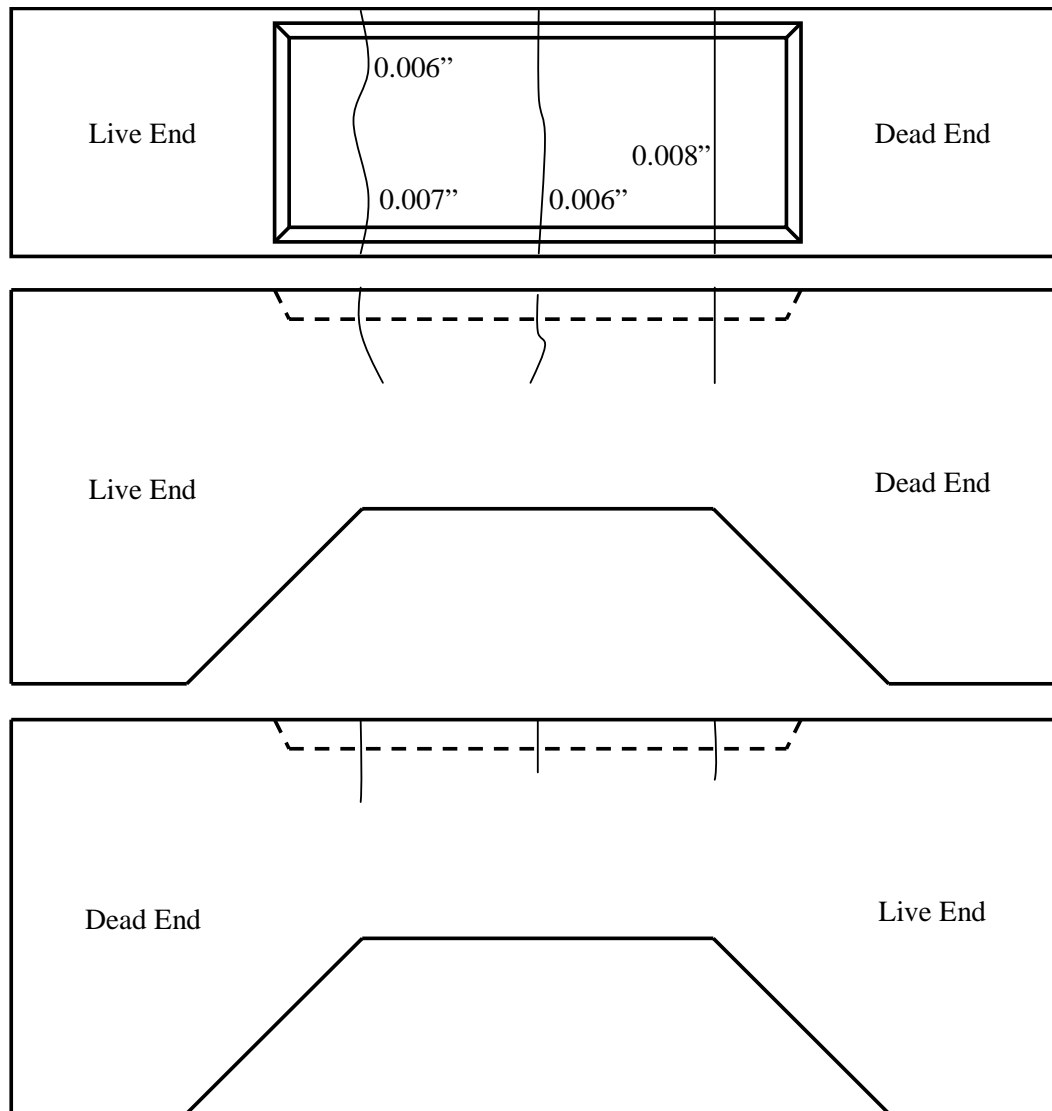


*Figure 6.4: Beam 1.1 Crack Map*

#### 6.3.1.4 Beam 1.1 Comments

- The duct-bearing plate connection was not sealed with duct tape before casting. Small amounts of concrete were removed from inside the bearing plates before proceeding with the remainder of specimen procedures.

- A shrinkage crack formed in the grout on the top surface of the live end pocket protection. The crack was sealed with epoxy before the initiation of exposure cycles.

### 6.3.2 Beam 2.2

#### 6.3.2.1 Materials

*Table 6.6: Beam 2.2 Materials*

<b>Strand</b>	Hot Dip Galvanized
<b>Duct</b>	Corrugated Steel
<b>Coupler</b>	None
<b>Bearing Plate</b>	Non-Galvanized
<b>28-Day Concrete Strength, <math>f'_c</math></b>	4080 psi

#### 6.3.2.2 Important Dates

*Table 6.7: Beam 2.2 Important Dates*

<b>Casting</b>	October 18, 2004
<b>Prestress Application</b>	February 16, 2005
<b>Grouting</b>	February 17, 2005
<b>Anchorage Protection</b>	February 24, 2005
<b>Live Load Application</b>	March 3, 2005
<b>Exposure Initiation</b>	<i>Not Available</i>



### 6.3.2.3 Stressing History

#### Live Load Application Plot

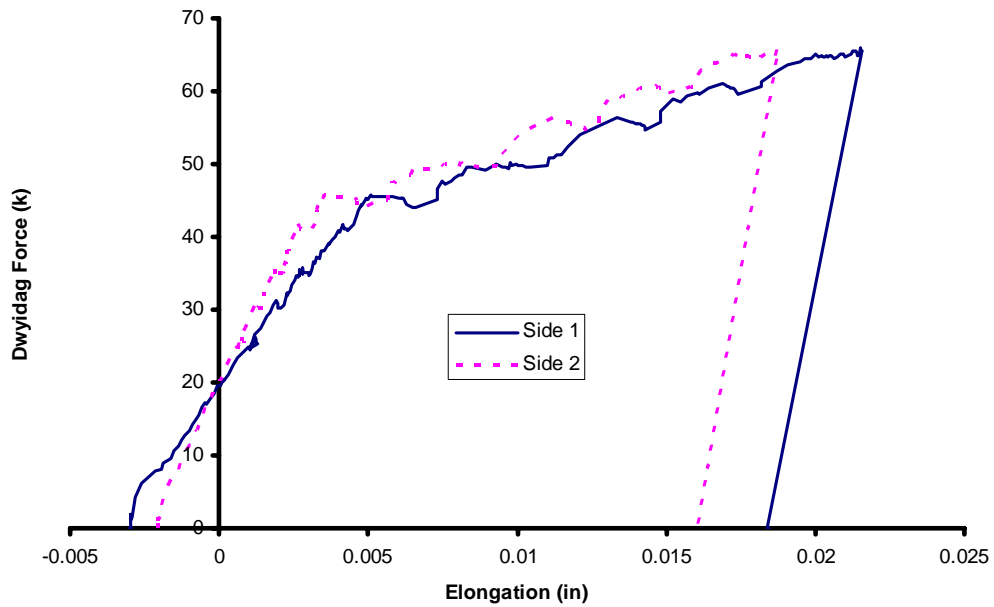


**Figure 6.5: Beam 2.2 Live Load Application Plot**

#### Crack Widths

The maximum measured crack width on the top of the specimen within the depression for the salt bath is 0.006 in. See the crack map within this section for additional information regarding location and widths of cracks.

### Crack Map

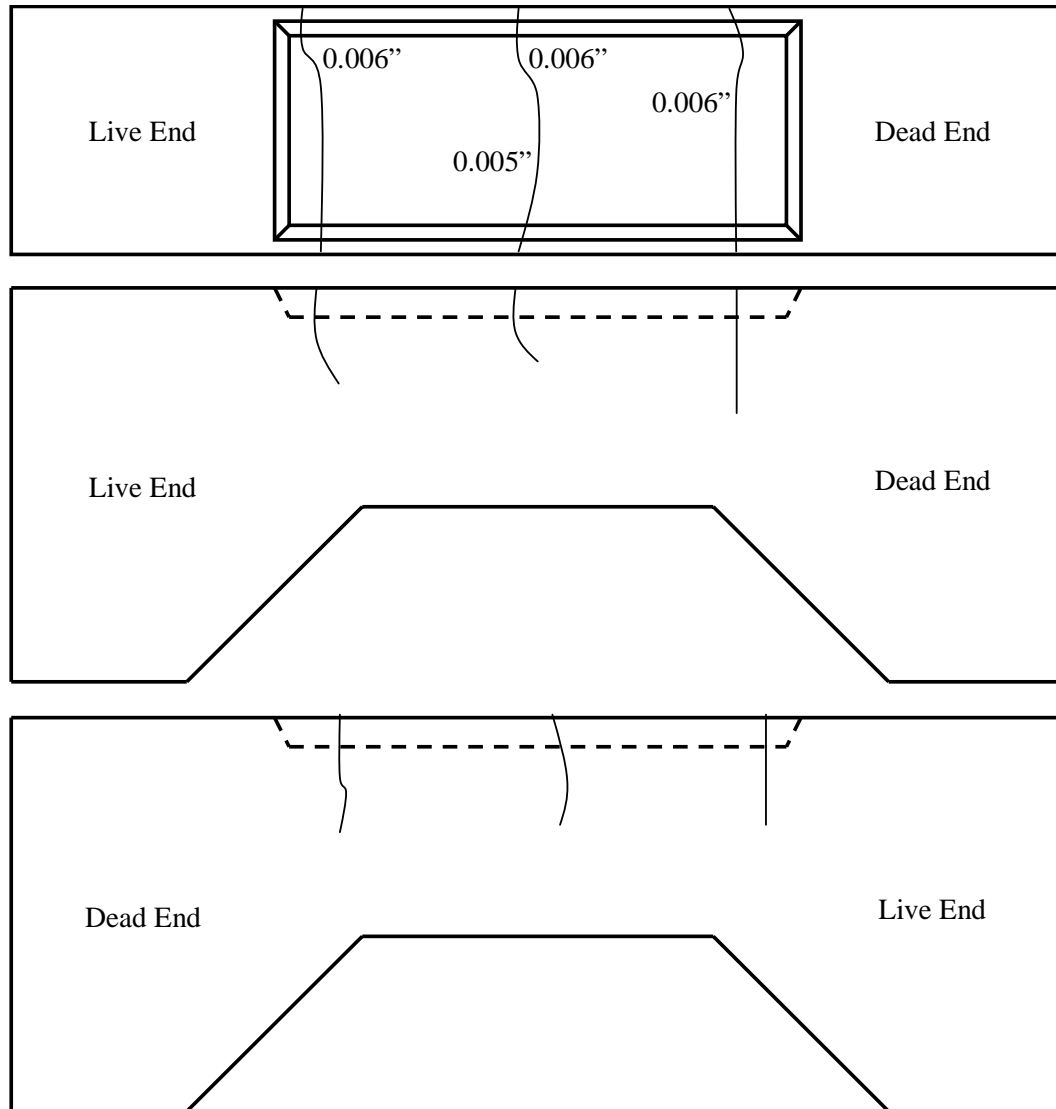


**Figure 6.6: Beam 2.2 Crack Map**

#### 6.3.2.4 Beam 2.2 Comments

- Measured crack widths were not as wide as most specimens. The live load force was limited to 65 kip to ensure sustainability of Dywidag assembly.

## **CHAPTER 7**

### **Conclusion**

#### **7.1 BRIEF SUMMARY**

This thesis focuses on the design and fabrication of a new compact research specimen for evaluation of corrosion resistance of potentially improved post-tensioning systems. The development of new post-tensioning materials and systems in recent years has made some of the durability research in this area obsolete. The current research is evaluating the corrosion resistance of both existing and potential post-tensioning materials as well as examining construction practices for the new systems. The new post-tensioning systems being investigated include combinations of strand, duct (with and without couplers), bearing plates and electrical isolation. Possible combinations of post-tensioning materials were identified using a specimen matrix (see Chapter 2).

The experimental program includes both long-term exposure tests and accelerated corrosion tests. The long-term program is modeled after previous post-tensioning durability research at the University of Texas under Project 1405. To provide continuity between the two projects and comparable results, this research used construction practices, exposure methods and monitoring conditions similar to those used in the previous research, with the exception that the current specimen uses only one-eighth of the materials used in previous specimens. The compact specimens should yield data fully comparable to that from the larger specimens of the previous project. The accelerated testing of the materials and evaluation of construction practices will be completed in ongoing phases of the project.

## 7.2 CONCLUSIONS

The overall performance of the Project 4562 research specimen during production was successful. The 4562 specimen uses much less materials than its 1405 predecessor while providing a comparable amount of project results (see Figure 7.1). The small scale of the 4562 research specimen also allows for convenient handling and long-term storage. When the live load was applied at the corbels of the specimen, cracks formed in the concrete surrounding the post-tensioning ducts in the reduced midsection of the beam. The cracks were opened to desired widths (see Section 3.1.3) by increasing the live load beyond cracking. Therefore, the small size and controlled cracking goals established at the beginning of the project were accomplished (see Sections 3.1.1 and 3.1.2). The remaining design criteria – post-tensioning hardware isolation and accelerated results – will be evaluated as Project 4562 continues (see Sections 3.1.3 and 3.1.4).



*Figure 7.1: New Specimens (Foreground) and Previous Specimens (Background) in Service at the North End of Ferguson Structural Engineering Lab*

### 7.3 RECOMMENDATIONS FOR SIMILAR RESEARCH

Over the course of the design and construction portion of the second phase of Project 4562, potential improvements to the research specimen became apparent. If similar specimens are utilized for future research, the following considerations may enhance construction practices and specimen performance:

- *Simpler Mild Reinforcement Cage:* The deformed reinforcement cage was too complex. The intricacy of the cage, especially at the corbels, made the epoxy-coated rebars difficult to fabricate and tie together.
- *More Steel Across the Corbel Plane:* The corbels of some specimens cracked during the live load application. The corbels were designed using ACI318-02 Section 11.9. The assumed design plane at the live end was not correct given the presence of the reentrant corner. The original assumed corbel design plane and a more appropriate corbel design plane are shown in Figure 7.2. Strut-and-tie modeling would also be an effective design tool for the irregular corbel region.
- *Exclude Reentrant Corner:* Cracks in the corbels formed during the live load application propagating from the reentrant corner at the live end of the specimen. The open live end was included to provide access for the equipment that was originally intended to prestress the specimens. Due to changes in the type of anchor heads after specimen production began, the original stressing equipment was not used. A monostrand ram was used to prestress the specimens. Because of the narrow nose of the monostrand ram, it did not require an open live end.

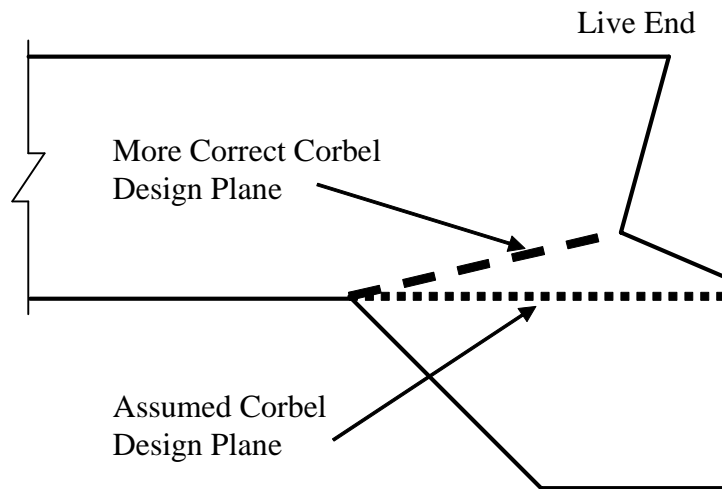


**Figure 7.2: Corbel Design Planes**

- *More Robust Grout Vent Connection in Uncoupled Ducts:* The grout vent installed in the uncoupled ducts of the research specimens would have been easier to work with had it been more robust. A great amount of care and time was taken to protect the existing grout vent during all phases of construction. Potential damage of the grout vent during construction may affect the ability of the duct to act as a protective barrier for the tendon.

#### **7.4 CONTINUATION OF PROJECT 4562 RESEARCH**

The design and construction of the research specimens was the initial portion of Project 4562 and the subject matter of this thesis. The next segments of Project 4562 are the continued exposure and monitoring, material testing, accelerated corrosion tests and finally autopsying the research specimens.

##### **7.4.1 Continued Exposure and Monitoring**

The tasks for the next phase will be:

1. Maintain the saltwater exposure cycles over the ducts – two weeks wet and two weeks dry (see Section 5.2).

2. Dead end anchorage saltwater exposure should be conducted every four weeks coinciding with the beginning of the wet cycle over the ducts.
3. Continue the nondestructive corrosion monitoring of the specimens by visual inspection and half-cell potential reading (see Section 5.3). Half-cell potential readings should be taken at the end of wet cycles over the ducts. The half-cell potential sampling grid within the depression in the top surface of the specimen is shown in Figure 5.7.

#### **7.4.2 Material Testing**

An important task remaining is to test each type of strand to determine its mechanical properties such as tensile strength, modulus of elasticity and representative stress-strain curve.

#### **7.4.3 Accelerated Corrosion Testing**

Another important task remaining is in addition to the long-term corrosion testing of the prestressed beams, subject each type of strand used in the Project 4562 to accelerated corrosion tests. The accelerated strand corrosion tests should be modeled after similar research conducted by Salcedo (2003) under the supervision of Schokker at Penn State University (PSU). The research specimen setup for the strand accelerated corrosion tests conducted by Salcedo is shown in Figure 7.3.

#### **7.4.4 Autopsy Research Specimens**

Far in the future, after an appropriate amount of time determined by half-cell potential readings, visual inspection and project schedule, the long-term research specimens should be opened in order to evaluate the corrosive performance of the post-tensioning materials within each specimen. For safety

purposes, remove the live load from the Dywidag bar before beginning the specimen autopsy.

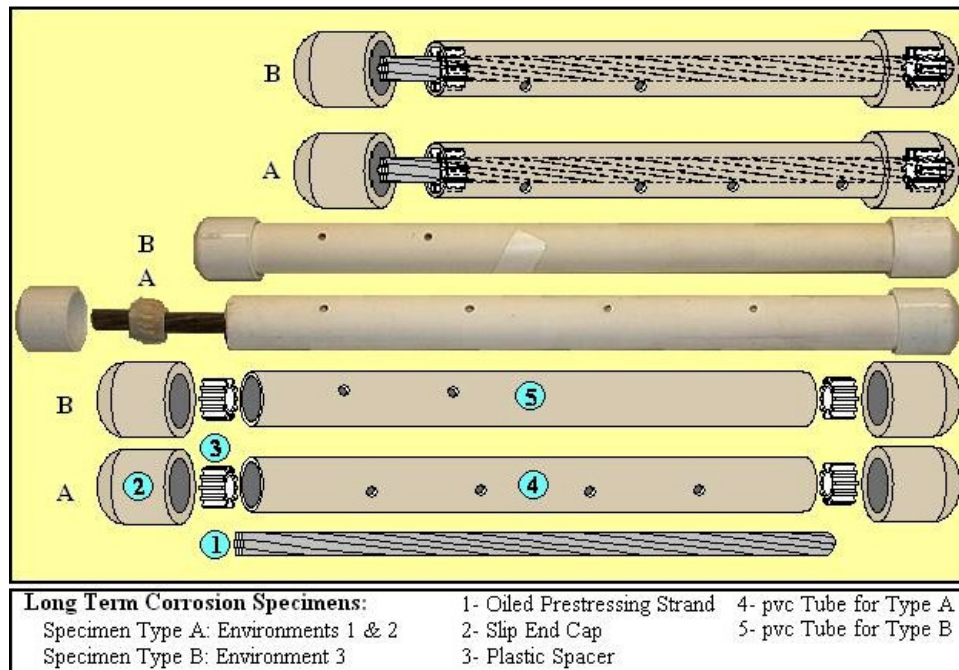


**Figure 7.3: PSU Strand Accelerated Corrosion Test Specimen (Salcedo 2003)**



# APPENDIX A

## Additional Material Information

### A.1 MATERIALS SUMMARY

*Table A.1: Material Acquisition Summary*

MATERIAL	SUPPLIER	CONTACT
Bearing Plates Galvanized Steel Duct PT Plus Plastic Duct and Couplers Hot Dip Galvanized Strand* 0.6" Strand Anchor Heads Wedges	VSL USA	Will Ferguson wferguson@structural.net 972.647.0200
EIT Systems	VSL Switzerland	Hans-Rudolf Ganz hrganz@vsl-schwiez.ch
76mm One-Way Ribbed Plastic Duct* 76mm Couplers* 85mm Two-Way Ribbed Plastic Duct* 85mm Coupler*	GTI	Joe Harrison joe.harrison@gti-usa.com 281.240.0550
Stainless Strand*	Techalloy	Jim Beitz jbeitz@techalloy.com 815.923.2131
Stainless Clad Strand*	DSI	Ron Bonomo ron.bonomo@dsiamerica.com
Copper Clad Strand*	Copperweld	Milton Lamb mlamb@copperweld.com info@copperweld.com
Epoxy Coated Strand*	Sumiden Wire	Steve Yoshida stevey@sumiden.com
Type V Epoxy*	Unitex	Susan Wintz 816.231.7700
Epoxy Coated Rebar	ABC Coating	Mary Boyette 972.937.9841 orders@abccoatingtx.com
Concrete	Capitol Aggregates	Ron Taff

\* - Material Donated to Research Project

All suppliers, except Capitol Aggregates, requested project results when available.

## A.2 WORKSHOP SUMMARY

**Table A.2: Post-Tensioning Durability Workshop Invitation List (Ferguson Structural Engineering Lab – April 14-15, 2003)**

NAME	AFFILIATION	EMAIL ADDRESS
Ron Bonomo	Dywidag Systems	ron.bonomo@dsiamerica.com
Eric Aigner	DSI HQ Engineering	<i>no email provided</i>
Jean-Philippe Fuzier	Freyssinet International	jpfuzier@freyssinet.com
Hans-Rudolf Ganz	VSL	hrganz@vsl-schweiz.ch
John Crigler	V Structural	jcrigler@structural.net
Steven Soltesz	Oregon DOT	Steven.M.Soltesz@odot.state.or.us
Jim Beitz	Techalloy Company	jbeitz@techalloy.com
Oscar Cano	MMFX Technologies	oscar.cano@mmfx.com
Salem S. Faza	MMFX Technologies	Salem.Faza@mmfxsteek.com
Tiger Kido	Sumiden Wire Products Corp.	tkido@sumidenwire.com
Steve Yoshida	Sumiden Wire Products Corp.	stevey@sumidenwire.com
Toshihiko Niki	Sumitomo Electric Industries	tniki@sei.co.jp
Jon Cornelius	Sumiden Wire Products Corp.	jonc@sumidenwire.com
Ken Fleck	Sumiden Wire Sales	<i>no email provided</i>
Yoshitaka Nishida	Anderson Technology Corp.	osaka@anderson-tech.co.jp
Nakamura	Anderson Technology Corp.	<i>no email provided</i>
Joe Harrison	General Technologies, Inc.	Joe.Harrison@gti-usa.net
Felix Sorkin	General Technologies, Inc.	<i>no email provided</i>
Ted Neff	PTI	tedneff@post-tensioning.org
Cliff Freyermuth*	ASBI	asbi@earthlink.net
Paul Johal*	PCI	pjohal@pcinst.com
Paul Virmani	FHWA	paul.virmani@fhwa.dot.gov
Jerry Porter	FHWA	<i>no email provided</i>
Brian Merrill	TxDOT	bmerrill@dot.state.tx.us
Randy Cox*	TxDOT	wrcox@dot.state.tx.us
Dean Van Landuyt*	TxDOT	dvanland@dot.state.tx.us
Tom Yarbrough	TxDOT RTI	tyarbro@dot.state.tx.us
Gilbert Sylva	TxDOT	gsylva@dot.state.tx.us
Randy Poston	WDP & Associates	rposton@wdpa.com
Andrea Schokker	Penn. State	ajs19@psu.edu
Harovel Wheat	UT	hwheat@mail.utexas.edu
John E. Breen	UT	jbreen@mail.utexas.edu
Michael E. Kreger	UT (currently Purdue Univ.)	kreger@purdue.edu
Ruben Salas	UT	Ruben_Salas@fsa.co.cr
Vijay Chandra	Parsons	ChandraV@pbworld.com
Trey Hamilton*	Univ. of Florida	hrh@ce.ufl.edu
Milton A. Lamb Jr.	LTV Copperweld Bimetallics	MLamb@copperweld.com

\* - Did Not Attend Workshop

## **APPENDIX B**

### **Additional Design Information**

#### **B.1 MILD REINFORCEMENT**

The drawings for the mild reinforcement are shown in Figures B.1 and B.2 of Section B.1.1. Given the complex geometry of the specimen and rebar, the details were drawn in AutoCAD to ensure the cage fit together.

The rebar order drawings sent to ABC Coating are shown in Figures B.3 through B.6 of Section B.1.2. Figure B.6 is an additional drawing of Bend 5 (see Figure B.4) requested by the fabricator to clarify dimensions and shape.

**B.1.1 Details**

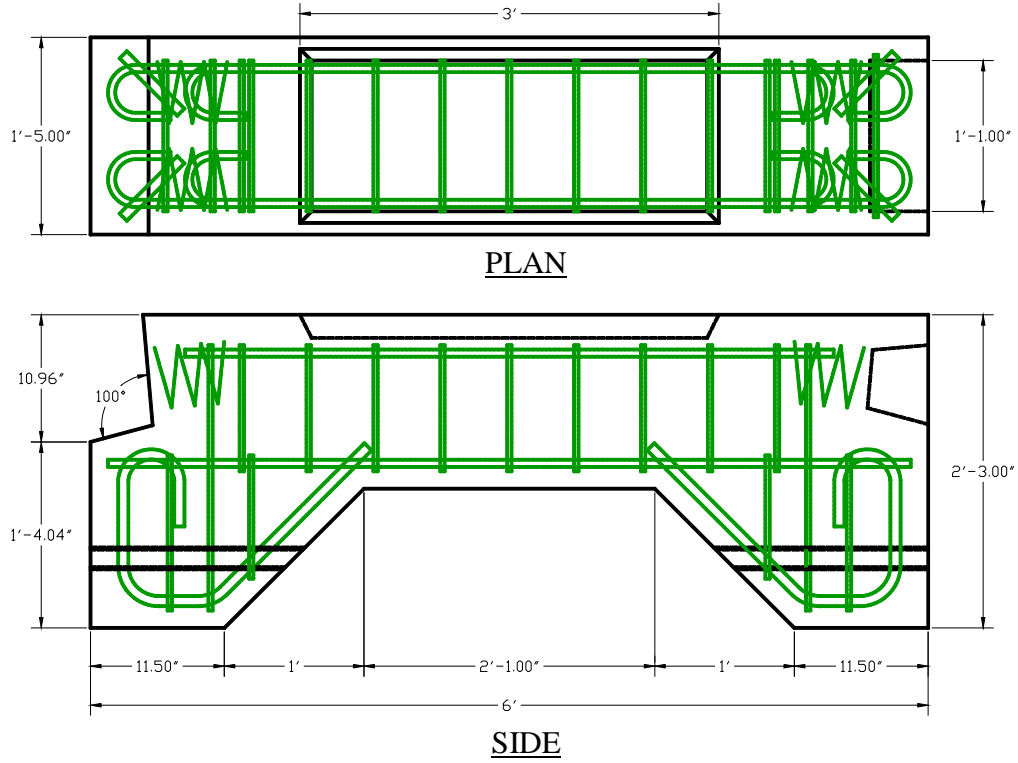


*Figure B.1: Mild Reinforcement Cage Details*

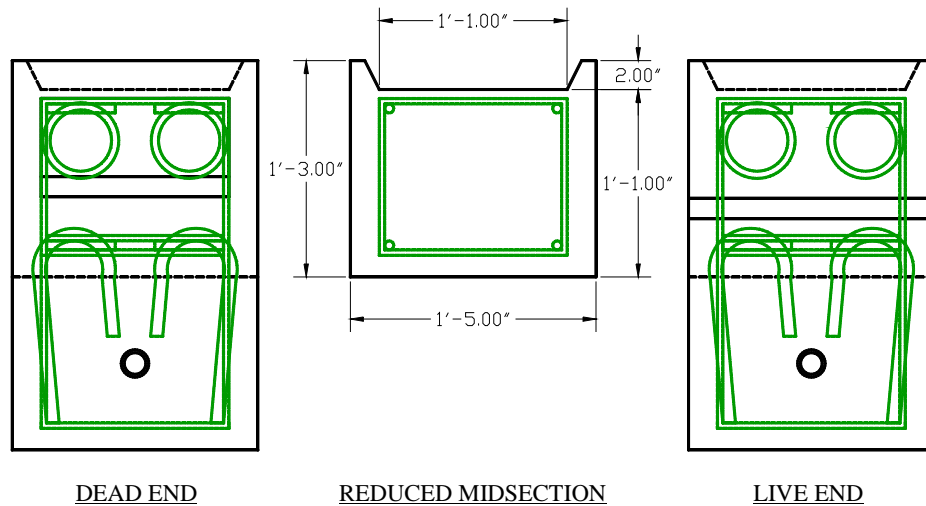


*Figure B.2: Ends and Midsection Details*

## B.1.2 Bar Dimensions

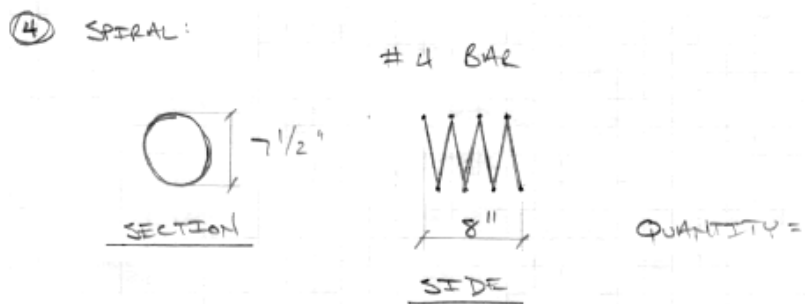
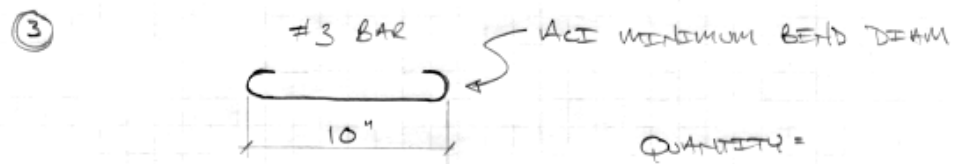
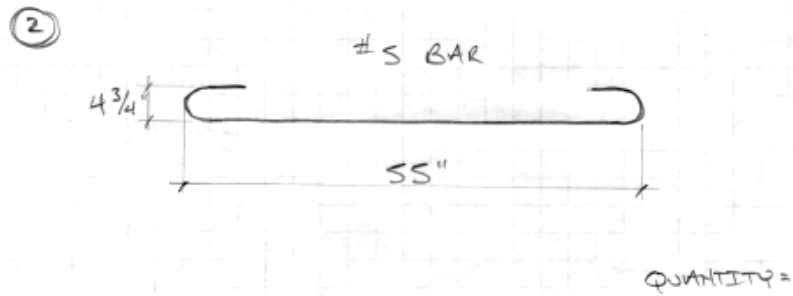
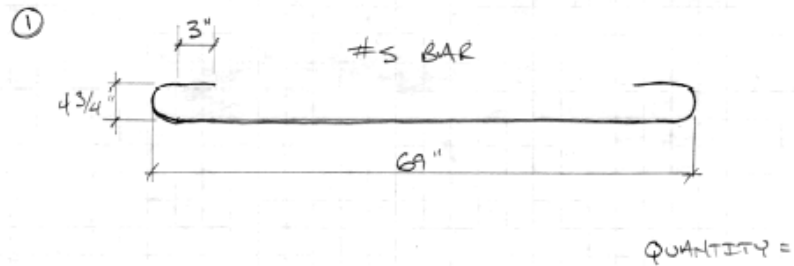
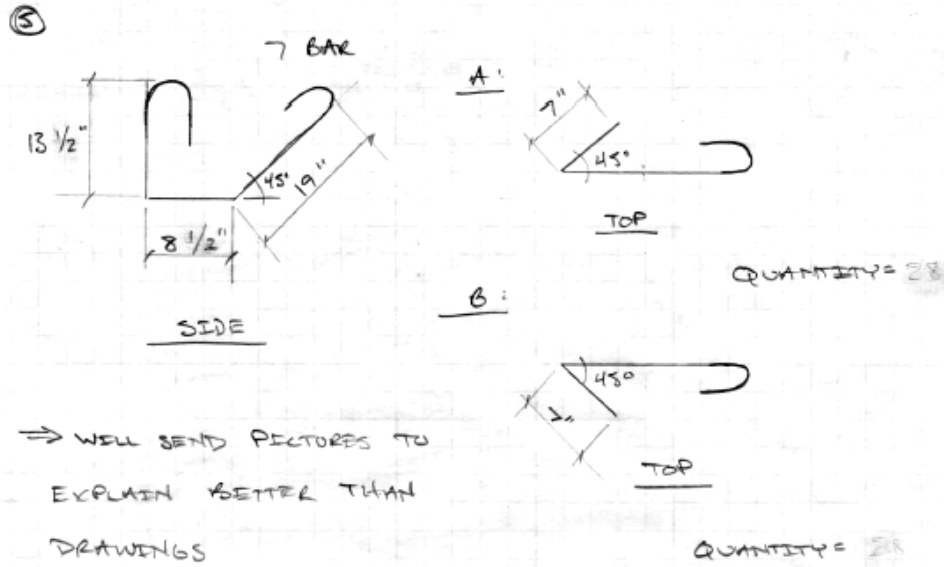


Figure B.3: Rebar Dimensions (1 of 3)



NOTE: ALL HOOPS - 3" TAILS  
MINIMUM BENDS ACCORDING TO ACI

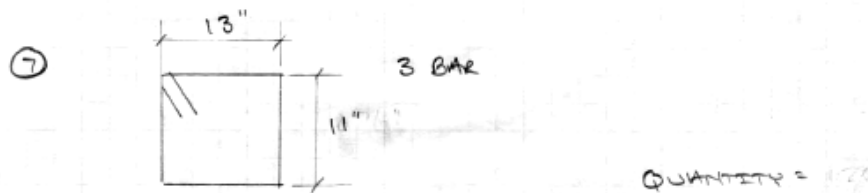
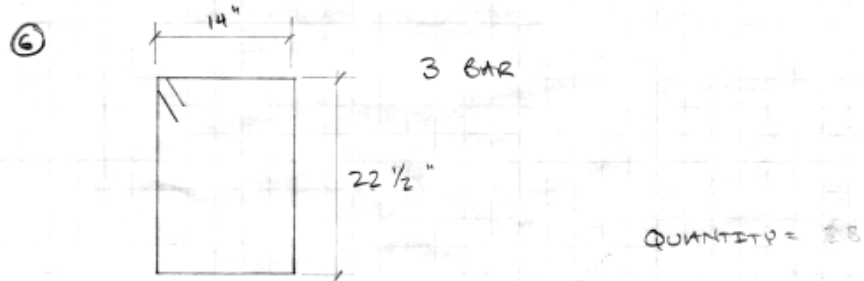
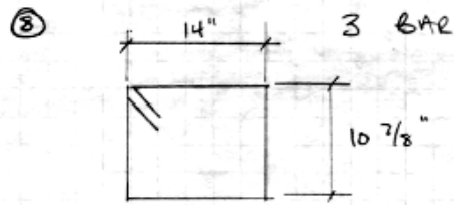
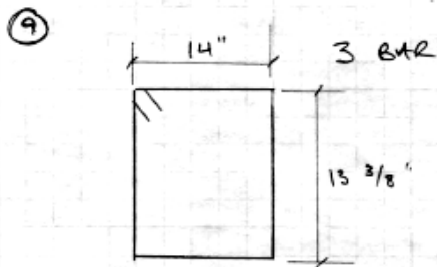


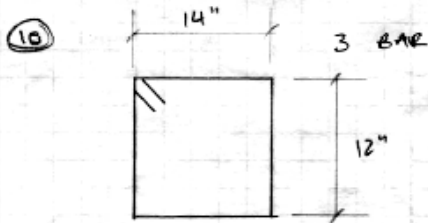
Figure B.4: Rebar Dimensions (2 of 3)



QUANTITY = 8



QUANTITY = 8



QUANTITY = 8

NOTE: ALL BAR GRADE 60 AND EPOXY COATED

Figure B.5: Rebar Dimensions (3 of 3)

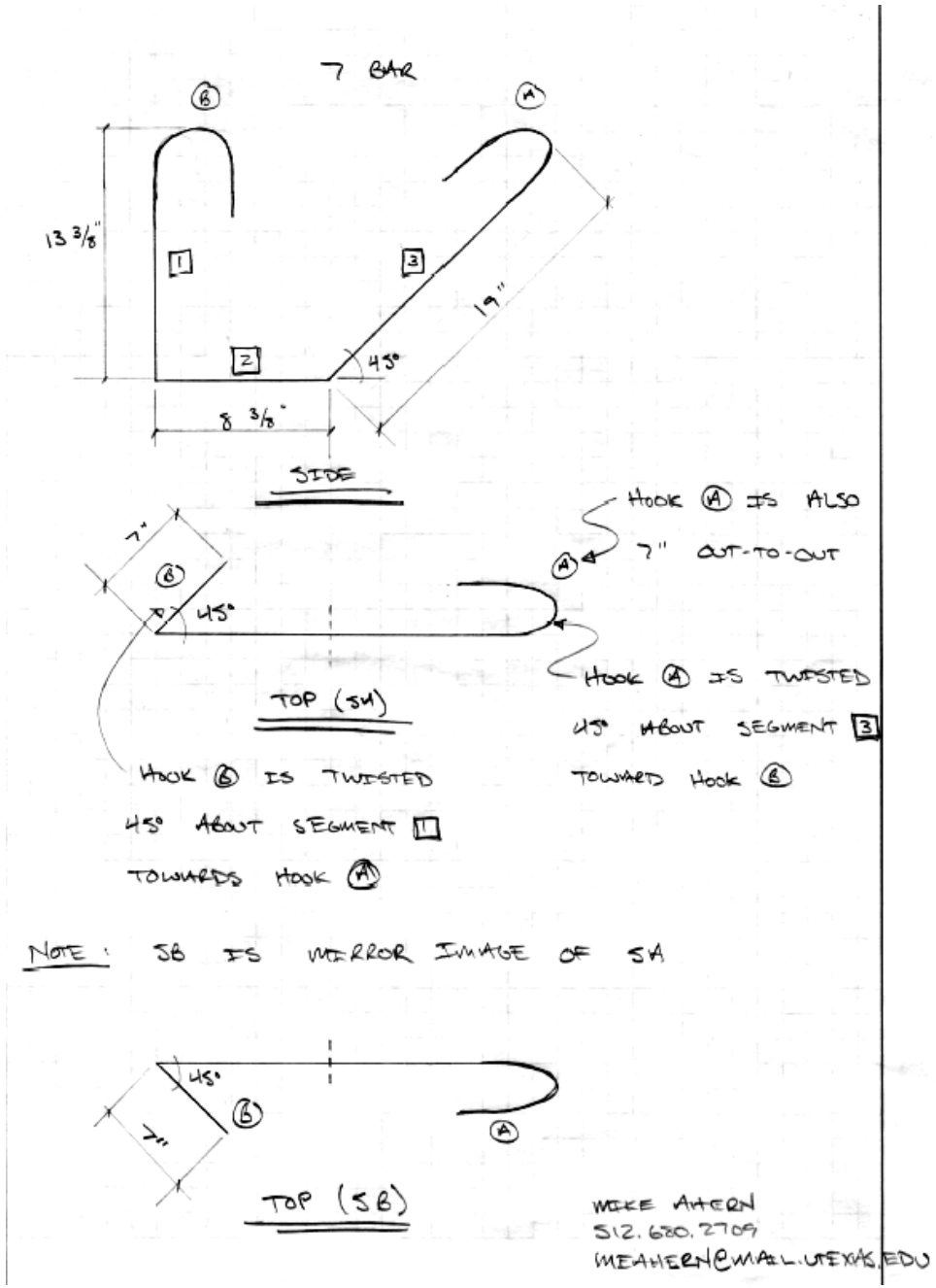
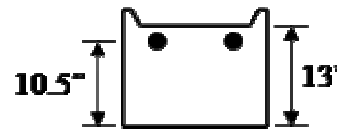


**Figure B.6: Bend 5 Detail**



## B.2 REFERENCE COMPARISON SPECIMEN DESIGN CALCULATIONS

### REFERENCE COMPARISON SPECIMEN DESIGN CALCULATIONS



Design Moment,  $M$

$$M = Fd \cdot ed$$

$Fd$  = expected Dywidag force =

55 k

$ed$  = eccentricity of Dywidag force with respect to neutral axis of reduced midsection =

15.5 in

$$M = \underline{\underline{852.5 \text{ k}\cdot\text{in}}}$$

Required Steel,  $A_{s,req}$

$$A_{s,req} = M / [f_s \cdot (d - a/2)]$$

$f_s$  = stress in flexural steel, assume '60%  $f_y$ ' (Gr. 60) at service level loads =

36 ksi

$d - a/2$  = moment arm between compression block and centroid of steel, assume '90%  $d$ ' =

9.45 in

$$A_{s,req} = \underline{\underline{2.506 \text{ in}^2}}$$

therefore, in addition to the two #5 bars in the existing reinforcement cage, use two #8 bars in place of the post-tensioning ducts

$$A_s = 2 \cdot A_5 + 2 \cdot A_8$$

$A_5$  = cross-sectional area of #5 rebar =

0.31 in<sup>2</sup>

$A_8$  = cross-sectional area of #8 rebar =

0.79 in<sup>2</sup>

$$A_s = \underline{\underline{2.2 \text{ in}^2}}$$

*slightly less than  $A_{s,req}$  for cracking purposes*

## APPENDIX C

### Beam Data

#### C.1 BEAM DATA

##### C.1.1 Beam 1.1

###### *C.1.1.1 Beam 1.1 Materials*

*Table C.1: Beam 1.1 Materials*

<b>Strand</b>	Conventional
<b>Duct</b>	Galvanized Corrugated Steel
<b>Coupler</b>	None
<b>Bearing Plate</b>	Non-Galvanized
<b>28-Day Concrete Strength, <math>f'_c</math></b>	4860 psi

###### *C.1.1.2 Beam 1.1 Important Dates*

*Table C.2: Beam 1.1 Important Dates*

<b>Casting</b>	August 16, 2004
<b>Prestress Application</b>	January 25, 2005
<b>Grouting</b>	January 27, 2005
<b>Anchorage Protection</b>	February 3, 2005
<b>Live Load Application</b>	February 22, 2005
<b>Exposure Initiation</b>	<i>Not Available</i>

### C.1.1.3 Beam 1.1 Stressing History

#### Live Load Application Plot

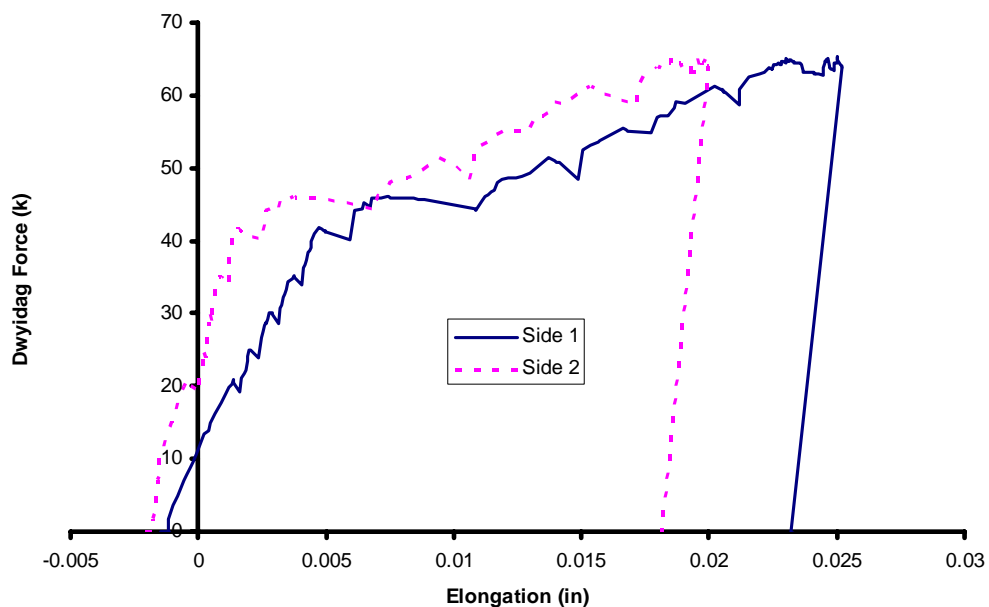


*Figure C.1: Beam 1.1 Live Load Application Plot*

#### Crack Widths

The maximum measured crack width on the top of the specimen within the depression for the salt bath is 0.008 in. See the crack map within this section for additional information regarding location and widths of cracks.

### Crack Map

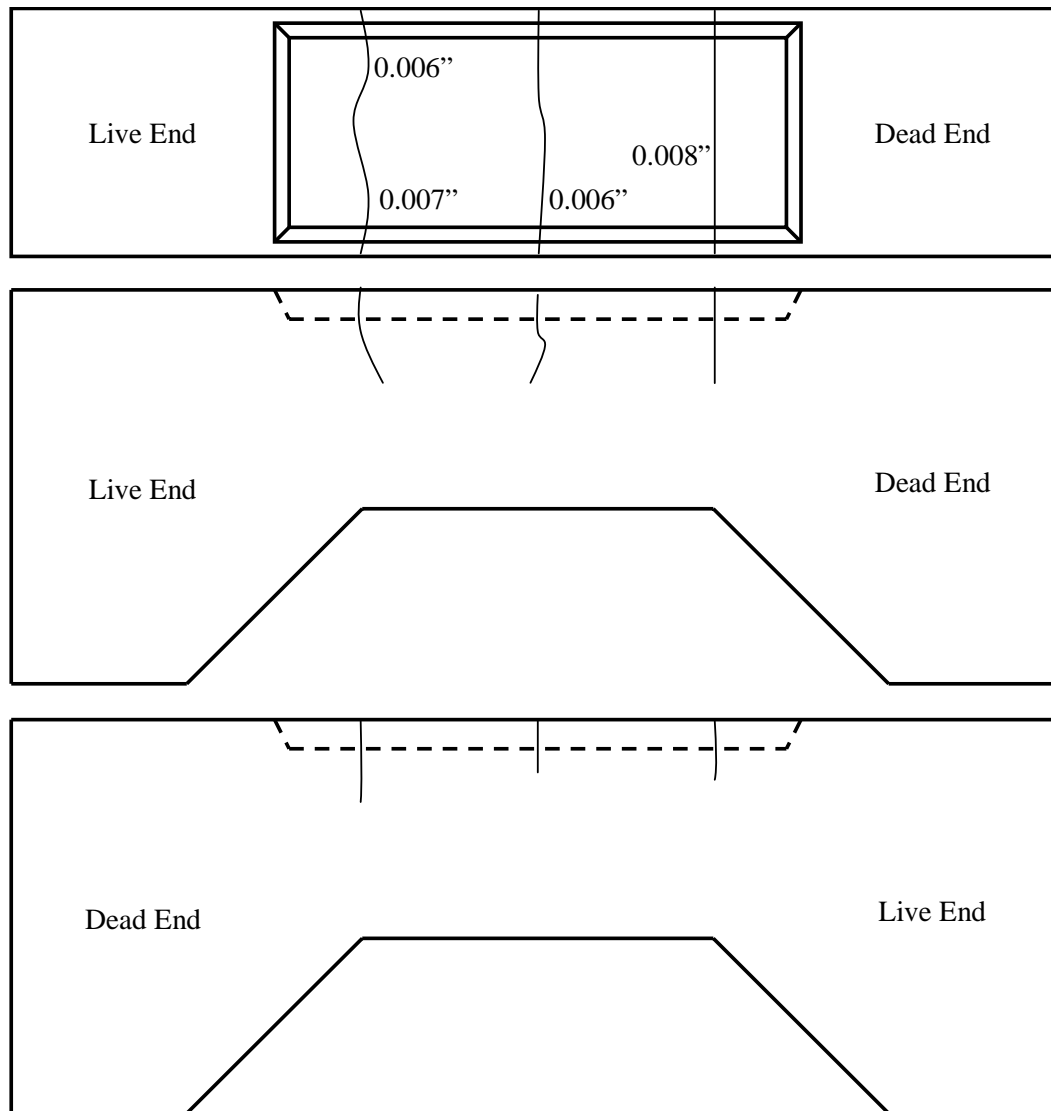


*Figure C.2: Beam 1.1 Crack Map*

#### *C.1.1.4 Beam 1.1 Comments*

- The duct-bearing plate connection was not sealed with duct tape before casting. Small amounts of concrete were removed from inside the bearing plates before proceeding with the remainder of specimen procedures.

- A shrinkage crack formed in the grout on the top surface of the live end pocket protection. The crack was sealed with epoxy before the initiation of exposure cycles.

## C.1.2 Beam 1.2

### C.1.2.1 Beam 1.2 Materials

*Table C.3: Beam 1.2 Materials*

<b>Strand</b>	Copper Clad
<b>Duct</b>	Galvanized Corrugated Steel
<b>Coupler</b>	None
<b>Bearing Plate</b>	Non-Galvanized
<b>28-Day Concrete Strength, <math>f'_c</math></b>	4860 psi

### C.1.2.2 Beam 1.2 Important Dates

*Table C.4: Beam 1.2 Important Dates*

<b>Casting</b>	August 16, 2004
<b>Prestress Application</b>	February 17, 2005
<b>Grouting</b>	February 17, 2005
<b>Anchorage Protection</b>	February 24, 2005
<b>Live Load Application</b>	March 3, 2005
<b>Exposure Initiation</b>	<i>Not Available</i>

### C.1.2.3 Beam 1.2 Stressing History

#### Live Load Application Plot

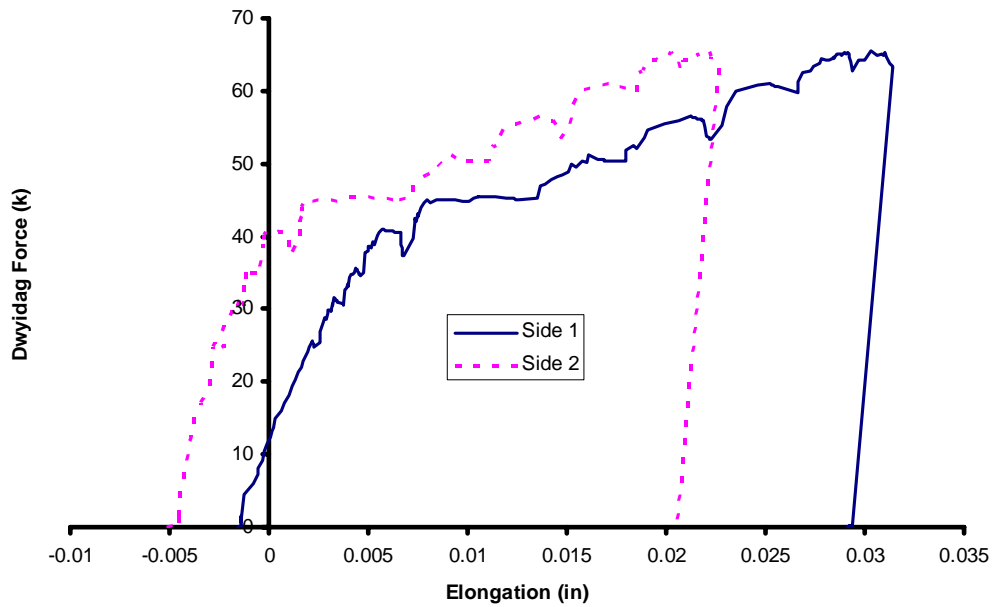


*Figure C.3: Beam 1.2 Live Load Application Plot*

#### Crack Widths

The maximum measured crack width on the top of the specimen within the depression for the salt bath is 0.009 in. See the crack map within this section for additional information regarding location and widths of cracks.

### Crack Map

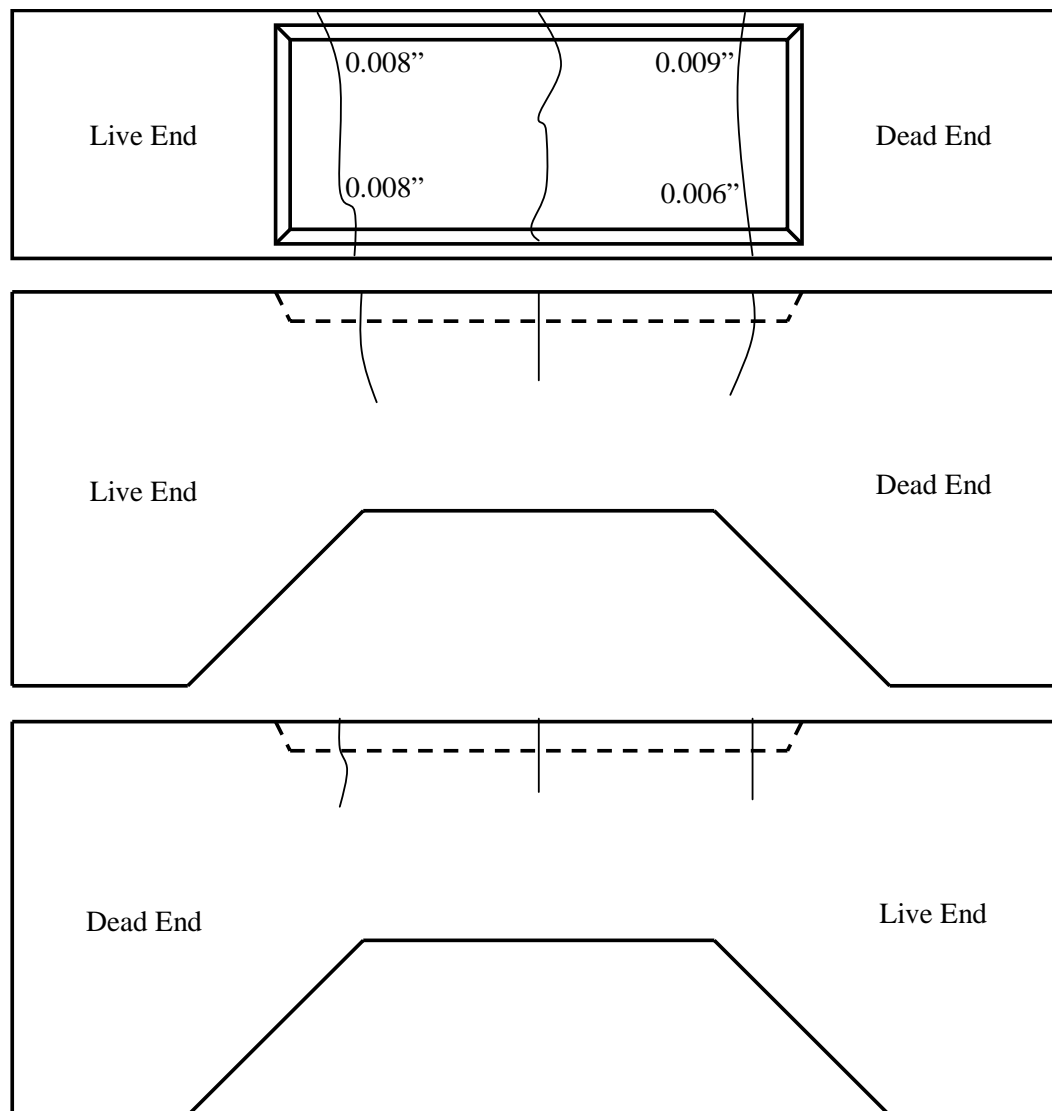


*Figure C.4: Beam 1.2 Crack Map*

#### *C.1.2.4 Beam 1.2 Comments*

- The duct-bearing plate connection was not sealed with duct tape before casting. Small amounts of concrete were removed from inside the bearing plates before proceeding with the remainder of specimen procedures.

- The back surface of one half of a two-part wedge cracked at the live end of the specimen, but the wedge remained intact and maintained the force in the strand.

### C.1.3 Beam 1.3

#### C.1.3.1 Beam 1.3 Materials

*Table C.5: Beam 1.3 Materials*

<b>Strand</b>	Stainless Clad (delivered Summer 2004)
<b>Duct</b>	Galvanized Corrugated Steel
<b>Coupler</b>	None
<b>Bearing Plate</b>	Non-Galvanized
<b>28-Day Concrete Strength, <math>f'_c</math></b>	4860 psi

#### C.1.3.2 Beam 1.3 Important Dates

*Table C.6: Beam 1.3 Important Dates*

<b>Casting</b>	August 16, 2004
<b>Prestress Application</b>	April 18, 2005
<b>Grouting</b>	April 18, 2005
<b>Anchorage Protection</b>	April 21, 2005
<b>Live Load Application</b>	April 26, 2005
<b>Exposure Initiation</b>	<i>Not Available</i>



### C.1.3.3 Beam 1.3 Stressing History

#### Live Load Application Plot

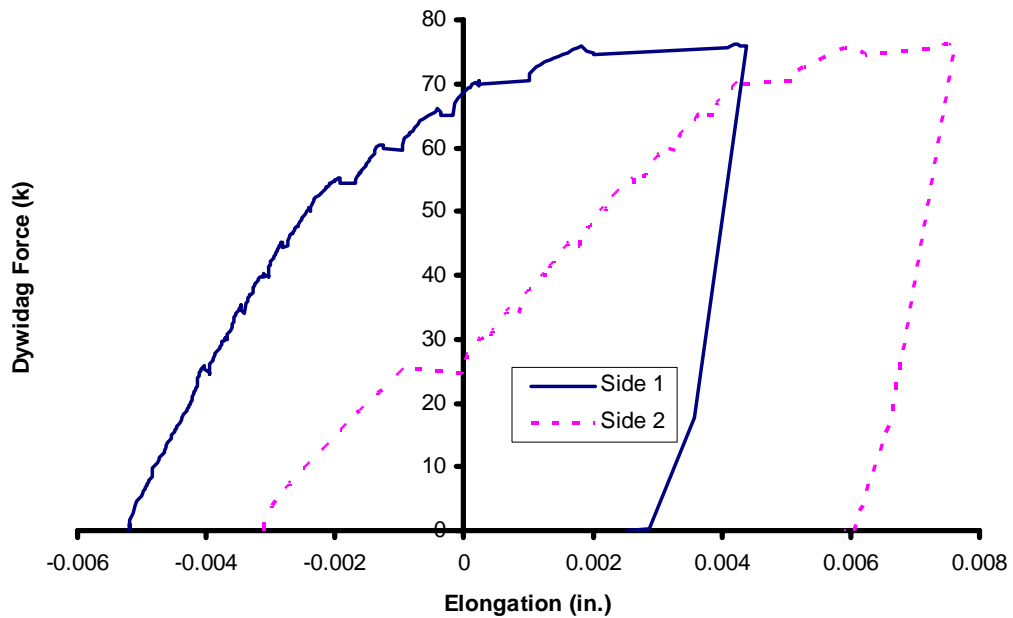


*Figure C.5: Beam 1.3 Live Load Application Plot*

#### Crack Widths

The maximum measured crack width on the top of the specimen within the depression for the salt bath is 0.003 in. See the crack map within this section for additional information regarding location and widths of cracks.

Crack Map

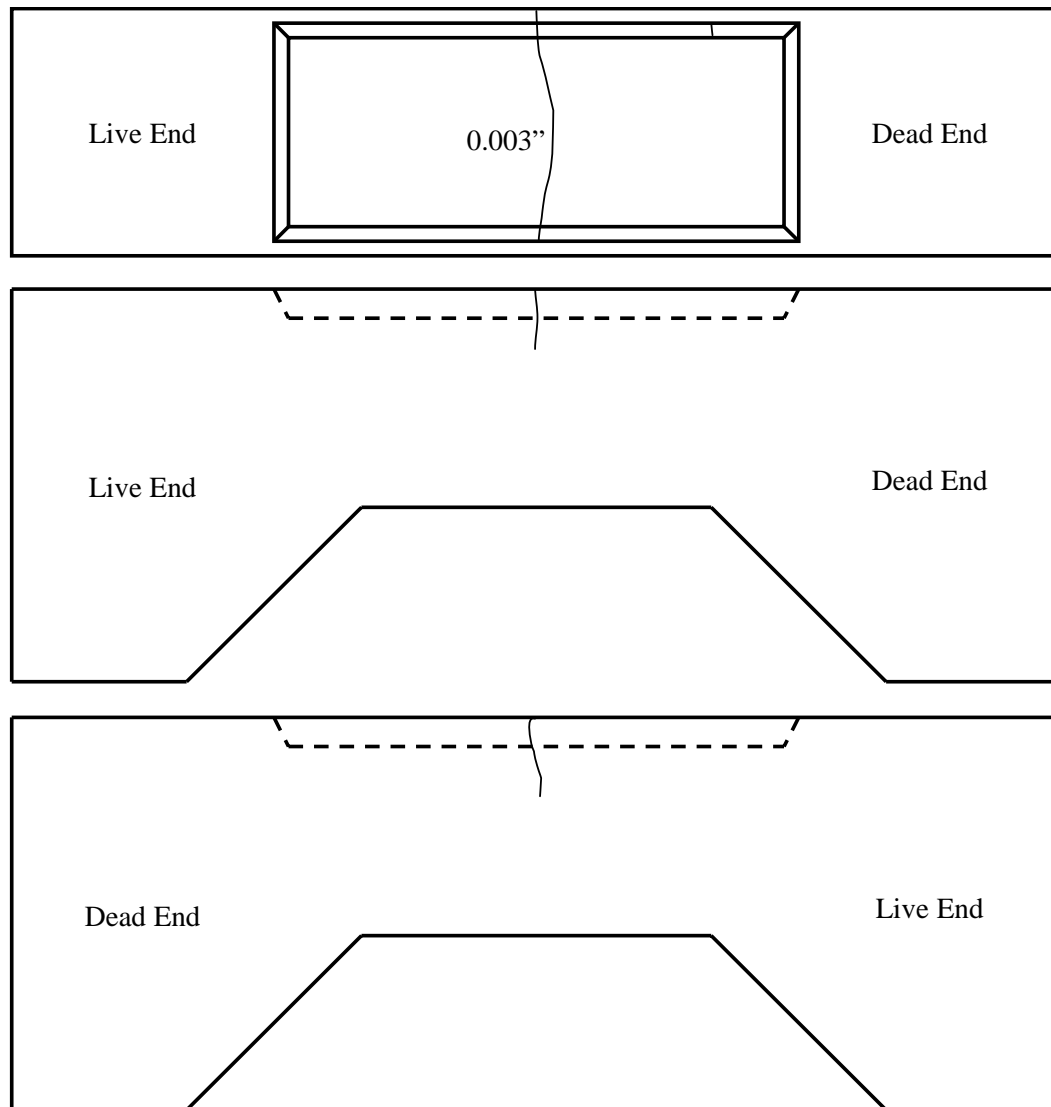


*Figure C.6: Beam 1.3 Crack Map*

***C.1.3.4 Beam 1.3 Comments***

- The duct-bearing plate connection was not sealed with duct tape before casting. Small amounts of concrete were removed from inside the bearing plates before proceeding with the remainder of specimen procedures.

- Since 0.6-in. strands were used in the specimen, the prestress force was larger than other specimens (see Section 3.2.1). Therefore, the live load required to crack the beam was larger. The live load was increased to 75 kip (see Figure C.6). The beam did not crack until 75 kip.
- After stressing was completed, cracks extending from the reentrant corner of the live end pocket were observed in the corbels. The corbel cracking was present in the trial specimens, but inclined #3 bars were added to the reinforcement cage through the crack plane in order to control corbel cracking in future specimens.

#### **C.1.4 Beam 1.4**

##### ***C.1.4.1 Beam 1.4 Materials***

***Table C.7: Beam 1.4 Materials***

<b>Strand</b>	Conventional
<b>Duct</b>	Galvanized Corrugated Steel
<b>Coupler</b>	None
<b>Bearing Plate</b>	Galvanized
<b>28-Day Concrete Strength, <math>f'_c</math></b>	4860 psi

**C.1.4.2 Beam 1.4 Important Dates**

**Table C.8: Beam 1.4 Important Dates**

<b>Casting</b>	August 16, 2004
<b>Prestress Application</b>	January 25, 2005
<b>Grouting</b>	January 27, 2005
<b>Anchorage Protection</b>	February 3, 2005
<b>Live Load Application</b>	February 22, 2005
<b>Exposure Initiation</b>	<i>Not Available</i>

**C.1.4.3 Beam 1.4 Stressing History**

Live Load Application Plot

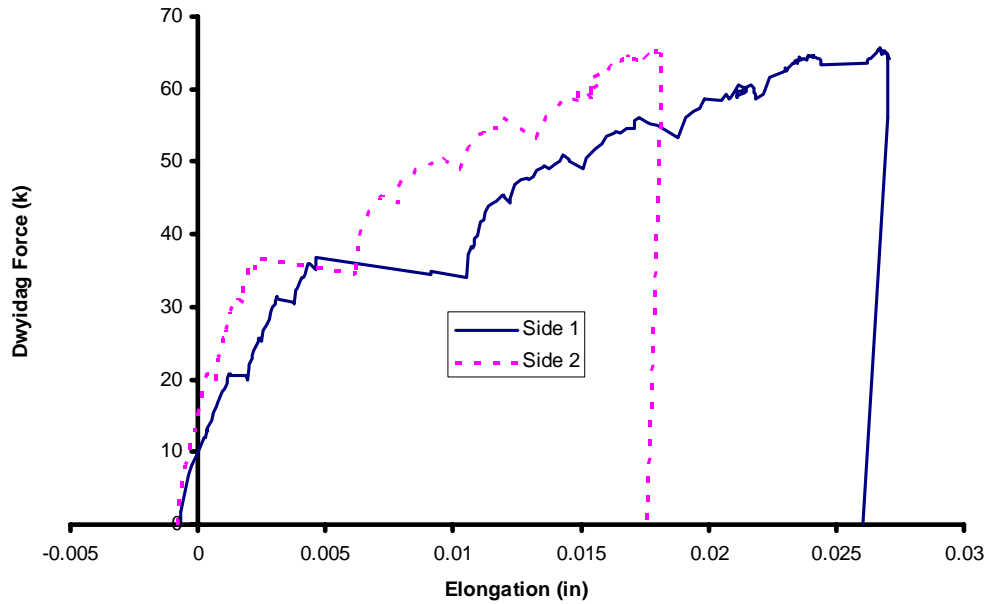


**Figure C.7: Beam 1.4 Live Load Application Plot**

### Crack Widths

The maximum measured crack width on the top of the specimen within the depression for the salt bath is 0.009 in. See the crack map within this section for additional information regarding location and widths of cracks.

### Crack Map

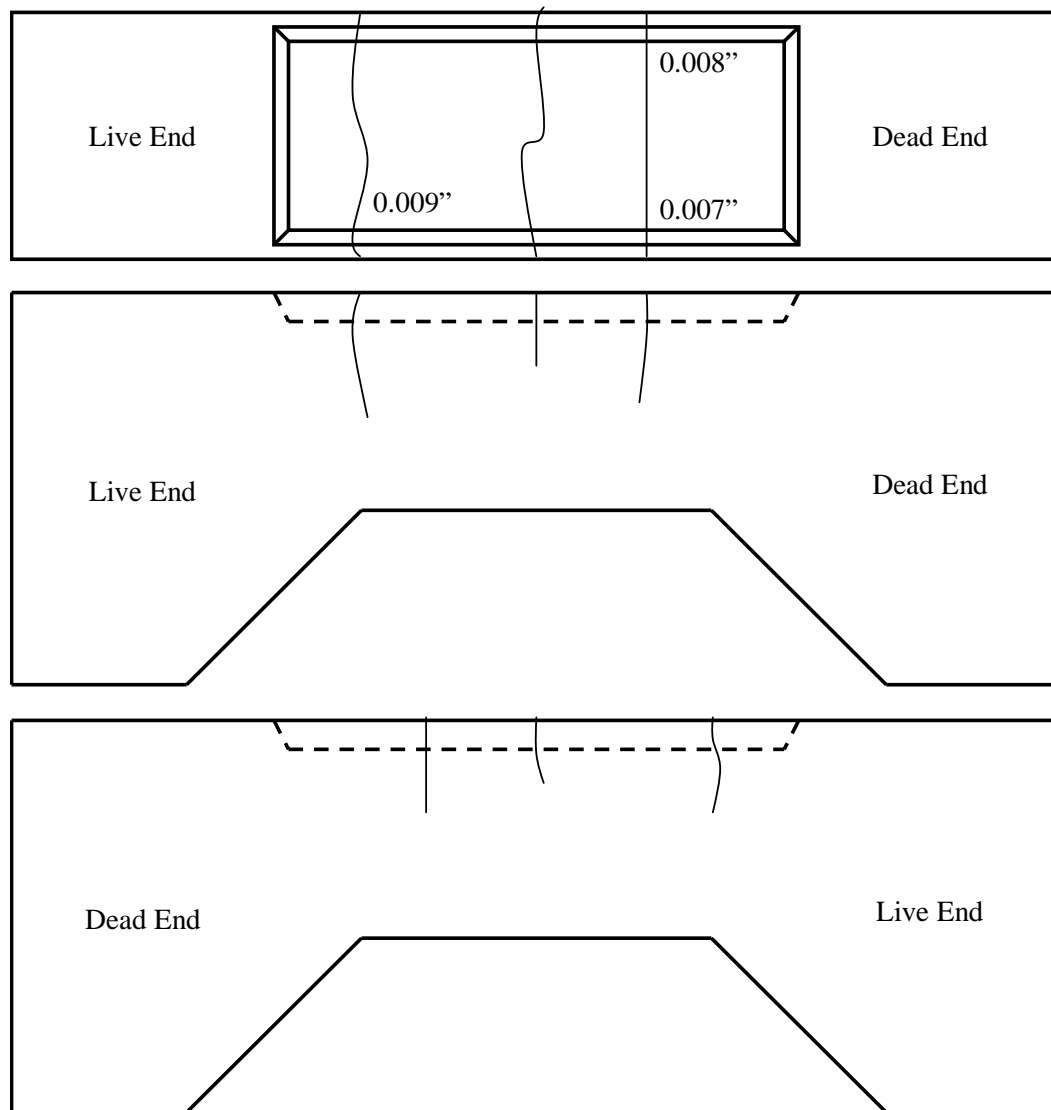


*Figure C.8: Beam 1.4 Crack Map*

#### ***C.1.4.4 Beam 1.4 Comments***

- The duct-bearing plate connection was not sealed with duct tape before casting. Small amounts of concrete were removed from inside the bearing plates before proceeding with the remainder of specimen procedures.

#### **C.1.5 Beam 2.1**

##### ***C.1.5.1 Beam 2.1 Materials***

***Table C.9: Beam 2.1 Materials***

<b>Strand</b>	Epoxy Coated, Flow-Filled
<b>Duct</b>	Galvanized Corrugated Steel
<b>Coupler</b>	None
<b>Bearing Plate</b>	Non-Galvanized
<b>28-Day Concrete Strength, <math>f'_c</math></b>	4080 psi

##### ***C.1.5.2 Beam 2.1 Important Dates***

***Table C.10: Beam 2.1 Important Dates***

<b>Casting</b>	October 18, 2004
<b>Prestress Application</b>	<i>Not Available</i>
<b>Grouting</b>	<i>Not Available</i>
<b>Anchorage Protection</b>	<i>Not Available</i>
<b>Live Load Application</b>	<i>Not Available</i>
<b>Exposure Initiation</b>	<i>Not Available</i>

### ***C.1.5.3 Beam 2.1 Stressing History***

*Not Available*

### ***C.1.5.4 Beam 2.1 Comments***

*Not Available*

## **C.1.6 Beam 2.2**

### ***C.1.6.1 Beam 2.2 Materials***

***Table C.11: Beam 2.2 Materials***

<b>Strand</b>	Hot Dip Galvanized
<b>Duct</b>	Galvanized Corrugated Steel
<b>Coupler</b>	None
<b>Bearing Plate</b>	Non-Galvanized
<b>28-Day Concrete Strength, <math>f'_c</math></b>	4080 psi

### ***C.1.6.2 Beam 2.2 Important Dates***

***Table C.12: Beam 2.2 Important Dates***

<b>Casting</b>	October 18, 2004
<b>Prestress Application</b>	February 16, 2005
<b>Grouting</b>	February 17, 2005
<b>Anchorage Protection</b>	February 24, 2005
<b>Live Load Application</b>	March 3, 2005
<b>Exposure Initiation</b>	<i>Not Available</i>

### C.1.6.3 Beam 2.2 Stressing History

#### Live Load Application Plot

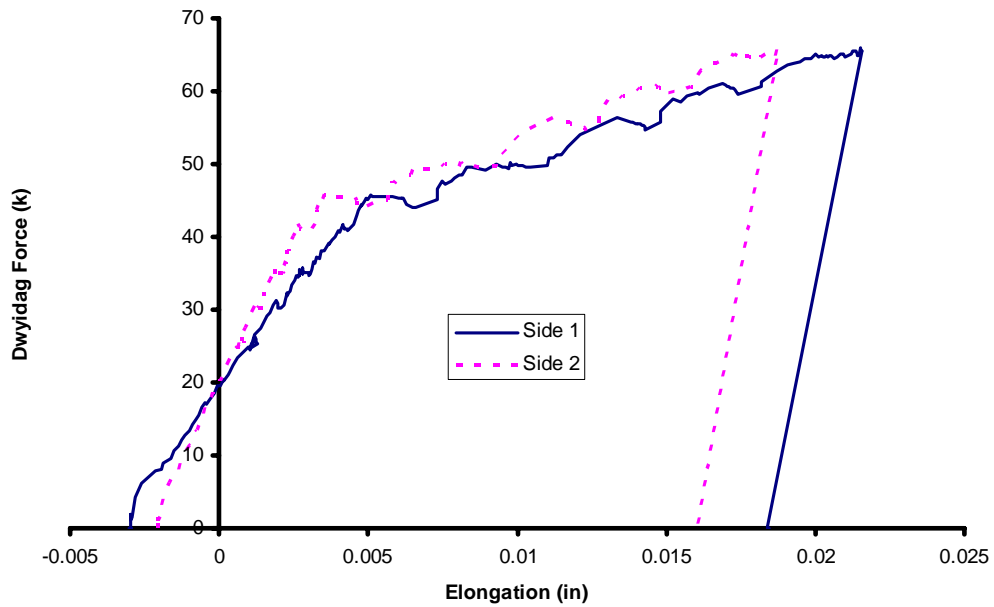


*Figure C.9: Beam 2.2 Live Load Application Plot*

#### Crack Widths

The maximum measured crack width on the top of the specimen within the depression for the salt bath is 0.006 in. See the crack map within this section for additional information regarding location and widths of cracks.



Crack Map

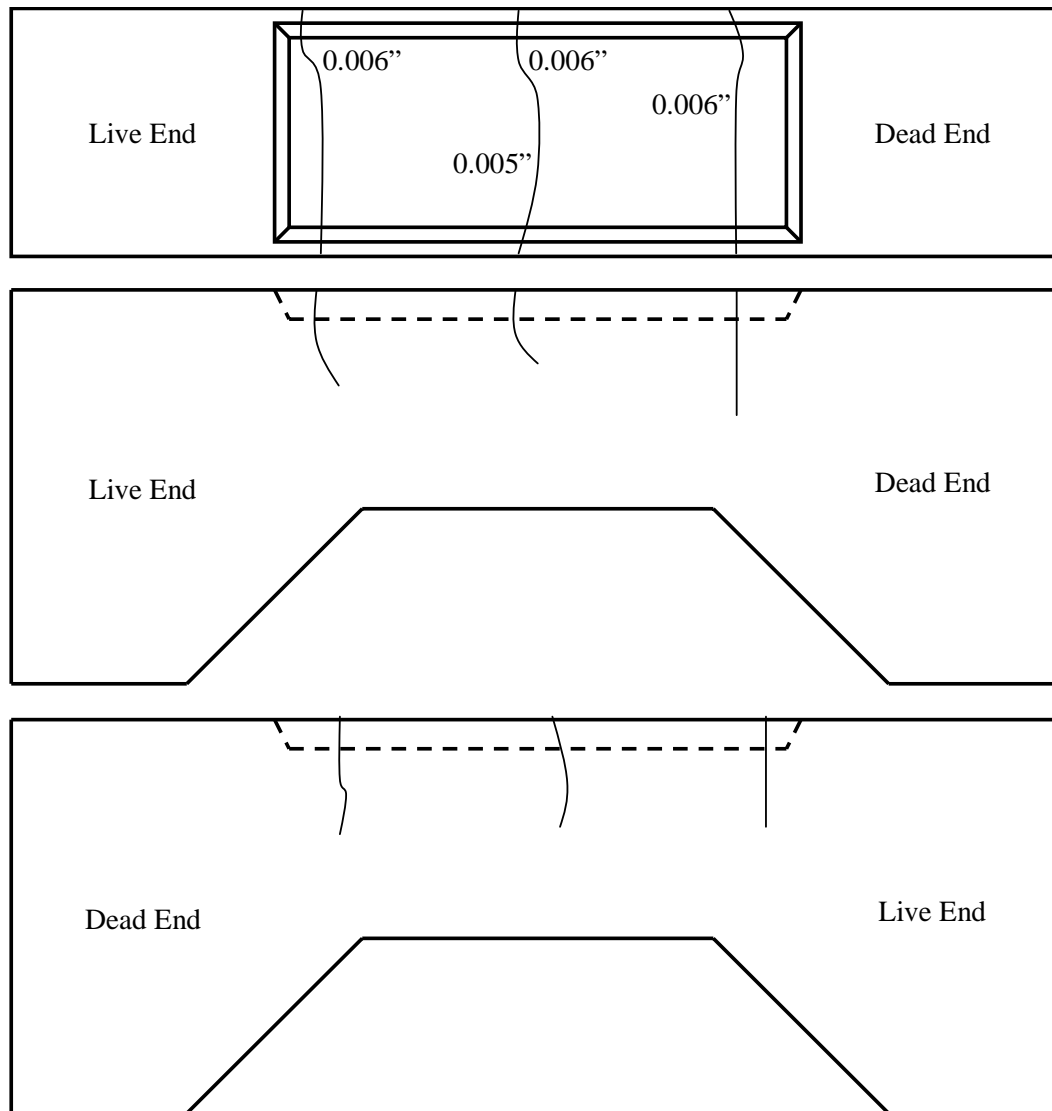


*Figure C.10: Beam 2.2 Crack Map*

*C.1.6.4 Beam 2.2 Comments*

- Measured crack widths were not as wide as most specimens. The live load force was limited to 65 kips to ensure sustainability of Dywidag assembly.

### C.1.7 Beam 2.3

#### C.1.7.1 Beam 2.3 Materials

*Table C.13: Beam 2.3 Materials*

<b>Strand</b>	Conventional
<b>Duct</b>	GTI One-Way Ribbed Plastic
<b>Coupler</b>	GTI Snap-On (Duct 1)
<b>Bearing Plate</b>	Non-Galvanized
<b>28-Day Concrete Strength, <math>f'_c</math></b>	4080 psi

#### C.1.7.2 Beam 2.3 Important Dates

*Table C.14: Beam 2.3 Important Dates*

<b>Casting</b>	October 18, 2004
<b>Prestress Application</b>	January 27, 2005
<b>Grouting</b>	February 1, 2005
<b>Anchorage Protection</b>	February 3, 2005
<b>Live Load Application</b>	February 22, 2005
<b>Exposure Initiation</b>	<i>Not Available</i>

### C.1.7.3 Beam 2.3 Stressing History

#### Live Load Application Plot

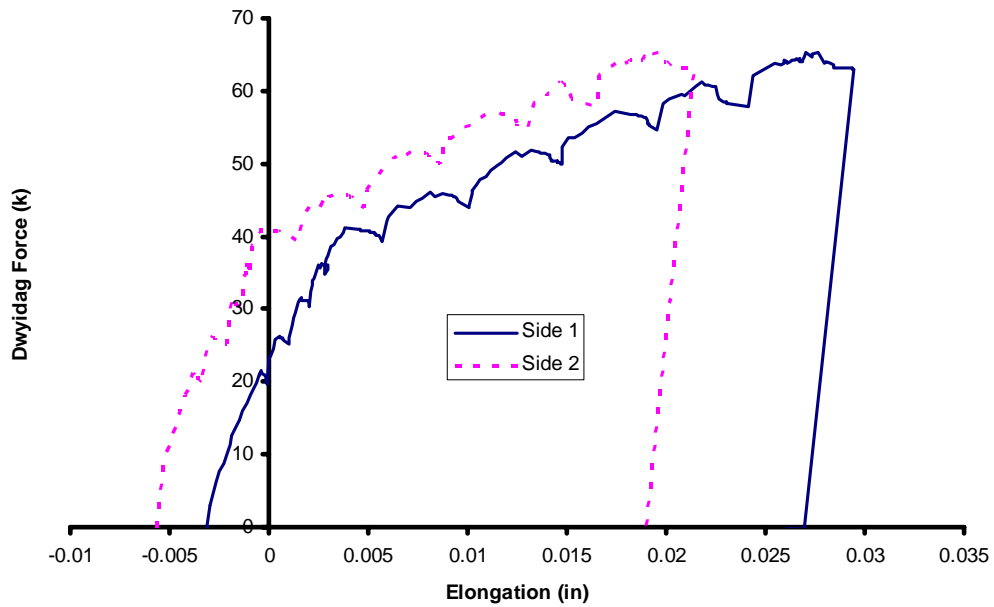


*Figure C.11: Beam 2.3 Live Load Application Plot*

#### Crack Widths

The maximum measured crack width on the top of the specimen within the depression for the salt bath is 0.009 in. See the crack map within this section for additional information regarding location and widths of cracks.

### Crack Map

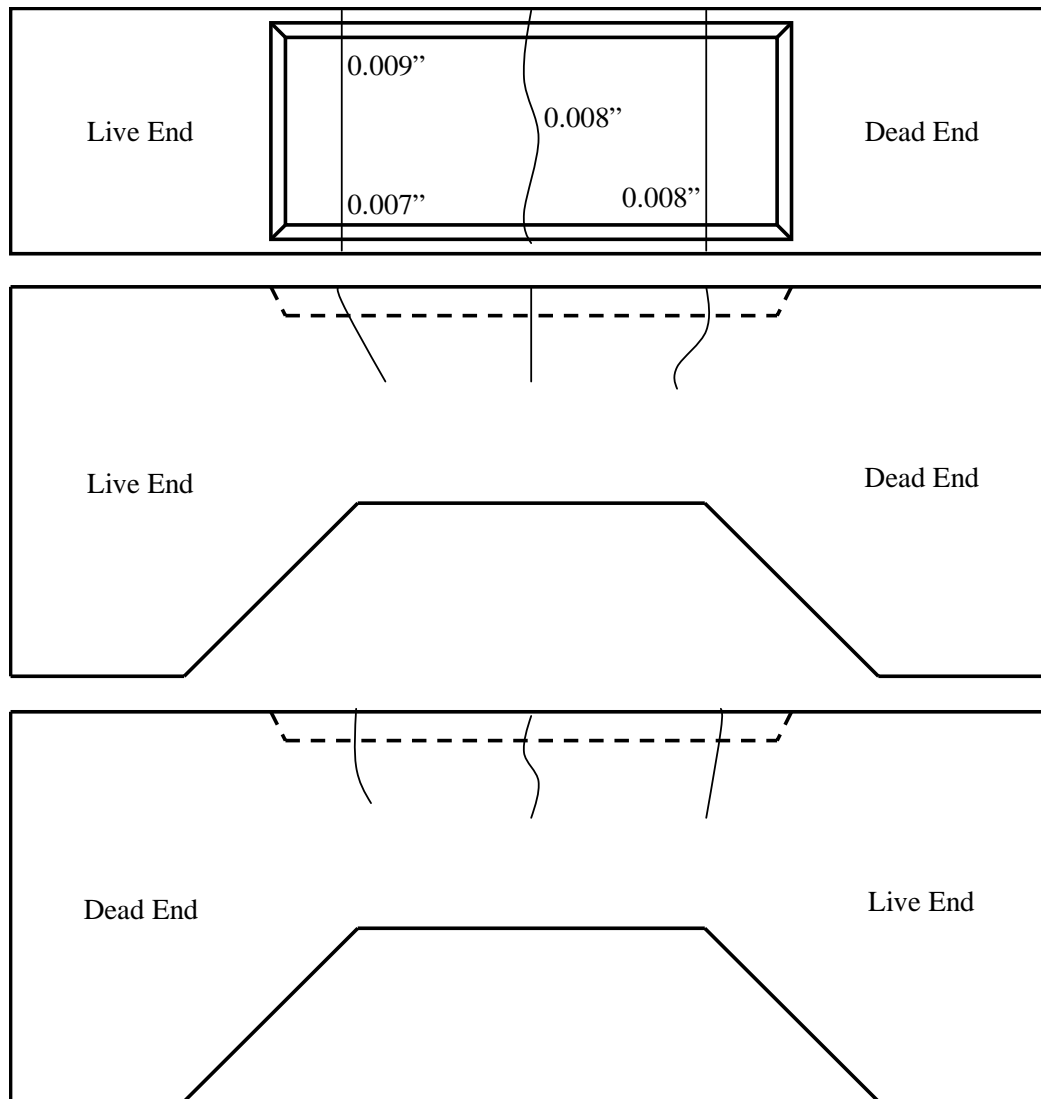


*Figure C.12: Beam 2.3 Crack Map*

#### *C.1.7.4 Beam 2.3 Comments*

- Beam 2.3 was not grouted within 48 hours of stressing as described in Section 4.9; instead, the specimen was grouted 5 days after prestressing.

## C.1.8 Beam 2.4

### C.1.8.1 Beam 2.4 Materials

*Table C.15: Beam 2.4 Materials*

<b>Strand</b>	Copper Clad
<b>Duct</b>	GTI One-Way Ribbed Plastic
<b>Coupler</b>	GTI Snap-On (Duct 1)
<b>Bearing Plate</b>	Non-Galvanized
<b>28-Day Concrete Strength, <math>f'_c</math></b>	4080 psi

### C.1.8.2 Beam 2.4 Important Dates

*Table C.16: Beam 2.4 Important Dates*

<b>Casting</b>	October 18, 2004
<b>Prestress Application</b>	February 16, 2005
<b>Grouting</b>	February 17, 2005
<b>Anchorage Protection</b>	February 24, 2005
<b>Live Load Application</b>	March 3, 2005
<b>Exposure Initiation</b>	<i>Not Available</i>

### ***C.1.8.3 Beam 2.4 Stressing History***

#### **Live Load Application Plot**

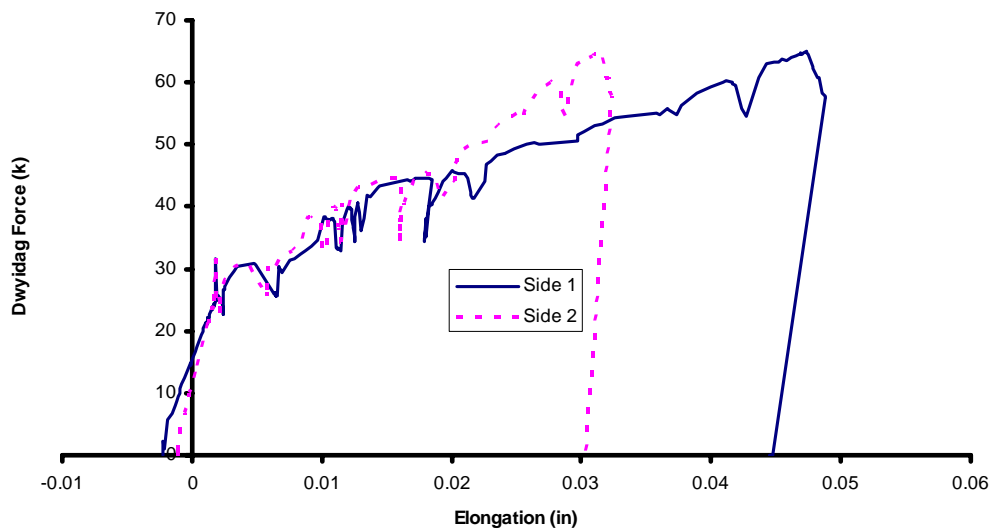


***Figure C.13: Beam 2.4 Live Load Application Plot***

#### **Crack Widths**

The maximum measured crack width on the top of the specimen within the depression for the salt bath is 0.016 in. See the crack map within this section for additional information regarding location and widths of cracks.

Crack Map

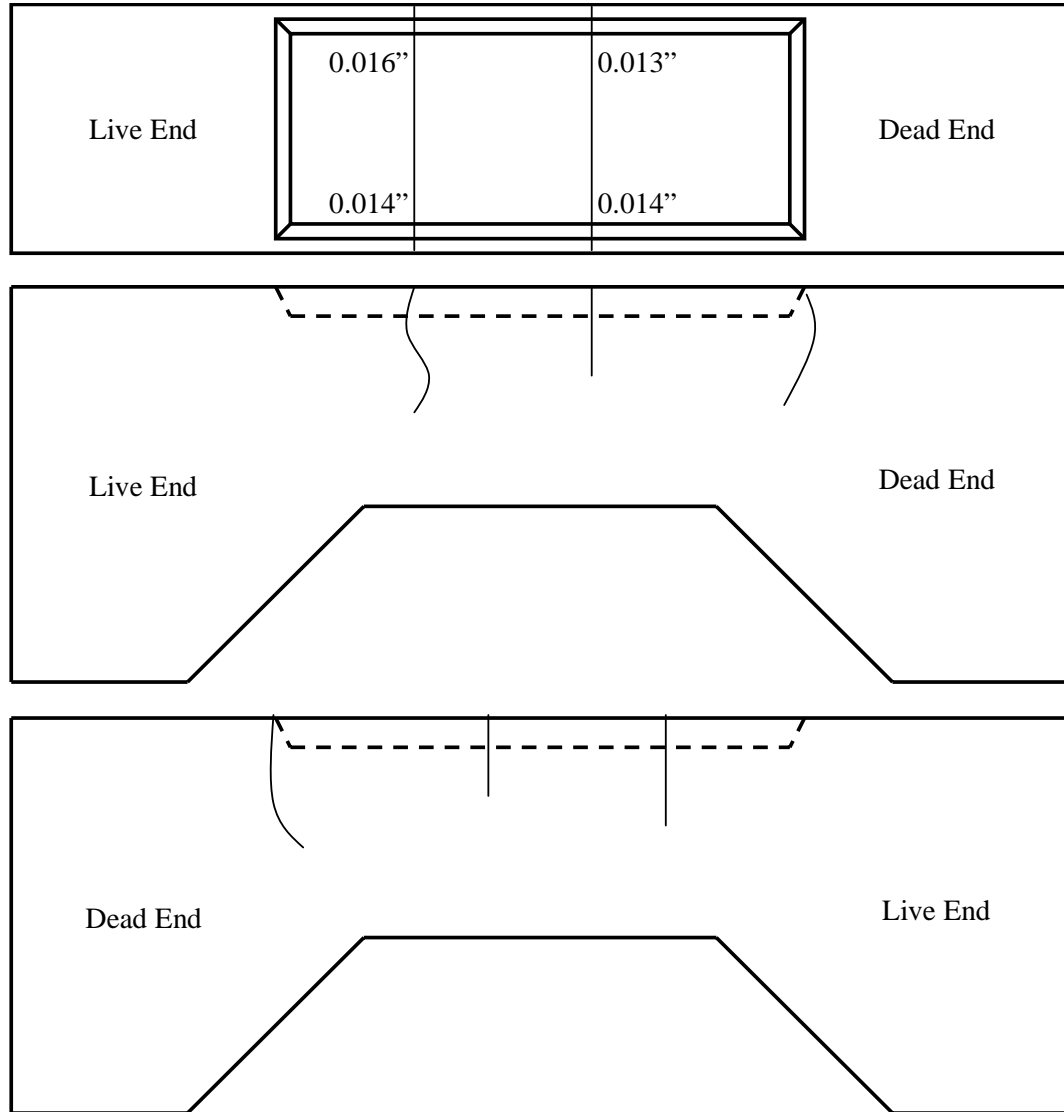


*Figure C.14: Beam 2.4 Crack Map*

**C.1.8.4 Beam 2.4 Comments**

- A portion of all three wedges in the live end anchorhead of duct 2 were partially cracked, but the wedge remained intact. A picture of the damaged wedges is included with the electronic thesis.

- The copper clad strand was delivered to FSEL in an approximately 3 ft. diameter roll. After being cut to length the strand remained curved. In addition to the irregular form, the individual wires of the copper clad strand began to separate at the cut ends. The curved shape and open ends made strand placement in the ducts difficult. The leading end of the strand was taped to keep it from separating and protect the duct. A lead wire was attached in order to guide the leading end of the strand as it was pushed in from the dead end of the beam. Even with the precautions taken, the end of the strand scrapped the interior of the plastic duct. Plastic shavings were observed exiting the duct after the strand was pushed through the duct.
- During the initial stages of applying the live load, a problem was noticed with the electronics. The use of an ungrounded extension cord on the hydraulic pump was affecting the data acquisition system. The problem was rectified before continuing with the Dywidag stressing.
- Initial cracking occurred at a lower load and the final crack widths were larger than most specimens.
- After stressing was completed, cracks extending from the reentrant corner of the live end pocket were observed in the corbels. The corbel cracking was present in the trial specimens, but inclined #3 bars were added to the reinforcement cage through the crack plane in order to control corbel cracking in future specimens.



### C.1.9 Beam 3.1

#### C.1.9.1 Beam 2.1 Materials

*Table C.17: Beam 3.1 Materials*

<b>Strand</b>	Conventional
<b>Duct</b>	GTI Two-Way Ribbed Plastic
<b>Coupler</b>	GTI Slip-On (Duct 1)
<b>Bearing Plate</b>	Non-Galvanized
<b>28-Day Concrete Strength, <math>f'_c</math></b>	7260 psi

#### C.1.9.2 Beam 2.1 Important Dates

*Table C.18: Beam 3.1 Important Dates*

<b>Casting</b>	December 8, 2004
<b>Prestress Application</b>	January 27, 2005
<b>Grouting</b>	February 1, 2005
<b>Anchorage Protection</b>	February 3, 2005
<b>Live Load Application</b>	February 22, 2005
<b>Exposure Initiation</b>	<i>Not Available</i>

### C.1.9.3 Beam 2.1 Stressing History

#### Live Load Application Plot

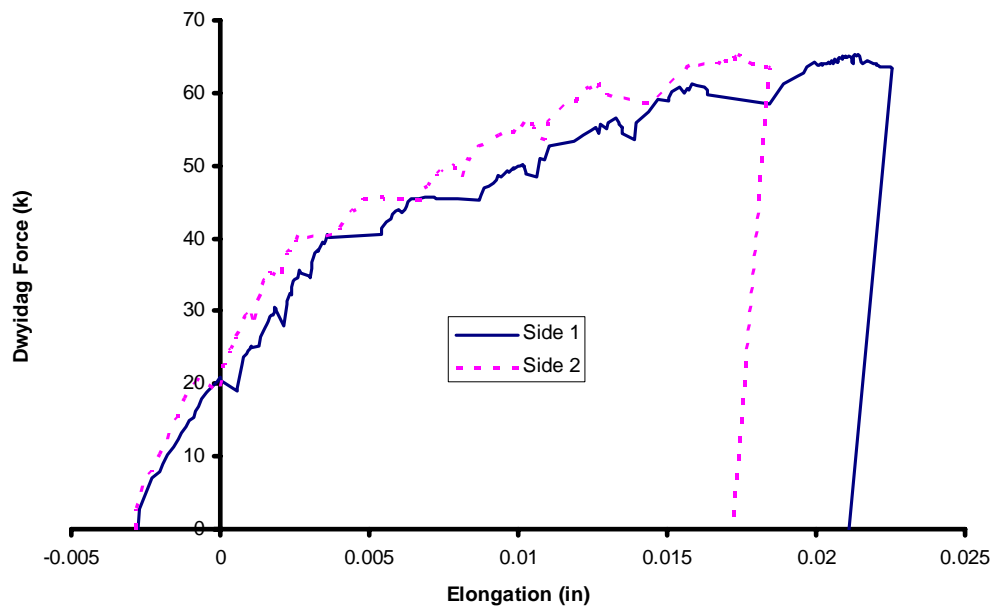


*Figure C.15: Beam 3.1 Live Load Application Plot*

#### Crack Widths

The maximum measured crack width on the top of the specimen within the depression for the salt bath is 0.010 in. See the crack map within this section for additional information regarding location and widths of cracks.

Crack Map

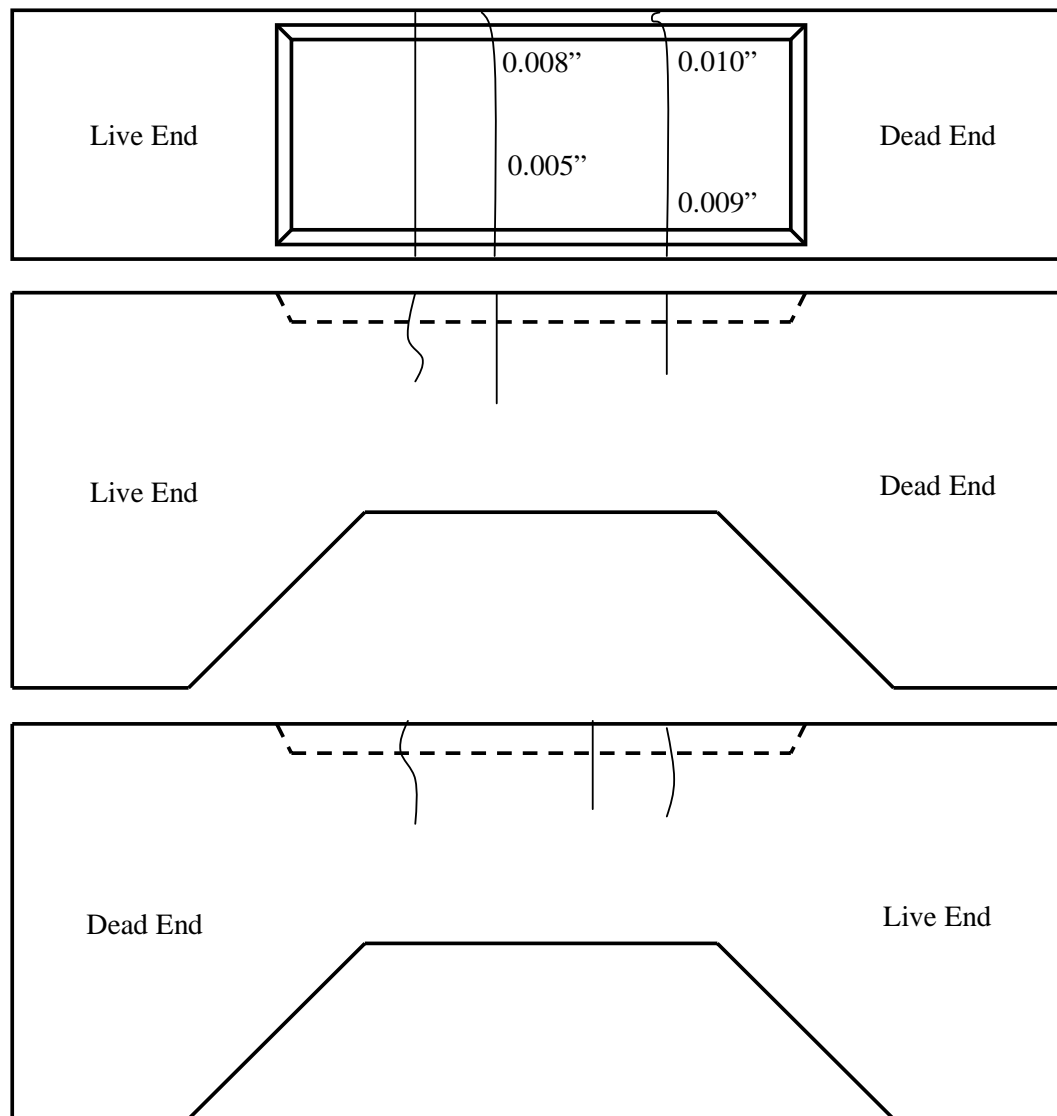


*Figure C.16: Beam 3.1 Crack Map*

*C.1.9.4 Beam 3.1 Comments*

- Beam 3.1 was not grouted within 48 hours of stressing as described in Section 4.9; instead, the specimen was grouted 5 days after prestressing.

### C.1.10 Beam 3.2

#### C.1.10.1 Beam 3.2 Materials

*Table C.19: Beam 3.2 Materials*

<b>Strand</b>	Hot-Dip Galvanized
<b>Duct</b>	GTI Two-Way Ribbed Plastic
<b>Coupler</b>	GTI Slip-On (Duct 1)
<b>Bearing Plate</b>	Non-Galvanized
<b>28-Day Concrete Strength, <math>f'_c</math></b>	7260 psi

#### C.1.10.2 Beam 3.2 Important Dates

*Table C.20: Beam 3.2 Important Dates*

<b>Casting</b>	December 8, 2004
<b>Prestress Application</b>	March 9, 2005
<b>Grouting</b>	March 9, 2005
<b>Anchorage Protection</b>	March 15, 2005
<b>Live Load Application</b>	March 22, 2005
<b>Exposure Initiation</b>	<i>Not Available</i>

### *C.1.10.3 Beam 3.2 Stressing History*

#### Live Load Application Plot

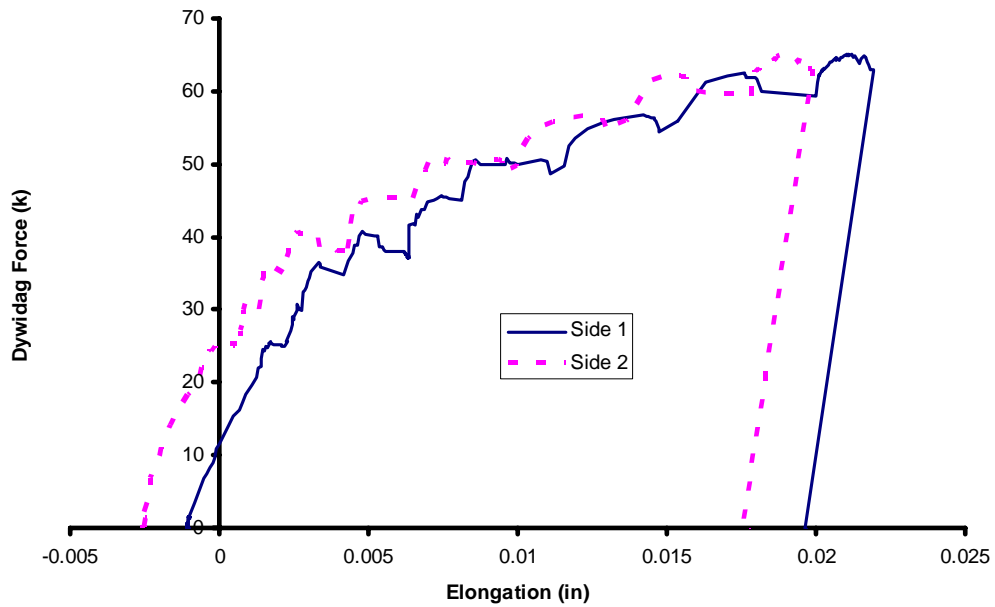
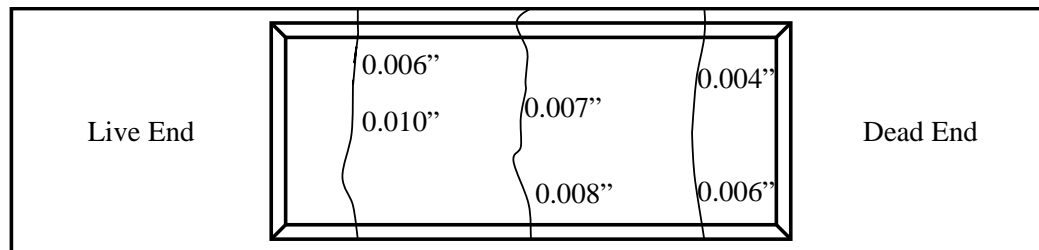


*Figure C.17: Beam 3.2 Live Load Application Plot*

#### Crack Widths

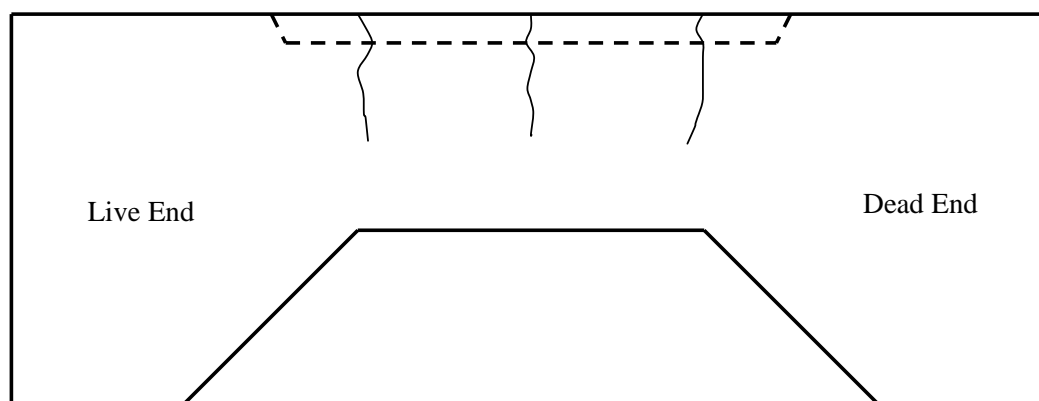
The maximum measured crack width on the top of the specimen within the depression for the salt bath is 0.010 in. See the crack map within this section for additional information regarding location and widths of cracks.

Crack Map

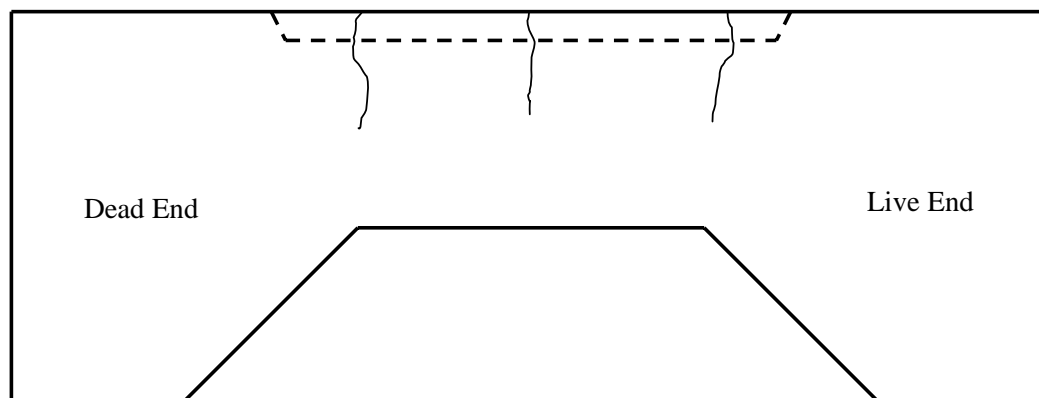


0.008"

Plan



Elevation



Elevation

**Figure C.18: Beam 3.2 Crack Map**

#### ***C.1.10.4 Beam 3.2 Comments***

- While grouting duct 2, small air bubbles were observed near the base of the grout vent at the middle of the beam.

#### **C.1.11 Beam 3.3**

##### ***C.1.11.1 Beam 3.3 Materials***

***Table C.21: Beam 3.3 Materials***

<b>Strand</b>	Copper Clad
<b>Duct</b>	GTI Two-Way Ribbed Plastic
<b>Coupler</b>	GTI Slip-On (Duct 1)
<b>Bearing Plate</b>	Non-Galvanized
<b>28-Day Concrete Strength, <math>f'_c</math></b>	7260 psi

##### ***C.1.11.2 Beam 3.3 Important Dates***

***Table C.22: Beam 3.3 Important Dates***

<b>Casting</b>	December 8, 2004
<b>Prestress Application</b>	February 16, 2005
<b>Grouting</b>	February 17, 2005
<b>Anchorage Protection</b>	February 24, 2005
<b>Live Load Application</b>	March 3, 2005
<b>Exposure Initiation</b>	<i>Not Available</i>

### C.1.11.3 Beam 3.3 Stressing History

#### Live Load Application Plot

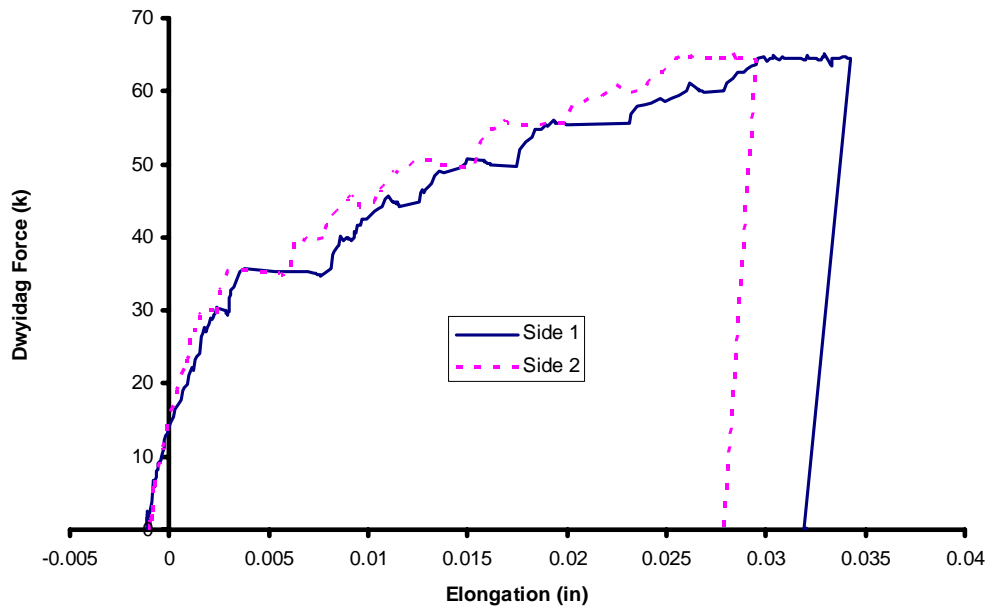


**Figure C.19: Beam 3.3 Live Load Application Plot**

#### Crack Widths

The maximum measured crack width on the top of the specimen within the depression for the salt bath is 0.011 in. See the crack map within this section for additional information regarding location and widths of cracks.



Crack Map

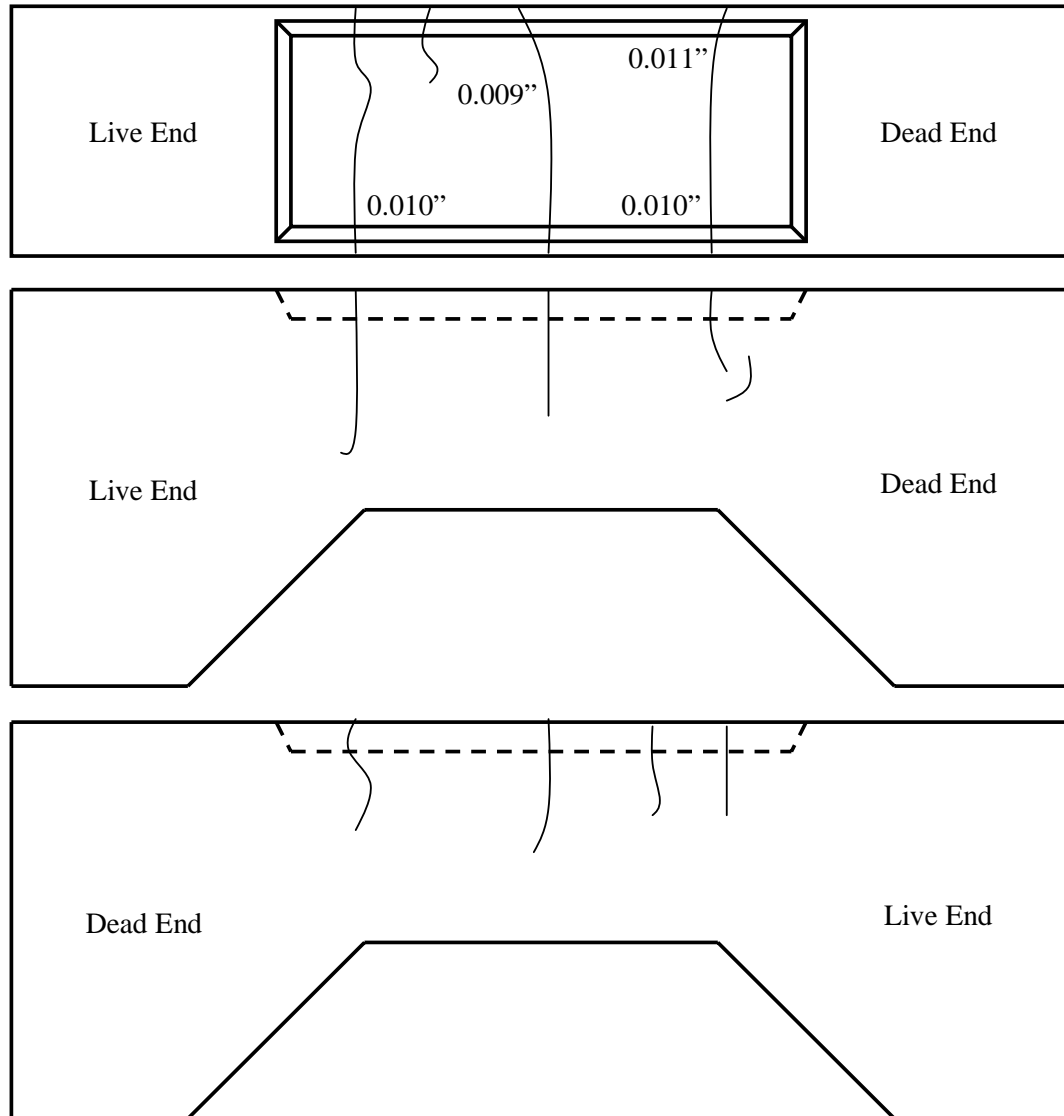


*Figure C.20: Beam 3.3 Crack Map*

***C.1.11.4 Beam 3.3 Comments***

- Grout did not flow from temporary grout cap vent at the dead end of duct 2 as it had for all other specimens. When the cap was removed, water

dripped from the rubber gasket of the grout cap and the back of the anchor head was only partially filled. To ensure full grouting in the tendon, grout was injected into a hole drilled through the epoxy plug in the anchor head, but the tendon was well grouted and no additional grout was needed. As an extra precaution, the temporary cap was replaced and filled with grout. Pictures of the anchor head immediately after removing the partially filled temporary grout cap are included in the electronic version of the thesis.

### **C.1.12 Beam 3.4**

#### *C.1.12.1 Beam 3.4 Materials*

*Table C.23: Beam 3.4 Materials*

<b>Strand</b>	Hot-Dip Galvanized
<b>Duct</b>	VSL One-Way Ribbed Plastic
<b>Coupler</b>	VSL Snap-On (Duct 1)
<b>Bearing Plate</b>	Non-Galvanized
<b>28-Day Concrete Strength, <math>f'_c</math></b>	7260 psi

**C.1.12.2 Beam 3.4 Important Dates**

**Table C.24: Beam 3.4 Important Dates**

<b>Casting</b>	December 8, 2004
<b>Prestress Application</b>	March 9, 2005
<b>Grouting</b>	March 9, 2005
<b>Anchorage Protection</b>	March 15, 2005
<b>Live Load Application</b>	March 22, 2005
<b>Exposure Initiation</b>	<i>Not Available</i>

**C.1.12.3 Beam 3.4 Stressing History**

Live Load Application Plot

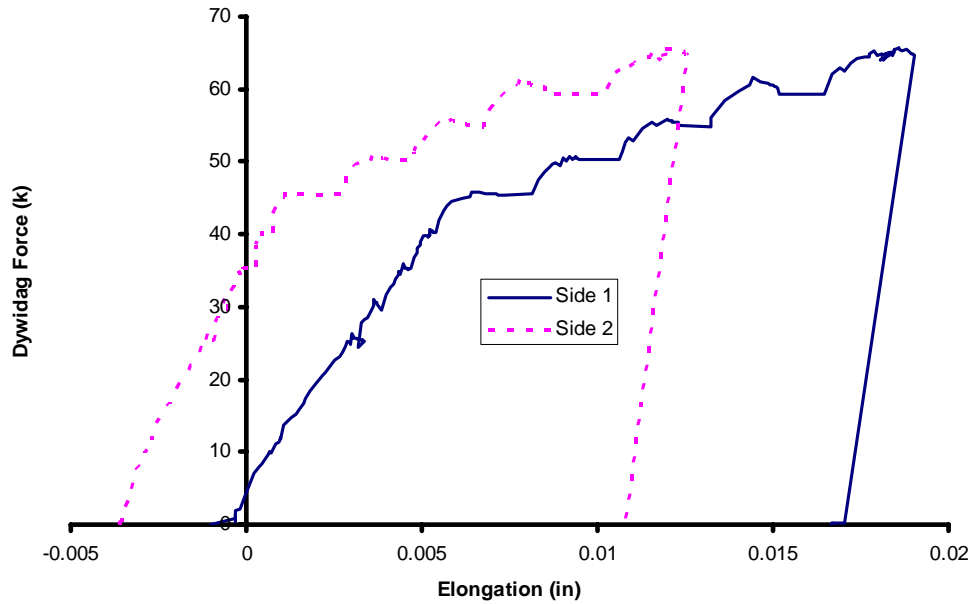


**Figure C.21: Beam 3.4 Live Load Application Plot**

### Crack Widths

The maximum measured crack width on the top of the specimen within the depression for the salt bath is 0.005 in. See the crack map within this section for additional information regarding location and widths of cracks.

### Crack Map

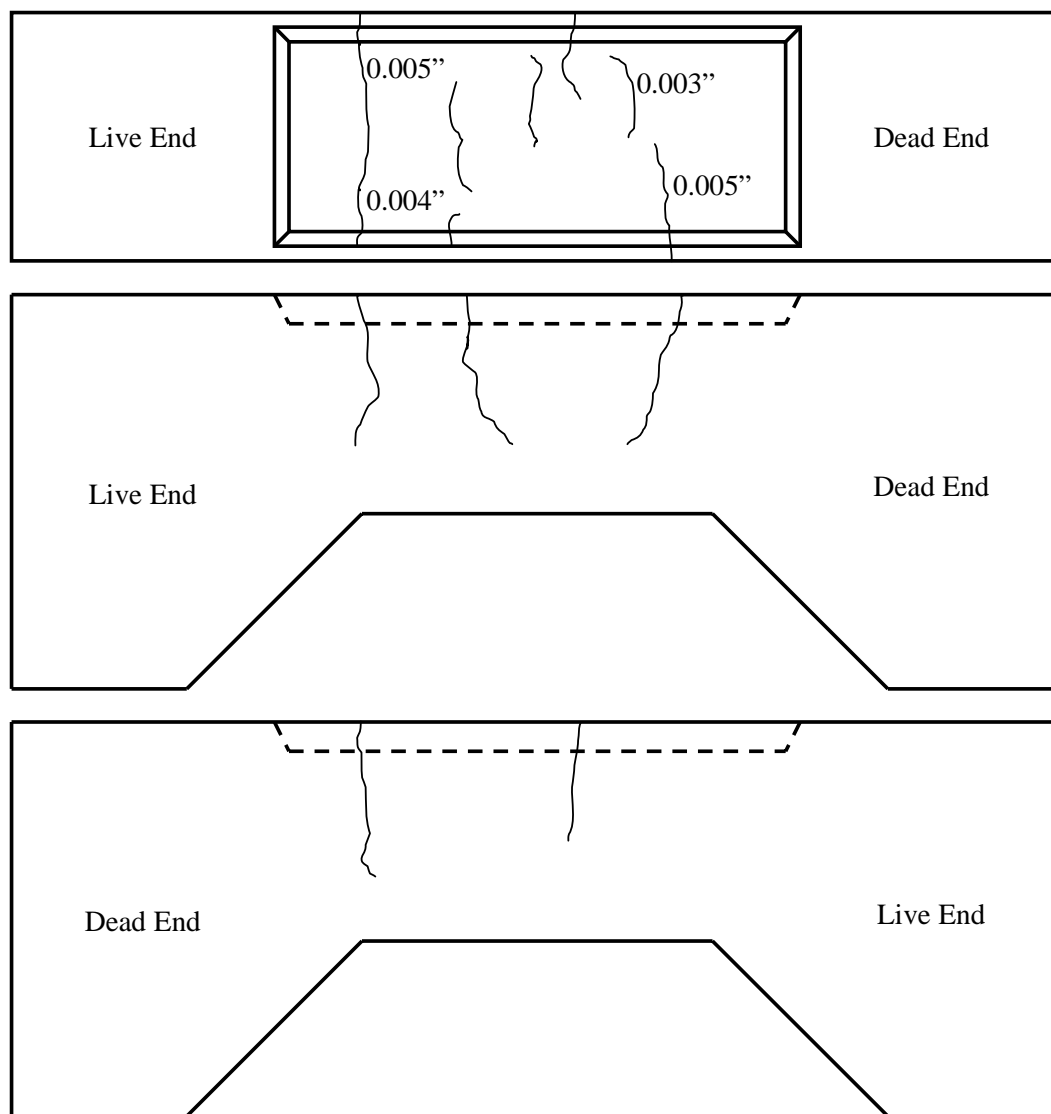


*Figure C.22: Beam 3.4 Crack Map*

#### ***C.1.12.4 Beam 3.4 Comments***

- Measured crack widths were not as wide as most specimens. The live load force was limited to 65 kips to ensure sustainability of Dywidag assembly.
- After stressing was completed, cracks extending from the reentrant corner of the live end pocket were observed in the corbels. The corbel cracking was present in the trial specimens, but inclined #3 bars were added to the reinforcement cage through the crack plane in order to control corbel cracking in future specimens.

#### **C.1.13 Beam 4.1**

##### ***C.1.13.1 Beam 4.1 Materials***

***Table C.25: Beam 4.1 Materials***

<b>Strand</b>	Stainless
<b>Duct</b>	Galvanized Corrugated Steel
<b>Coupler</b>	None
<b>Bearing Plate</b>	Non-Galvanized
<b>28-Day Concrete Strength, <math>f'_c</math></b>	7120 psi

**C.1.13.2 Beam 4.1 Important Dates**

**Table C.26: Beam 4.1 Important Dates**

<b>Casting</b>	February 10, 2004
<b>Prestress Application</b>	March 9, 2005
<b>Grouting</b>	March 9, 2005
<b>Anchorage Protection</b>	March 15, 2005
<b>Live Load Application</b>	March 22, 2005
<b>Exposure Initiation</b>	<i>Not Available</i>

**C.1.13.3 Beam 4.1 Stressing History**

Live Load Application Plot

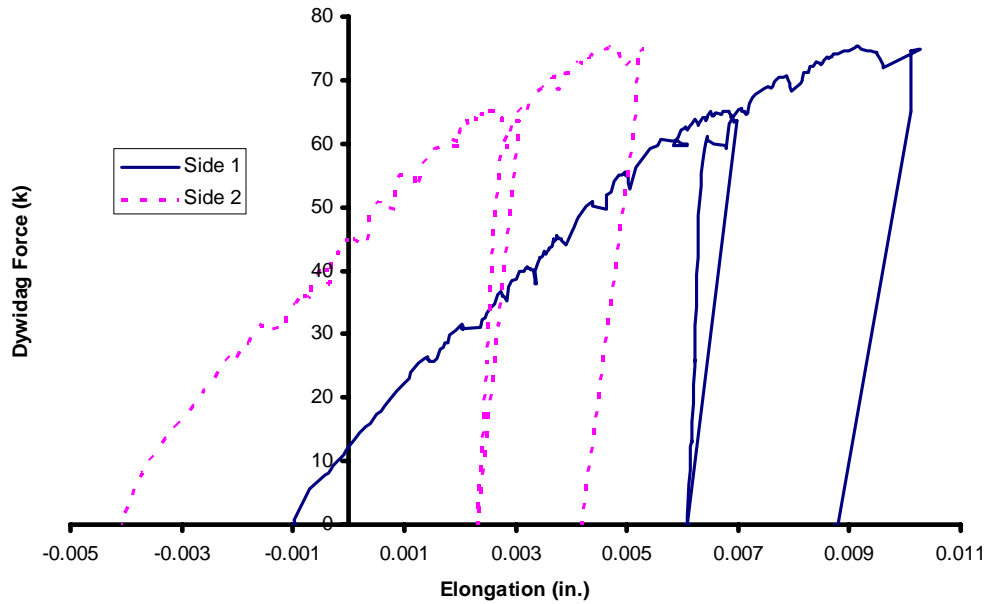


**Figure C.23: Beam 4.1 Live Load Application Plot**

### Crack Widths

The maximum measured crack width on the top of the specimen within the depression for the salt bath is 0.004 in. See the crack map within this section for additional information regarding location and widths of cracks.

### Crack Map

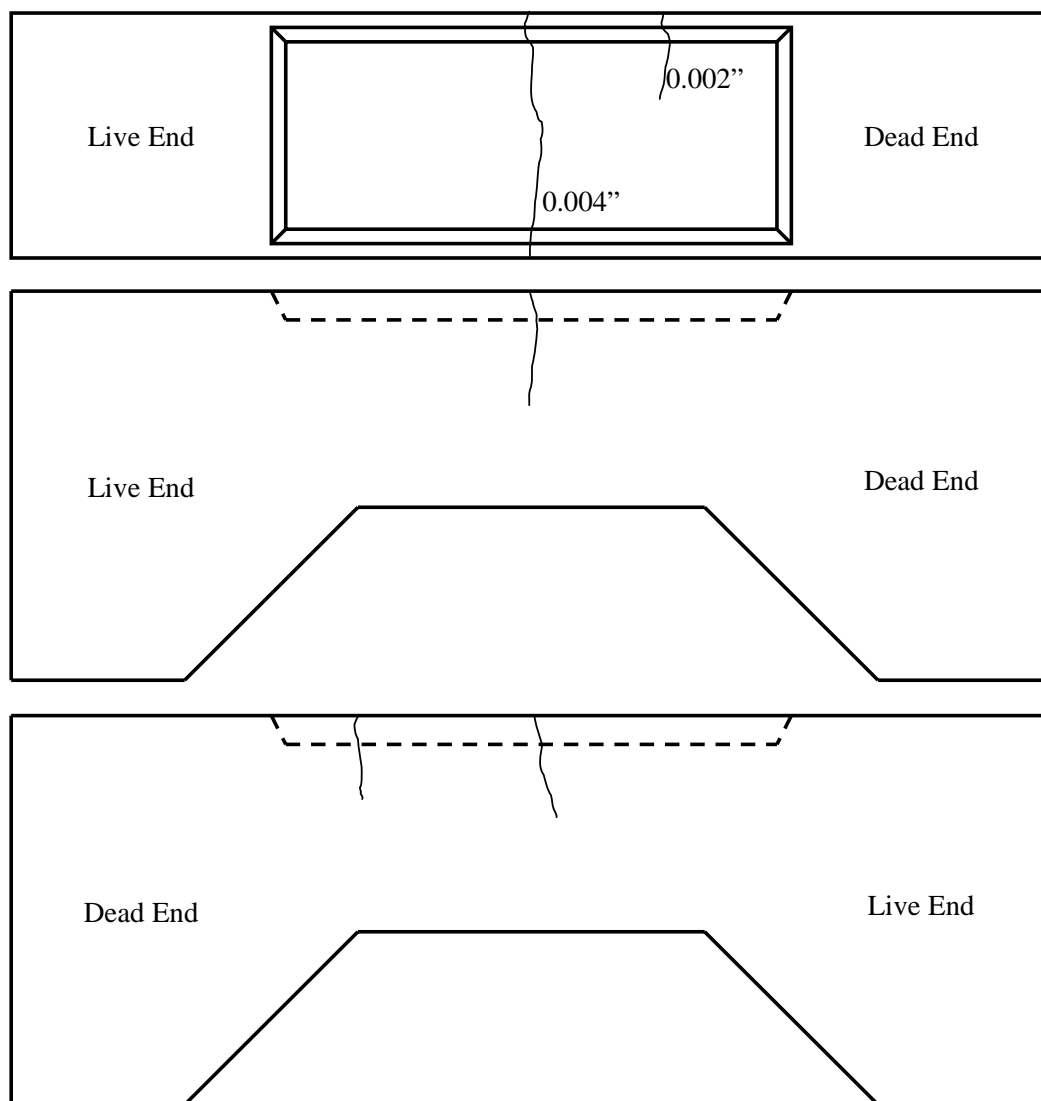


**Figure C.24: Beam 4.1 Crack Map**

#### ***C.1.13.4 Beam 4.1 Comments***

- Since 0.6-in. strands were used in the specimen, the prestress force was larger than other specimens (see Section 3.2.1). Therefore, the live load required to crack the beam was larger. The specimen was originally stressed to 65k similarly to other specimens, but the cracks in the top surface of the beam were too narrow for research purposes. To improve the cracking, the live load was increased to 75 kips by stressing the Dywidag bar again (see Figure C.23).
- Despite the increased live load, the cracks in Beam 4.1 are relatively narrow compared to other specimens.
- The duct 1 side wall of the dead end anchorage pocket wall was broken when the plastic-covered, wood pocket forms were removed. The damaged portion of the anchorage pocket was repaired when the pocket was filled with grout. A picture of the damaged pocket is included with the electronic version of the thesis.
- After stressing was completed, cracks extending from the reentrant corner of the live end pocket were observed in the corbels. The corbel cracking was present in the trial specimens, but inclined #3 bars were added to the reinforcement cage through the crack plane in order to control corbel cracking in future specimens.



## C.1.14 Beam 4.2

### C.1.14.1 Beam 4.2 Materials

*Table C.27: Beam 4.2 Materials*

<b>Strand</b>	Stainless
<b>Duct</b>	VSL One-Way Ribbed Plastic
<b>Coupler</b>	VSL Snap-On (Duct 1)
<b>Bearing Plate</b>	Non-Galvanized
<b>28-Day Concrete Strength, <math>f'_c</math></b>	7120 psi

### C.1.14.2 Beam 4.2 Important Dates

*Table C.28: Beam 4.2 Important Dates*

<b>Casting</b>	February 10, 2004
<b>Prestress Application</b>	March 9, 2005
<b>Grouting</b>	March 9, 2005
<b>Anchorage Protection</b>	March 15, 2005
<b>Live Load Application</b>	March 22, 2005
<b>Exposure Initiation</b>	<i>Not Available</i>

### C.1.14.3 Beam 4.2 Stressing History

#### Live Load Application Plot

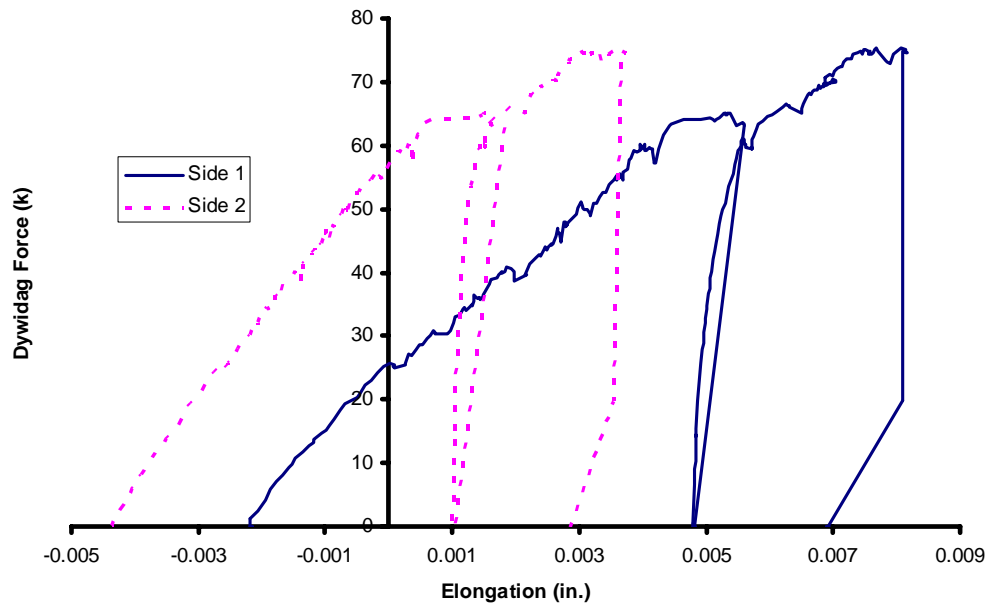


*Figure C.25: Beam 4.2 Live Load Application Plot*

#### Crack Widths

The maximum measured crack width on the top of the specimen within the depression for the salt bath is 0.003 in. See the crack map within this section for additional information regarding location and widths of cracks.

### Crack Map

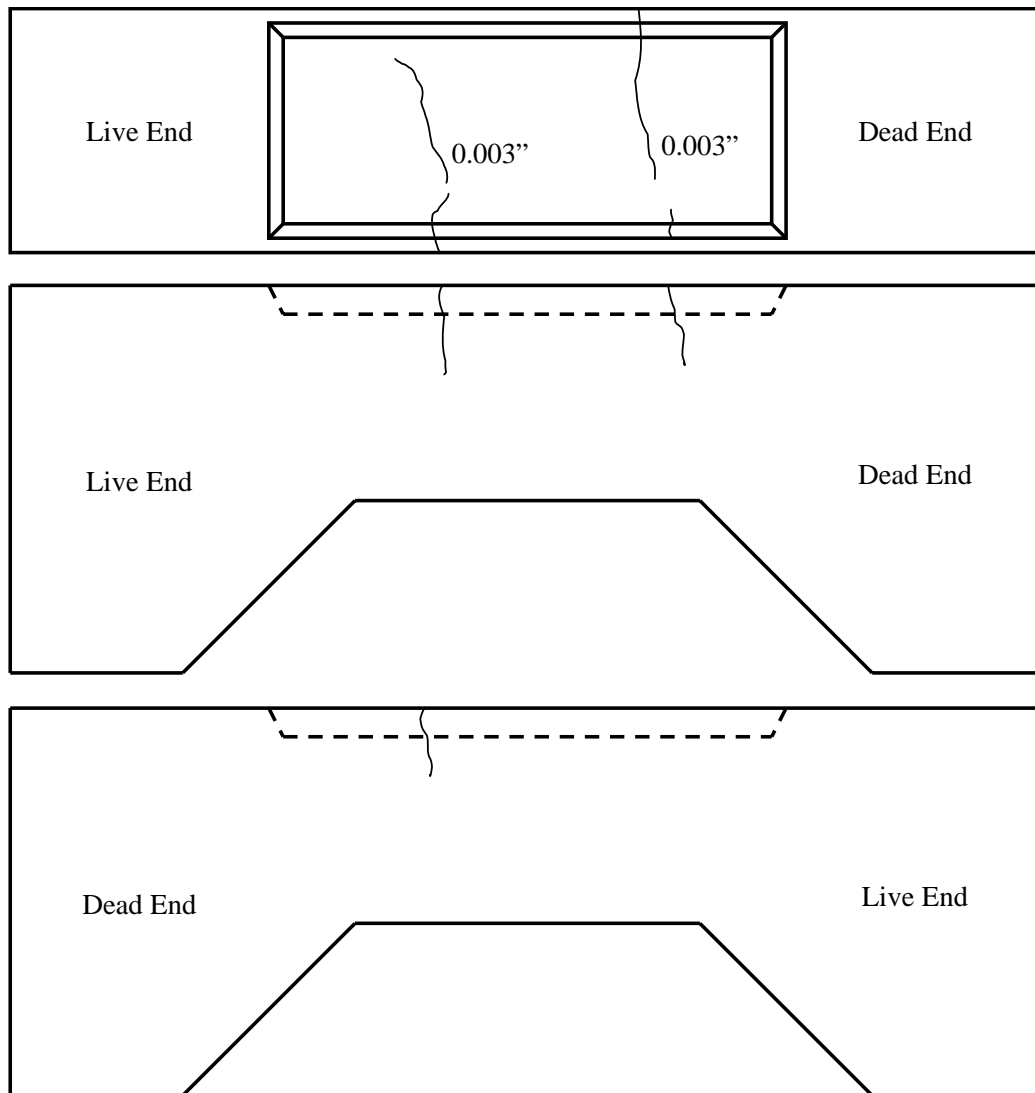


*Figure C.26: Beam 4.2 Crack Map*

#### ***C.1.14.4 Beam 4.2 Comments***

- Since 0.6-in. strands were used in the specimen, the prestress force was larger than other specimens (see Section 3.2.1). Therefore, the live load required to crack the beam was larger. The specimen was originally

stressed to 65k similarly to other specimens, but the cracks in the top surface of the beam were too narrow for research purposes. To improve the cracking, the live load was increased to 75 kips by stressing the Dywidag bar again (see Figure C.25).

- Despite the increased live load, the cracks in Beam 4.1 are relatively narrow compared to other specimens.

### **C.1.15 Beam 4.3**

Beam 4.3 is a reinforced concrete specimen to compare with the other prestressed specimens. The passive longitudinal steel reinforcement is epoxy coated. The epoxy coated rebar for the comparison specimens was supplied by ABC Coating – the same company that provided the epoxy coated rebar for the general reinforcement cage.

#### ***C.1.15.1 Beam 4.3 Materials***

***Table C.29: Beam 4.3 Materials***

<b>Strand</b>	None
<b>Duct</b>	None
<b>Coupler</b>	None
<b>Bearing Plate</b>	None
<b>28-Day Concrete Strength, <math>f'_c</math></b>	7120 psi

**C.1.15.2 Beam 4.3 Important Dates**

**Table C.30: Beam 4.3 Important Dates**

<b>Casting</b>	February 10, 2004
<b>Prestress Application</b>	Not Applicable
<b>Grouting</b>	Not Applicable
<b>Anchorage Protection</b>	Not Applicable
<b>Live Load Application</b>	March 8, 2005
<b>Exposure Initiation</b>	<i>Not Available</i>

**C.1.15.3 Beam 4.3 Stressing History**

Live Load Application Plot

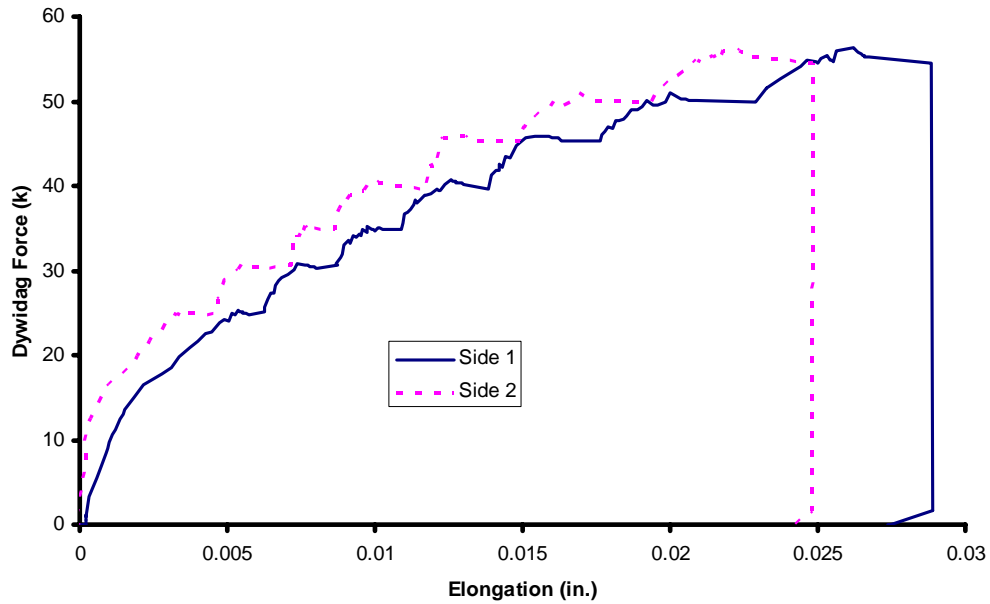


**Figure C.27: Beam 4.3 Live Load Application Plot**

### Crack Widths

The maximum measured crack width on the top of the specimen within the depression for the salt bath is 0.008 in. See the crack map within this section for additional information regarding location and widths of cracks.

### Crack Map

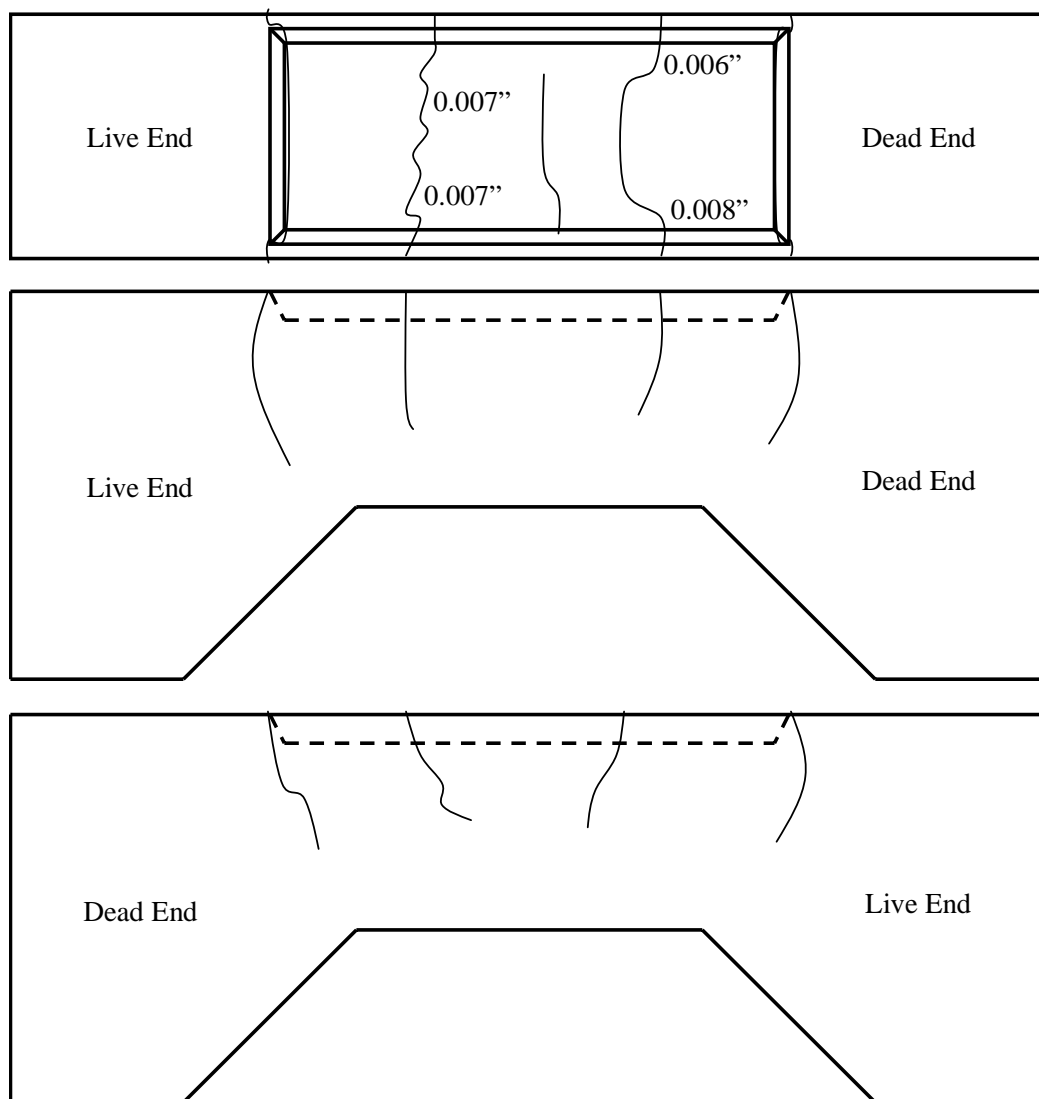


**Figure C.28: Beam 4.3 Crack Map**

#### ***C.1.15.4 Beam 4.3 Comments***

- Loading was stopped at 55 kips due to the amount of cracking and sustained crack widths. As the load was increased, more cracks formed instead of existing cracks opening wider.
- Beam 4.3 is not prestressed. Therefore, cracking occurs at a lower applied live load (see Figure C.29)

#### **C.1.16 Beam 4.4**

Beam 4.4 is a reinforced concrete specimen to compare with the other prestressed specimens. The passive longitudinal steel reinforcement is uncoated. The bare rebar for the comparison specimens was supplied by ABC Coating – the same company that provided the epoxy coated rebar for the general reinforcement cage.

##### ***C.1.16.1 Beam 4.4 Materials***

***Table C.31: Beam 4.4 Materials***

<b>Strand</b>	None
<b>Duct</b>	None
<b>Coupler</b>	None
<b>Bearing Plate</b>	None
<b>28-Day Concrete Strength, <math>f'_c</math></b>	7120 psi

**C.1.16.2 Beam 4.4 Important Dates**

**Table C.32: Beam 4.4 Important Dates**

<b>Casting</b>	February 10, 2004
<b>Prestress Application</b>	Not Applicable
<b>Grouting</b>	Not Applicable
<b>Anchorage Protection</b>	Not Applicable
<b>Live Load Application</b>	March 8, 2005
<b>Exposure Initiation</b>	<i>Not Available</i>

**C.1.16.3 Beam 4.4 Stressing History**

Live Load Application Plot

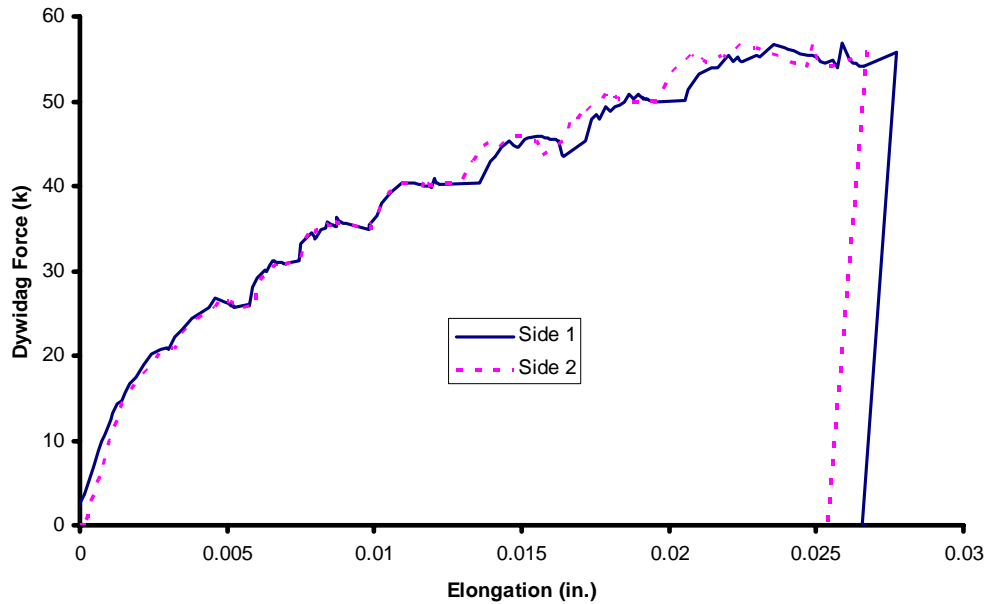


**Figure C.29: Beam 4.4 Live Load Application Plot**



### Crack Widths

The maximum measured crack width on the top of the specimen within the depression for the salt bath is 0.008 in. See the crack map within this section for additional information regarding location and widths of cracks.

### Crack Map

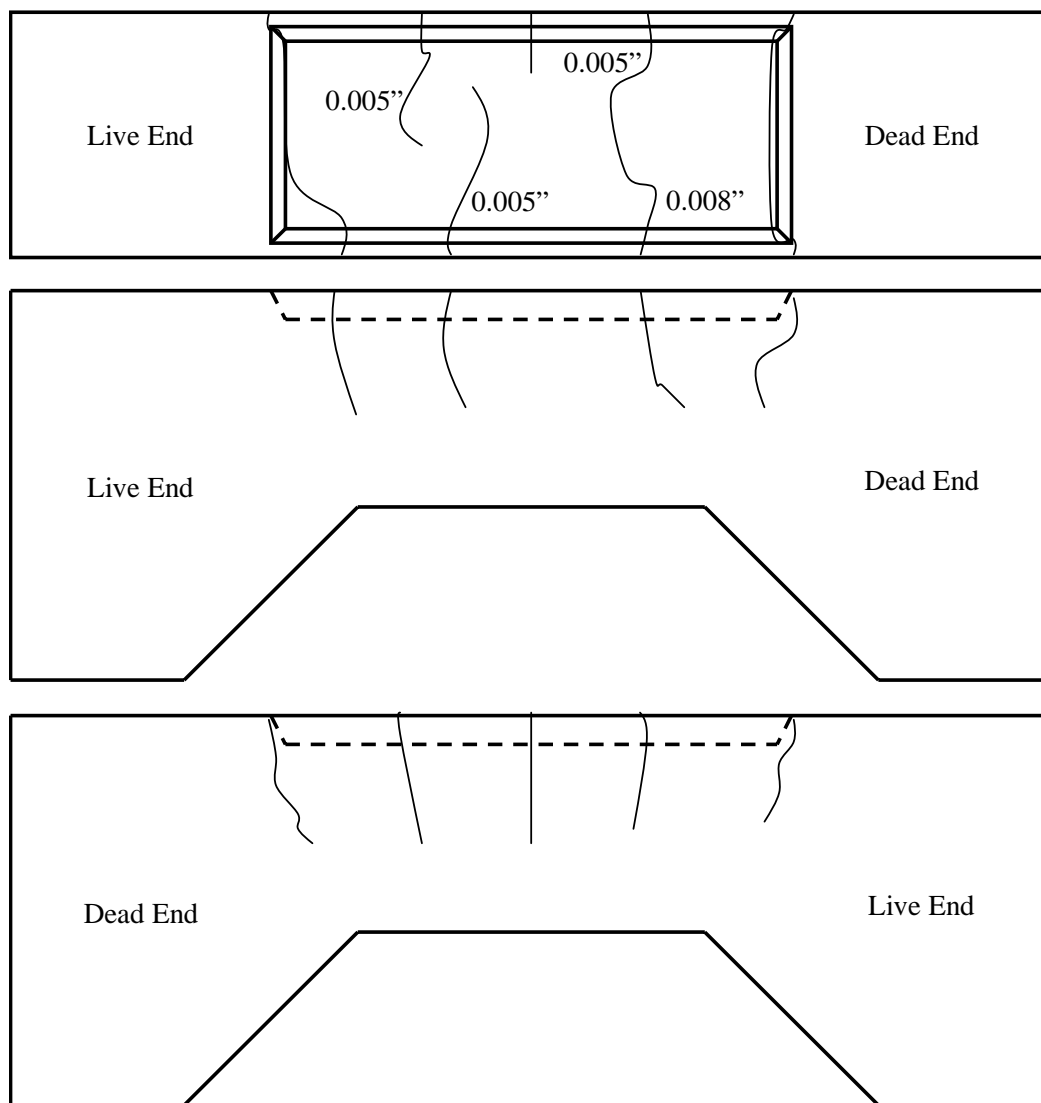


**Figure C.30: Beam 4.4 Crack Map**

#### ***C.1.16.4 Beam 4.4 Comments***

- Loading was stopped at 55 kips due to the amount of cracking and sustained crack widths. As the load was increased, more cracks formed instead of existing cracks opening wider.
- Beam 4.3 is not prestressed. Therefore, cracking occurs at a lower applied live load (see Figure C.31)

#### **C.1.17 Beam 5.1**

##### ***C.1.17.1 Beam 5.1 Materials***

***Table C.33: Beam 5.1 Materials***

<b>Strand</b>	Conventional
<b>Duct</b>	GTI Two-Way Ribbed Plastic
<b>Coupler</b>	GTI Slip-On (Duct 1)
<b>Bearing Plate</b>	Galvanized
<b>28-Day Concrete Strength, <math>f'_c</math></b>	6180 psi

##### ***C.1.17.2 Beam 5.1 Important Dates***

***Table C.34: Beam 5.1 Important Dates***

<b>Casting</b>	March 3, 2005
<b>Prestress Application</b>	March 16, 2005
<b>Grouting</b>	March 17, 2005
<b>Anchorage Protection</b>	April 21, 2005
<b>Live Load Application</b>	April 26, 2005
<b>Exposure Initiation</b>	<i>Not Available</i>

### C.1.17.3 Beam 5.1 Stressing History

#### Live Load Application Plot

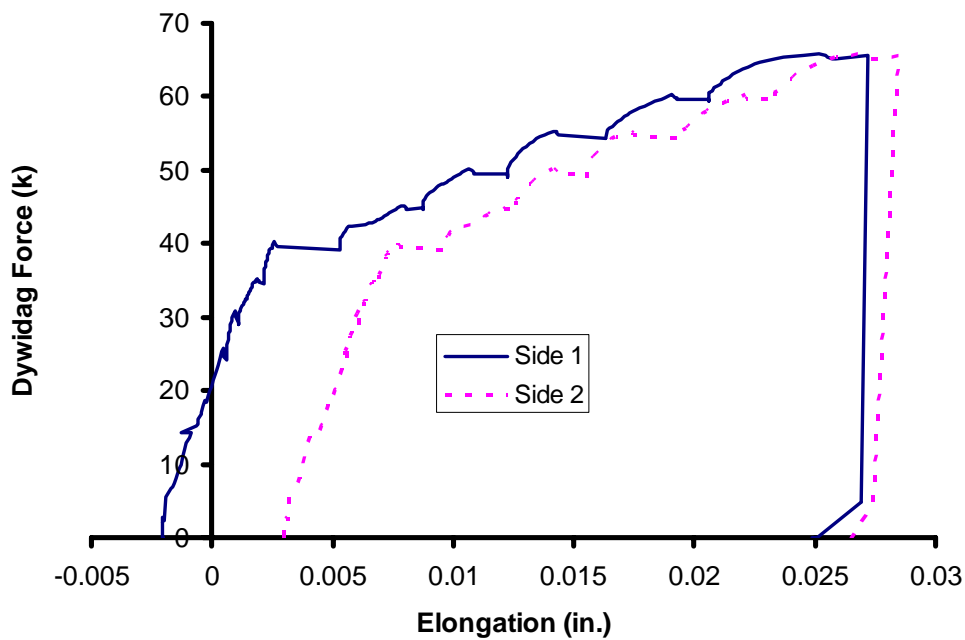


*Figure C.31: Beam 5.1 Live Load Application Plot*

#### Crack Widths

The maximum measured crack width on the top of the specimen within the depression for the salt bath is 0.007 in. See the crack map within this section for additional information regarding location and widths of cracks.

Crack Map

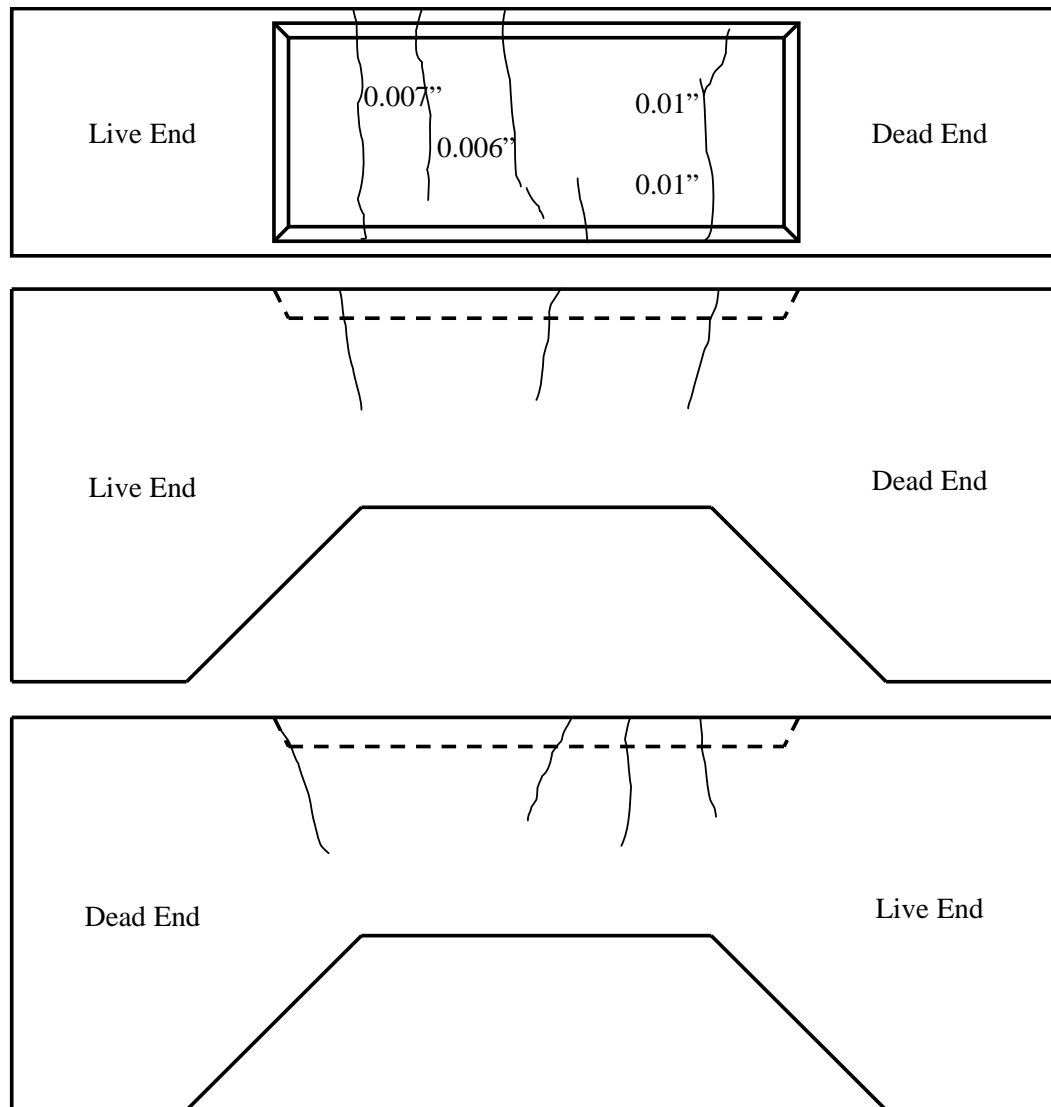


*Figure C.32: Beam 5.1 Crack Map*

***C.1.17.4 Beam 5.1 Comments***

- While grouting Duct 2, small air bubbles were observed 6 in. from the center of the specimen towards the live end.

- After stressing was completed, cracks extending from the reentrant corner of the live end pocket were observed in the corbels. The corbel cracking was present in the trial specimens, but inclined #3 bars were added to the reinforcement cage through the crack plane in order to control corbel cracking in future specimens.

### C.1.18 Beam 5.2

#### C.1.18.1 Beam 5.2 Materials

*Table C.35: Beam 5.2 Materials*

<b>Strand</b>	Stainless Clad (delivered Spring 2005)
<b>Duct</b>	GTI Two-Way Ribbed Plastic
<b>Coupler</b>	GTI Slip-On (Duct 1)
<b>Bearing Plate</b>	Non-Galvanized
<b>28-Day Concrete Strength, <math>f'_c</math></b>	6180 psi

#### C.1.18.2 Beam 5.2 Important Dates

*Table C.36: Beam 5.2 Important Dates*

<b>Casting</b>	March 3, 2005
<b>Prestress Application</b>	April 18, 2005
<b>Grouting</b>	April 18, 2005
<b>Anchorage Protection</b>	April 21, 2005
<b>Live Load Application</b>	April 26, 2005
<b>Exposure Initiation</b>	<i>Not Available</i>

### C.1.18.3 Beam 5.2 Stressing History

#### Live Load Application Plot

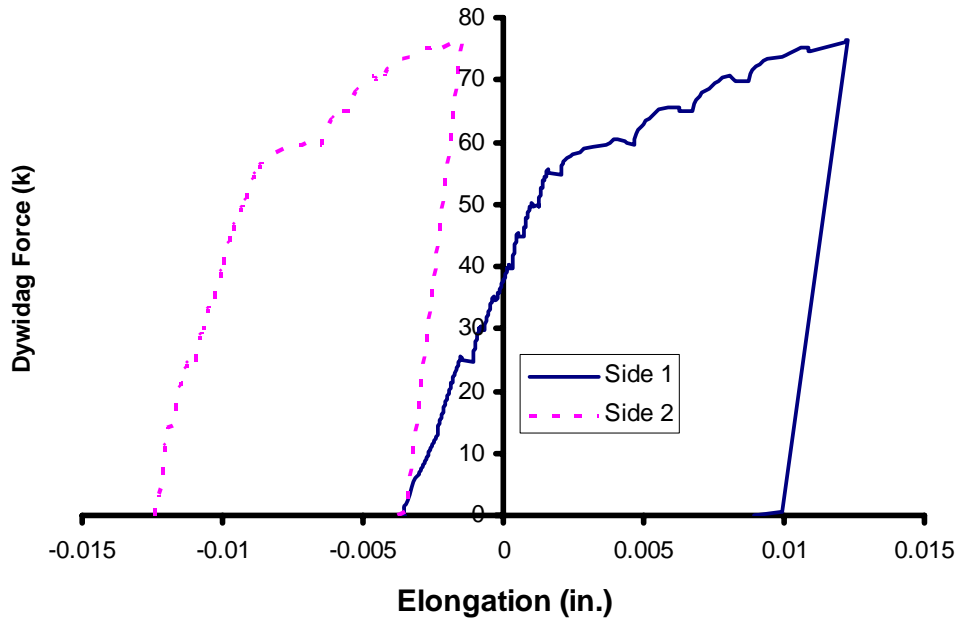


*Figure C.33: Beam 5.2 Live Load Application Plot*

#### Crack Widths

The maximum measured crack width on the top of the specimen within the depression for the salt bath is 0.003 in. See the crack map within this section for additional information regarding location and widths of cracks.

Crack Map

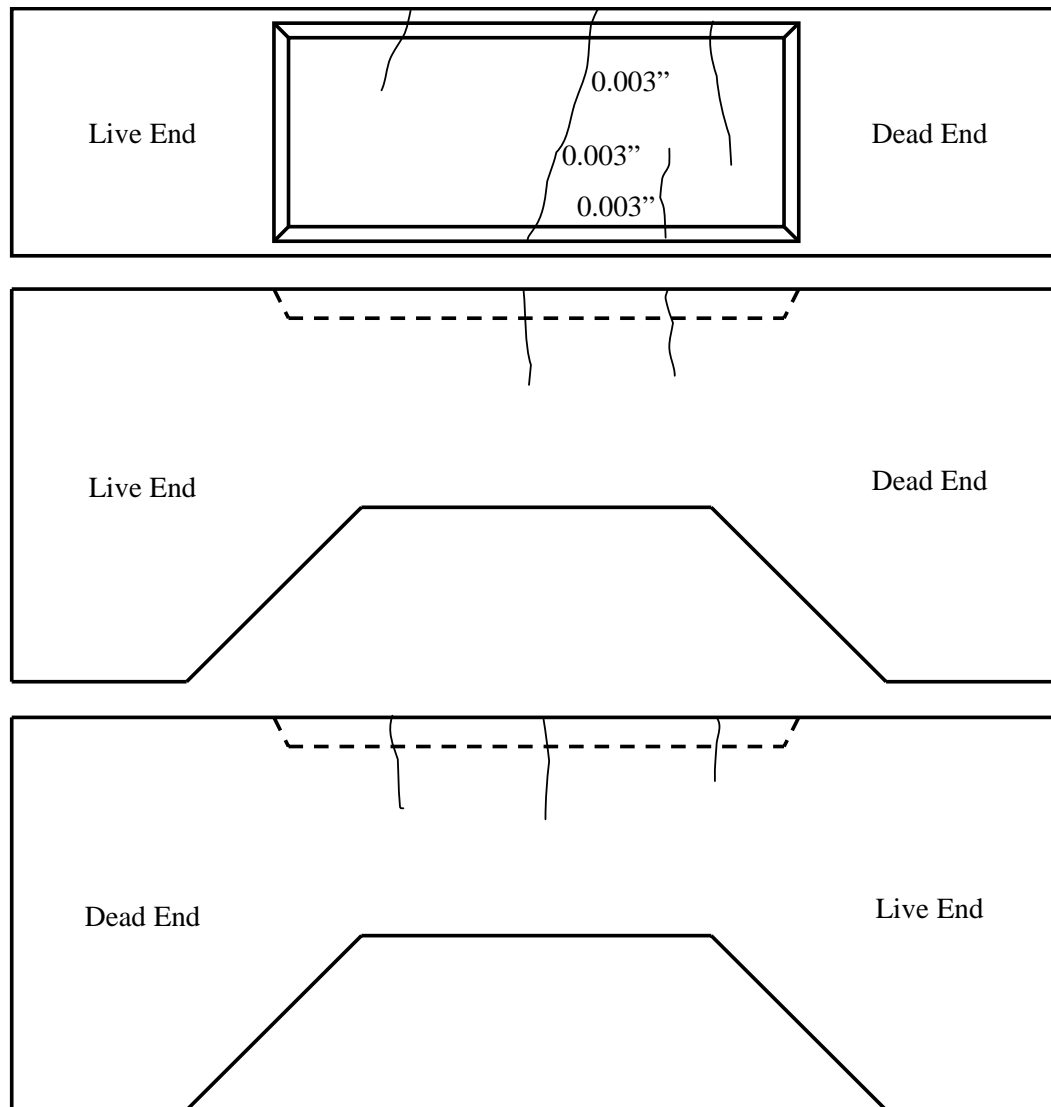


*Figure C.34: Beam 5.2 Crack Map*

***C.1.18.4 Beam 5.2 Comments***

- While grouting Duct 2, small air bubbles were observed 6 in. from the center of the specimen towards the live end.

- While reducing the live-load application data of Beam 5.2, it was determined the data acquisition system on side 1 was disturbed. Efforts were made to quantify the prestress data error and correct the subsequent live-load application data.
- After stressing was completed, cracks extending from the reentrant corner of the live end pocket were observed in the corbels. The corbel cracking was present in the trial specimens, but inclined #3 bars were added to the reinforcement cage through the crack plane in order to control corbel cracking in future specimens.
- Since 0.6-in. strands were used in the specimen, the prestress force was larger than other specimens (see Section 3.2.1). Therefore, the live load required to crack the beam was larger. The live load was increased to 75 kip (see Figure C.33).

### **C.1.19 Beam 5.3**

#### *C.1.19.1 Beam 5.3 Materials*

*Table C.37: Beam 5.3 Materials*

<b>Strand</b>	Stainless
<b>Duct</b>	GTI Two-Way Ribbed Plastic
<b>Coupler</b>	GTI Slip-On (Duct 1)
<b>Bearing Plate</b>	Non-Galvanized
<b>28-Day Concrete Strength, <math>f'_c</math></b>	6180 psi



*C.1.19.2 Beam 5.3 Important Dates*

*Table C.38: Beam 5.3 Important Dates*

<b>Casting</b>	March 3, 2005
<b>Prestress Application</b>	March 16, 2005
<b>Grouting</b>	March 17, 2005
<b>Anchorage Protection</b>	April 21, 2005
<b>Live Load Application</b>	April 26, 2005
<b>Exposure Initiation</b>	<i>Not Available</i>

*C.1.19.3 Beam 5.3 Stressing History*

Live Load Application Plot

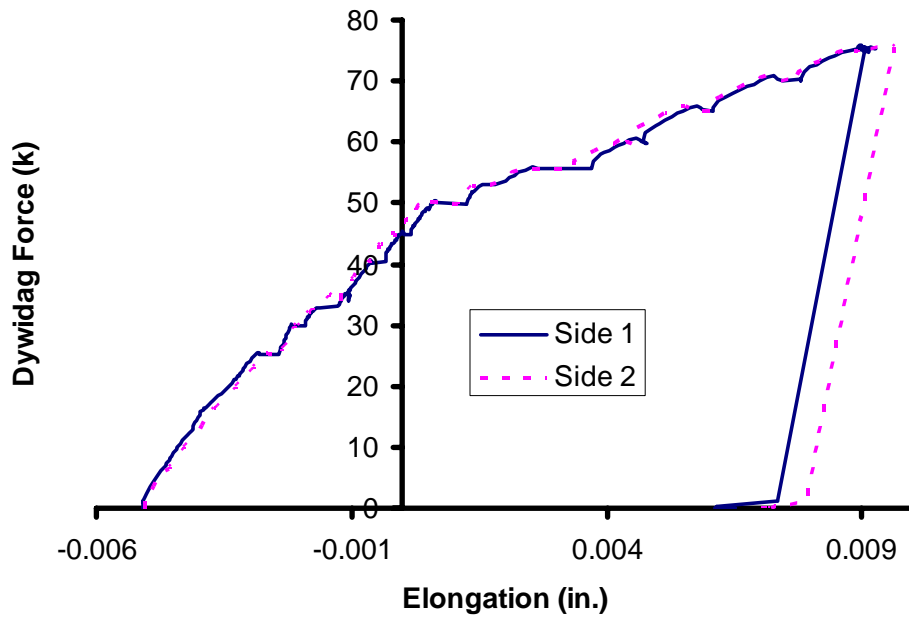


*Figure C.35: Beam 5.3 Live Load Application Plot*

Crack Widths

The maximum measured crack width on the top of the specimen within the depression for the salt bath is 0.006 in. See the crack map within this section for additional information regarding location and widths of cracks.

Crack Map

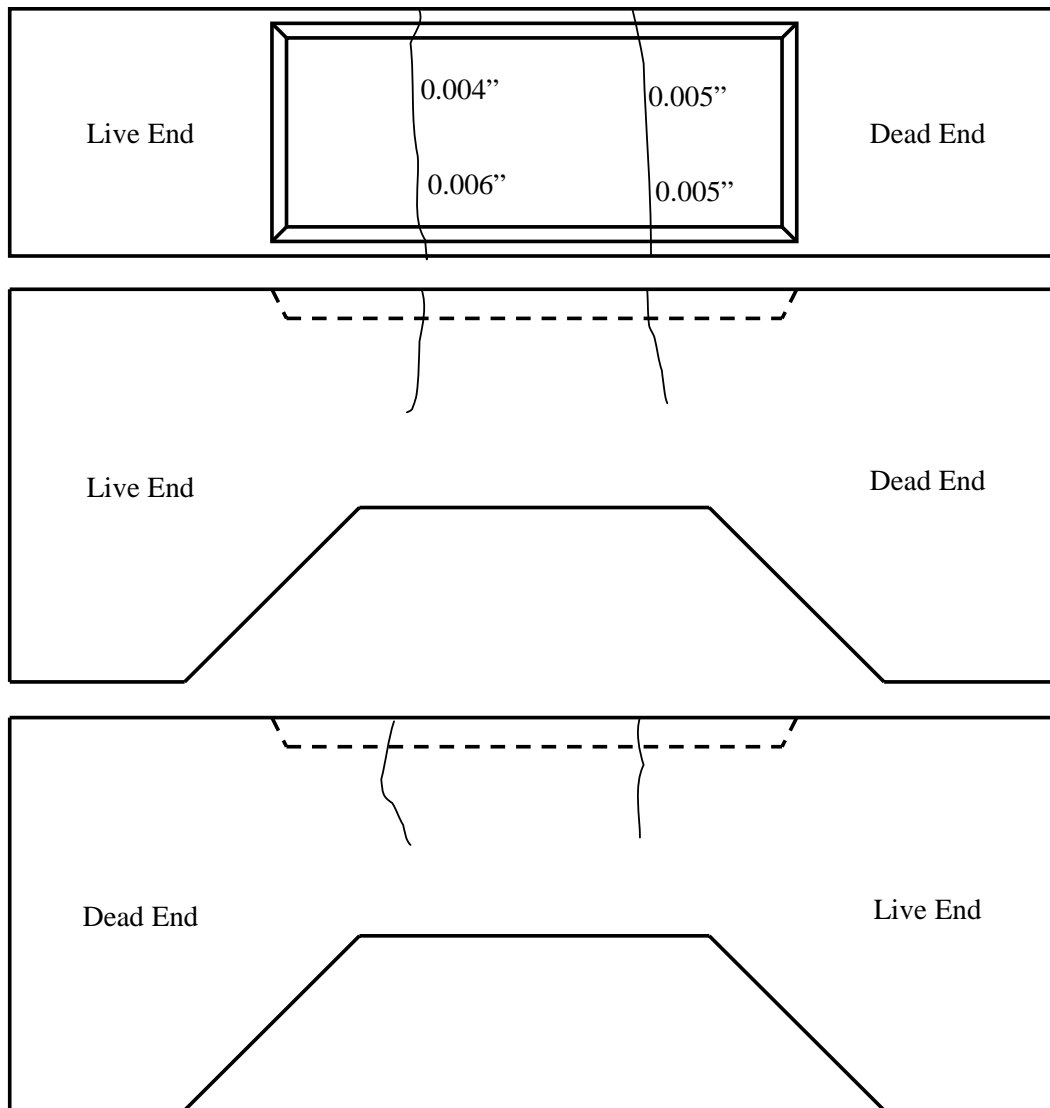


***Figure C.36: Beam 5.3 Crack Map***

***C.1.19.4 Beam 5.3 Comments***

- While grouting duct 2, small air bubbles were observed near the base of the grout vent at the middle of the beam.
- Since 0.6-in. strands were used in the specimen, the prestress force was larger than other specimens (see Section 3.2.1). Therefore, the live load required to crack the beam was larger. The live load was increased to 75 kip (see Figure C.35).
- After stressing was completed, cracks extending from the reentrant corner of the live end pocket were observed in the corbels. The corbel cracking was present in the trial specimens, but inclined #3 bars were added to the reinforcement cage through the crack plane in order to control corbel cracking in future specimens.
- In addition to cracking the live end corbel, the dead end corbel was also cracked during the live-load application process. The crack at the dead end corbel was sealed with epoxy before applying the pre-mixed concrete patch (see Section 4.10).

### C.1.20 Beam 6.1

#### C.1.20.1 Beam 6.1 Materials

*Table C.39: Beam 6.1 Materials*

<b>Strand</b>	Electroplated Galvanized
<b>Duct</b>	Galvanized Corrugated Steel
<b>Coupler</b>	None
<b>Bearing Plate</b>	Non-Galvanized
<b>28-Day Concrete Strength, <math>f'_c</math></b>	5730 psi

#### C.1.20.2 Beam 6.1 Important Dates

*Table C.40: Beam 6.1 Important Dates*

<b>Casting</b>	March 17, 2005
<b>Prestress Application</b>	<i>Not Available</i>
<b>Grouting</b>	<i>Not Available</i>
<b>Anchorage Protection</b>	<i>Not Available</i>
<b>Live Load Application</b>	<i>Not Available</i>
<b>Exposure Initiation</b>	<i>Not Available</i>

#### C.1.20.3 Beam 6.1 Stressing History

*Not Available*

#### C.1.20.4 Beam 6.1 Comments

*Not Available*

### C.1.21 Beam 6.2

#### C.1.21.1 Beam 6.2 Materials

*Table C.41: Beam 6.2 Materials*

<b>Strand</b>	Electroplated Galvanized
<b>Duct</b>	VSL One-Way Ribbed Plastic
<b>Coupler</b>	VSL Snap-On (Duct 1)
<b>Bearing Plate</b>	Non-Galvanized
<b>28-Day Concrete Strength, <math>f'_c</math></b>	5730 psi

#### C.1.21.2 Beam 6.2 Important Dates

*Table C.42: Beam 6.2 Important Dates*

<b>Casting</b>	March 17, 2005
<b>Prestress Application</b>	<i>Not Available</i>
<b>Grouting</b>	<i>Not Available</i>
<b>Anchorage Protection</b>	<i>Not Available</i>
<b>Live Load Application</b>	<i>Not Available</i>
<b>Exposure Initiation</b>	<i>Not Available</i>

#### C.1.21.3 Beam 6.2 Stressing History

*Not Available*

#### C.1.21.4 Beam 6.2 Comments

*Not Available*

### C.1.22 Beam 6.3

#### C.1.22.1 Beam 6.3 Materials

*Table C.43: Beam 6.3 Materials*

<b>Strand</b>	Electroplated Galvanized
<b>Duct</b>	GTI Two-Way Ribbed Plastic
<b>Coupler</b>	GTI Slip-On (Duct 1)
<b>Bearing Plate</b>	Non-Galvanized
<b>28-Day Concrete Strength, <math>f'_c</math></b>	5730 psi

#### C.1.22.2 Beam 6.3 Important Dates

*Table C.44: Beam 6.3 Important Dates*

<b>Casting</b>	March 17, 2005
<b>Prestress Application</b>	<i>Not Available</i>
<b>Grouting</b>	<i>Not Available</i>
<b>Anchorage Protection</b>	<i>Not Available</i>
<b>Live Load Application</b>	<i>Not Available</i>
<b>Exposure Initiation</b>	<i>Not Available</i>

#### C.1.22.3 Beam 6.3 Stressing History

*Not Available*

#### C.1.22.4 Beam 6.3 Comments

*Not Available*

### C.1.23 Beam 7.1

#### C.1.23.1 Beam 7.1 Materials

*Table C.45: Beam 7.1 Materials*

<b>Strand</b>	Conventional
<b>Duct</b>	VSL One-Way Ribbed Plastic
<b>Coupler</b>	VSL Snap-On
<b>Bearing Plate</b>	CS2000 (EIT)
<b>28-Day Concrete Strength, <math>f'_c</math></b>	<i>Not Available</i>

#### C.1.23.2 Beam 7.1 Important Dates

*Table C.46: Beam 7.1 Important Dates*

<b>Casting</b>	May 5, 2005
<b>Prestress Application</b>	<i>Not Available</i>
<b>Grouting</b>	<i>Not Available</i>
<b>Anchorage Protection</b>	<i>Not Available</i>
<b>Live Load Application</b>	<i>Not Available</i>
<b>Exposure Initiation</b>	<i>Not Available</i>

#### C.1.23.3 Beam 7.1 Stressing History

*Not Available*

#### ***C.1.23.4 Beam 7.1 Comments***

- The shrink sleeve over the dead end trumpet to duct connection split during heating near the hole provided in the sleeve for the grout vent. The split sleeve was patched with an additional piece of shrink sleeve material.

#### **Beam 7.2**

#### ***C.1.23.5 Beam 7.2 Materials***

***Table C.47: Beam 7.2 Materials***

<b>Strand</b>	Conventional
<b>Duct</b>	VSL One-Way Ribbed Plastic
<b>Coupler</b>	VSL Snap-On
<b>Bearing Plate</b>	CS2000 (EIT)
<b>28-Day Concrete Strength, <math>f'_c</math></b>	<i>Not Available</i>

#### ***C.1.23.6 Beam 7.2 Important Dates***

***Table C.48: Beam 7.2 Important Dates***

<b>Casting</b>	May 5, 2005
<b>Prestress Application</b>	<i>Not Available</i>
<b>Grouting</b>	<i>Not Available</i>
<b>Anchorage Protection</b>	<i>Not Available</i>
<b>Live Load Application</b>	<i>Not Available</i>
<b>Exposure Initiation</b>	<i>Not Available</i>



**C.1.23.7 Beam 7.2 Stressing History**

*Not Available*

**C.1.23.8 Beam 7.2 Comments**

*Not Available*

**C.1.24 Beam 7.3**

**C.1.24.1 Beam 7.3 Materials**

**Table C.49: Beam 7.3 Materials**

<b>Strand</b>	Hot Dip Galvanized
<b>Duct</b>	VSL One-Way Ribbed
<b>Coupler</b>	VSL Snap-On
<b>Bearing Plate</b>	CS2000 (EIT)
<b>28-Day Concrete Strength, <math>f'_c</math></b>	<i>Not Available</i>

**C.1.24.2 Beam 7.3 Important Dates**

**Table C.50: Beam 7.3 Important Dates**

<b>Casting</b>	May 5, 2005
<b>Prestress Application</b>	<i>Not Available</i>
<b>Grouting</b>	<i>Not Available</i>
<b>Anchorage Protection</b>	<i>Not Available</i>
<b>Live Load Application</b>	<i>Not Available</i>
<b>Exposure Initiation</b>	<i>Not Available</i>

### ***C.1.24.3 Beam 7.3 Stressing History***

*Not Available*

### ***C.1.24.4 Beam 7.3 Comments***

- The shrink sleeve over the live end trumpet to duct connection split during heating near the hole provided in the sleeve for the grout vent. The split sleeve was patched with an additional piece of shrink sleeve material.

### **C.1.25 Beam 7.4**

#### ***C.1.25.1 Beam 7.4 Materials***

***Table C.51: Beam 7.4 Materials***

<b>Strand</b>	Epoxy Coated, Flow Filled
<b>Duct</b>	VSL One-Way Ribbed Plastic
<b>Coupler</b>	VSL Snap-On
<b>Bearing Plate</b>	CS2000 (EIT)
<b>28-Day Concrete Strength, <math>f'_c</math></b>	<i>Not Available</i>

***C.1.25.2 Beam 7.4 Important Dates***

***Table C.52: Beam 7.4 Important Dates***

<b>Casting</b>	May 5, 2005
<b>Prestress Application</b>	<i>Not Available</i>
<b>Grouting</b>	<i>Not Available</i>
<b>Anchorage Protection</b>	<i>Not Available</i>
<b>Live Load Application</b>	<i>Not Available</i>
<b>Exposure Initiation</b>	<i>Not Available</i>

***C.1.25.3 Beam 7.4 Stressing History***

*Not Available*

***C.1.25.4 Beam 7.4 Comments***

- The shrink sleeve over the dead end trumpet to duct connection split during heating near the hole provided in the sleeve for the grout vent. The split sleeve was patched with an additional piece of shrink sleeve material.

## REFERENCES

**ACI Committee 222**, “*Corrosion of Metals in Concrete*,” (ACI 222R-96), American Concrete Institute, Detroit, MI, 1996, pp. 30.

**ASTM**, “*Standard Test Method for Determining the Effects of Chemical Admixtures on the Corrosion of Embedded Steel Reinforcement in Concrete Exposed to Chloride Environments*,” ASTM G109-92, American Society for Testing and Materials, Philadelphia, PA, 1992.

**ASTM**, “*Standard Test Method for Half-Cell Potentials of Uncoated Reinforcing Steel in Concrete*,” ASTM C876-91, American Society for Testing and Materials, Philadelphia, PA., 1991.

**Breen, J.E. and Kreger, M.E.**, “*Durability Design of Post-Tensioning Substructure Elements*,” Texas Department of Transportation Center for Transportation Research, November, 5, 2003.

**Collins, M. and Mitchell, D.**, *Prestressed Concrete Structures*, Response Publications, Toronto, 1997.

**FHWA**, “*Post-Tensioning Tendon Installation and Grouting Manual*,” Corven Engineering, Inc., Tallahassee, FL, May 26, 2004.

**fib Bulletin 11**, “*Factory Applied Corrosion Protection of Prestressing Steel*,”  
Task Group 9.1, fib, Lausanne (Switzerland), 2001.

**fib Commission 5**, “*Durability Specifics for Prestressed Concrete Structures: Durability of Post-Tensioning Tendons*,” Second Workshop on Durability of Post-Tensioning Tendons, fib, Zurich (Switzerland), October 2004.

**FLDOT**, “*New Direction for Florida Post-Tensioned Bridges*,” Corven Engineering, Inc., Volume 1 of 5, Tallahassee, FL, February 15, 2002.

**Fontana, M.G.**, *Corrosion Engineering*, McGraw-Hill Book Company, New York, NY, 1986.

**Freyermuth, C.L.**, “*Status of the durability of post-tensioning tendons in the United States*,” Durability of Post-tensioning tendons, fib-IABSE Technical Report, Bulletin 15, Workshop 15-16 November, Ghent (Belgium), 2001, pp. 43-50.

**Jones, D.A.**, *Principles and Prevention of Corrosion (Second Edition)*, Prentice Hall, Upper Saddle River, NJ, 1996.

**Miller, M.D.**, “*Durability Survey of Segmental Concrete Bridges*,” American Segmental Bridge Institute, ASBI, Second Edition, September 2000.

**Nilson, Darwin and Dolan**, *Design of Concrete Structures: 13<sup>th</sup> Edition*, McGraw-Hill, New York, New York, 2004.

- Rosenberg, A., Hansson, C.M. and Andrade, C.,** “*Mechanisms of Corrosion of Steel in Concrete,*” Materials Science of Concrete I, The American Ceramic Society, 1989, pp. 285-313.
- Salas, R.M.,** “*Accelerated Corrosion Testing, Evaluation and Durability Design of Bonded Post-Tensioned Concrete Tendons,*” Ph.D. Dissertation, The University of Texas at Austin, August 2003.
- Salcedo, R.E.,** “*Effects of Emulsifiable Oils Used as Temporary Corrosion Protection in Grouted Post-Tensioning Tendons,*” Master’s Thesis, Pennsylvania State University, 2003.
- Schokker, A.J.,** “*Improving Corrosion Resistance of Post-Tensioned Substructures Emphasizing High Performance Grouts,*” Ph.D. Dissertation, The University of Texas at Austin, May 1999.
- Terraserver,** <http://terraserver.microsoft.com>, Microsoft Corp., March 29, 2005.
- Theryo, T., García, P., Nickas, W.,** “*Lessons Learned from the Vertical Tendon Corrosion Investigation of the Sunshine Skyway Bridge High Level Approach Piers,*” Proceedings of the first fib Congress: Concrete Structures in the 21<sup>st</sup> Century, Session 8, Osaka (Japan), 2002.
- VSL,** “*Grouting of Post-Tensioning Tendons,*” VSL Report Series 5, VSL International Ltd., Lyssach (Switzerland), 2002.

**VSL**, “*Corrosion: The VSL Weapons*,” VSL News: Issue Two-2003, VSL International Ltd., Bern (Switzerland), 2003.

**West, J.S.**, “*Durability Design of Post-Tensioned Bridge Substructures*,” Ph.D. Dissertation, The University of Texas at Austin, May 1999.

**Yunovich, M., Thompson, N.G.**, “*Corrosion of Highway Bridges: Economic Impact and Control Methodologies*,” Concrete International, January 2003, pp.52-57.

## VITA

Michael Ahern was born on April 8, 1981 to Joseph and Kathy Ahern at Bethesda Naval Hospital in Bethesda, Maryland. He is the youngest of three children – brother Christopher and sister Elizabeth. Due to his father’s career in the Coast Guard, he had the opportunity to live in several different parts of the United States before graduating from Taravella High School in Coral Springs, Florida in June 1999. Michael entered the University of Florida in Gainesville the following Fall. In May 2003 he graduated with honors from Florida with the degree Bachelor of Science in Civil Engineering. He left Florida for Austin, Texas to pursue a Master of Science in Structural Engineering at the University of Texas. While at Texas, he worked with Dr. John Breen to improve the durability of post-tensioned concrete structures. Michael graduated from Texas in May 2005 and accepted a position with Walter P. Moore in Austin.

Permanent Address: 1920 Hawaii Ave. NE

St. Petersburg, Florida 33703

This thesis was typed by the author.